

QUANTIFICATION AND SPATIAL ANALYSIS OF SEAGRASS LANDSCAPE
STRUCTURE THROUGH THE APPLICATION OF AERIAL AND ACOUSTIC
REMOTE SENSING

by

Jeffrey Peter Barrell

Submitted in partial fulfilment of the requirements
for the degree of Doctor of Philosophy

at

Dalhousie University
Halifax, Nova Scotia
July 2014

© Copyright by Jeffrey Peter Barrell, 2014

To my family

Table of Contents

List of Tables	vii
List of Figures.....	viii
Abstract.....	xi
List of Abbreviations Used.....	xii
Acknowledgements	xiv
Chapter 1. Introduction	1
1.1 Seagrass Ecology	2
1.1.1 Seagrass Spatial Structure	5
1.2 Spatial Analysis and Landscape Ecology	6
1.2.1 Quantification of Landscape Pattern	9
1.3 Remote Sensing of Coastal Habitats.....	10
1.4 Objectives and Outline.....	13
Chapter 2. Detecting Hot and Cold Spots in a Seagrass Landscape Using Local Indicators of Spatial Association	17

2.1	Introduction.....	17
2.2	Methods.....	24
2.2.1	Study Site and Acoustic Survey	24
2.2.2	Data Processing and Analysis	25
2.3	Results.....	33
2.3.1	Acoustic Survey	33
2.3.2	Geostatistical Analysis	33
2.3.3	Local Spatial Statistics	35
2.4	Discussion.....	39
2.4.1	G_i^* Considerations.....	39
2.4.2	Implications for Landscape Analysis	41
2.4.3	Conclusions	46

**Chapter 3. Evaluating the Accuracy of Seagrass Landscape Mapping
through Comparison of Acoustic and Satellite Remote Sensing Data..... 48**

3.1	Introduction.....	48
3.2	Methods.....	56
3.2.1	Study Site	56
3.2.2	Image Acquisition and Classification	58
3.2.3	Acoustic Survey and Analysis.....	59
3.2.4	Error Matrix and Threshold Formulation.....	60

3.3	Results.....	65
3.3.1	Image Classification.....	65
3.3.2	Acoustic Survey Results.....	66
3.3.3	Error Matrix Analysis.....	71
3.4	Discussion.....	80
3.4.1	Comparison of acoustic and satellite data.....	80
3.4.2	Factors affecting classification accuracy.....	82
3.4.3	Conclusions.....	87

Chapter 4. Use of High-Resolution Low-Altitude Aerial Photography for the

Characterization of Eelgrass (*Zostera marina* L.) and Blue Mussel

(*Mytilus edulis* L.) Landscape Structure at Multiple Spatial Scales 89

4.1	Introduction.....	89
4.2	Methods.....	96
4.2.1	Data Collection.....	96
4.2.2	Data Processing & Image Classification.....	98
4.2.3	Landscape- and Patch-Scale Analysis.....	99
4.3	Results.....	102
4.3.1	Landscape-Scale Analysis.....	102
4.3.2	Patch-Scale Analysis of Eelgrass.....	104
4.4	Discussion.....	112
4.4.1	Landscape-Scale Investigation.....	112

4.4.2 Patch-Scale Investigation	114
4.4.3 Drivers of Landscape Structure.....	117
4.4.4 Implications for Landscape Analysis	124
4.4.5 Conclusions.....	126
Chapter 5. Conclusions.....	128
5.1 Synopsis	128
5.2 Future Work	129
5.2.1 Applications to Management	130
5.2.2 Acoustic Remote Sensing	132
5.2.3 Aerial Remote Sensing	134
Appendix A. Technical Details.....	137
A.1 Acoustic System Specifications	137
A.2 Acoustic Ground Reference Data	138
Appendix B Copyright Information.....	143
References	146

List of Tables

Table 2-1. Results of G_i^* at five search radii indicating the number and proportion of points identified as hot or cold spots, and the mean and minimum number of neighboring points found around each hot or cold spot.....	35
Table 2-2. Neighborhood values for the G_i^* analysis at each of 3 spatial scales along with average seagrass percent cover and the number of discrete “patches” formed via buffering procedures.....	36
Table 3-1. Error matrix representing the possible outcomes in the comparison between acoustic and satellite datasets.	61
Table 3-2. Description of metrics derived from the error matrix along with the calculation used for their derivation.	64
Table 4-1. Landscape metrics used for characterizing configuration and composition of the landscape at three levels: patch, class (comprising all patches of each category), and landscape. Metrics are either defined in the literature (i.e., McGarigal et al. 2012) or adapted from similar metrics.....	99

List of Figures

Figure 1-1. Hierarchy of spatial scales represented in a seagrass landscape: (<i>left</i>) individual plant with leaf and rhizome structures, (<i>center</i>) a collection of plants forming a patch, and (<i>right</i>) landscape-scale mosaic of patches. All photos taken by J. Barrell at Eastern Passage, Nova Scotia, Canada.....	4
Figure 1-2. Aerial photograph showing patches of eelgrass and mussels distributed through a background matrix of soft sediments. Image collected from Eastern Passage, Nova Scotia, Canada (see Chapter 4).....	7
Figure 2-1. Map of the Richibucto estuary with the primary study location highlighted. (<i>Inset</i>) Location in eastern Canada.	23
Figure 2-2. (<i>Above</i>) Acoustic data tracks, showing the distribution of percent cover values. (<i>Below</i>) Histogram of the distribution of percent cover values.	30
Figure 2-3. Variogram map depicting anisotropy in the dataset with a lag size range from 2 -200 m.	31
Figure 2-4. (<i>Above</i>) Modeled omnidirectional variogram. (<i>Below</i>) anisotropic empirical variograms representing the east-west (crosses) and north-south (points) axes.	32
Figure 2-5. Map of seagrass percent cover interpolated using ordinary kriging.	34
Figure 2-6. Zones of high and low seagrass cover as derived from G_i^* analysis for (A) 30 m, (B) 40 m, and (C) 50 m neighborhood search radii. Overlap zones are indicated in blue.	37
Figure 3-1. Map of the study locations Site A and Site B within the Richibucto estuary, New Brunswick, Canada.	56
Figure 3-2. Classified map of sites A (<i>left</i>) and B (<i>right</i>) with the location of sampled acoustic points overlaid.	65
Figure 3-3. Spectral banding at site B affected the 2.4 m resolution multispectral imagery (<i>left</i>) more strongly than the 0.6 m resolution panchromatic image (<i>right</i>).	66
Figure 3-4. (<i>above</i>) Acoustic track map of site A from the October 2007 survey depicting percent cover of eelgrass; (<i>below</i>) histogram of seagrass percent cover at site A; mean $41.8 \pm 18.1\%$ (SD), $n = 2677$ points.	68
Figure 3-5. (<i>above</i>) Acoustic track map of site B from October 2007 showing percent cover of seagrass. (<i>below</i>) Histogram of seagrass percent cover at site B; $33.2 \pm 24.5\%$ (SD), $n = 4932$ points.	69

Figure 3-6. Prevalence of seagrass presence determined from the acoustic percent cover dataset at each examined threshold $t_0 - t_{100}$ for sites A and B.	71
Figure 3-7. Results of the kappa statistic at each threshold from $t_0 - t_{100}$ for sites A and B. Kappa measures the agreement of two binary classifications relative to random chance, ranging from 1 (perfect agreement) to 0 (random agreement) to -1 (systematic disagreement below that expected by random chance).	72
Figure 3-8. Trends in overall accuracy for sites A & B at each threshold value of seagrass percent cover ($t_0 - t_{100}$).	74
Figure 3-9. At each percent cover threshold, the proportion of points determined to be true positives (TP), true negatives (TN), false positives (FP), and false negatives (FN) for sites A (<i>above</i>) and B (<i>below</i>). The sum of TP and TN is equivalent to the overall accuracy, while the sum of FP and FN represents the misclassification rate. The ratio of classified positives (TP + FP) to classified negatives (TN + FN) is predetermined by the number of points falling in respective categories in the classified map.	75
Figure 3-10. Trends in positive predictive value (PPV) and negative predictive value (NPV) at sites A (<i>above</i>) and B (<i>below</i>) through threshold values of percent cover from 0 – 100% ($t_0 - t_{100}$).	78
Figure 3-11. Sensitivity (correctly predicted presences) and specificity (correctly predicted absences) of the classification scheme for sites A (<i>above</i>) and B (<i>below</i>) at threshold values of percent cover from 0 – 100% ($t_0 - t_{100}$).	79
Figure 4-1. (<i>above</i>) Outline of the landscape of interest; (<i>below</i>) approximate location of the study site in Eastern Passage, Nova Scotia, Canada (63° 29.7' W, 44° 36.5' N). Imagery source: QuickBird satellite.	96
Figure 4-2. Map showing the raw unclassified imagery (<i>left</i>) with classified bivalve and eelgrass patches superimposed (<i>right</i>). The area of interest for patch-scale analysis is outlined at right. The spatial resolution of the imagery is 0.045 m.	102
Figure 4-3. Depiction of the temporal change in four selected patches from imagery collected on 8 July 2008 (<i>left</i>) to 20 September 2010 (<i>right</i>). The spatial resolution (i.e., pixel edge length) of the 2008 and 2010 images are 0.0353 m and 0.0368 m respectively.	104
Figure 4-4. Change in patch area (m ²) for four patches from July 2008 to October 2010. Does not include internal gap areas. (<i>Inset</i>) Relative patch location by patch ID.	105
Figure 4-5. Change in circumscribing circle radius over the sampling period, measuring the radius of the smallest circumscribing circle for each patch. This metric estimates the maximum lateral expansion or retraction for each patch, and	

provides an estimate of patch linear extent. (<i>Inset</i>) Relative patch location by patch ID.....	106
Figure 4-6. Change in patch perimeter length (m) for four patches between the sampling dates, including internal perimeter associated with patch gaps (<i>Inset</i>) Relative patch location by patch ID.....	106
Figure 4-7. Change in interior patch gaps over the study period, expressed as a percentage of total patch area. (<i>Inset</i>) Relative patch location by patch ID.	107
Figure 4-8. Change in perimeter-to-area ratio for each patch between the sample dates. This metric provides an estimate of patch shape complexity. (<i>Inset</i>) Relative patch location by patch ID.....	107
Figure 4-9. Change in shape index over the sampling period, estimating complexity relative to a standardized square shape. (<i>Inset</i>) Relative patch location by patch ID.....	108
Figure 4-10. Change in the related circumscribing circle metric over the sample period. This metric measures the area of a patch relative to the area of its smallest circumscribing circle, providing estimates of patch density and elongation. (<i>Inset</i>) Relative patch location by patch ID.....	108
Figure 4-11. Change in the radius of gyration metric for each patch, calculated as the mean distance from each cell of the patch to the patch centroid. This metric estimates the weighted areal extent of each patch as well as patch elongation. (<i>Inset</i>) Relative patch location by patch ID.	109
Figure 4-12. Waterfowl (probably American black duck, <i>Anas rubripes</i>) grazing within eelgrass patches at the study site during imagery acquisition on 20 September 2010. Internal patch gaps are clearly evident.	120
Figure A-1. Map of locations sampled by drop-camera for the purpose of ground-truthing acoustic data gathered in the Richibucto estuary, with the classification of eelgrass presence or absence noted.....	138
Figure A-2. Characteristic acoustic results for areas with (<i>left</i>) absence and (<i>right</i>) presence of vegetation. Depicted for each category is (<i>top</i>) a screen capture from the underwater video; (<i>center</i>) echogram profile showing the structure of the seafloor; and (<i>bottom</i>) ping profile used through the classification algorithm.	140

Abstract

Biogenic components of the marine environment such as eelgrass (*Zostera marina* L.) provide numerous valuable ecosystem services and function as ecosystem engineers in the coastal environment. The spatial distribution and arrangement of eelgrass in the coastal landscape greatly influences ecological functions, necessitating mapping and monitoring of eelgrass habitat for effective management, though quantification of landscape structure has been hindered by challenges collecting and analyzing spatial data in the coastal zone. In this thesis, the spatial structure and distribution of eelgrass was studied through the application of acoustic and optical remote sensing and spatial analysis to quantify aspects of eelgrass landscape pattern. Single-beam acoustic data representing a seagrass landscape were collected and analyzed at multiple spatial scales through geostatistical methods and local spatial statistics (i.e., Getis-Ord G_i^*), identifying areas of high and low cover in a spatially continuous seagrass bed. Acoustic data from the same site were compared to a satellite-derived dataset using remote sensing techniques for the evaluation of map accuracy. Performance of the satellite classification algorithm was found to vary depending on the spatial scale and degree of fragmentation in the landscape, highlighting the strengths and weaknesses of the method, and contrasting the landscape conceptualization of acoustic and aerial remote sensing. The spatial resolution of modern satellite data has greatly improved, though at pixel size of 2.4 m the ability to discern fine-scale patterns is limited. In contrast, very high-resolution aerial photography (pixel size ~3 cm) collected at a second site from a tethered helium-balloon platform was classified to depict a complex landscape mosaic comprised of eelgrass and blue mussels (*Mytilus edulis* L.). The application of landscape pattern metrics with high-resolution imagery additionally allowed tracking the temporal change in eelgrass patch metrics over a period of 26 months. The multidisciplinary approach of this thesis advance the application of spatial analysis in coastal ecosystems through the novel use of spatial statistics and remote sensing. Continued research and technological developments promise to improve management and provide new insights to the spatial dynamics and function of coastal landscapes.

List of Abbreviations Used

Abbreviation

Definition

ADCP	Acoustic Doppler Current Profiler
DFO	Department of Fisheries and Oceans, Canada
ESS	Ecologically Significant Species
FN	False Negative
FP	False Positive
GCP	Ground Control Point
G_i^*	Getis-Ord G_i^* statistic
GIS	Geographic Information Systems
GPS	Global Positioning System
LISA	Local Indicators of Spatial Association
LLWLT	Lower Low Water, Large Tide
LPI	Largest Patch Index
MPA	Marine Protected Area
MSP	Marine Spatial Planning
NPV	Negative Predictive Value
OBIA	Object-Based Image Analysis
PPV	Positive Predictive Value
PVM	Predictive Vegetation Mapping

<i>Abbreviation</i>	<i>Definition</i>
SAV	Submerged Aquatic Vegetation
SPERA	Strategic Program for Ecosystem-Based Research and Advice
TIFF	Tagged Image File Format
TN	True Negative
TP	True Positive

Acknowledgements

I have many people to acknowledge and thank for their assistance in various aspects of the writing of this thesis. First, thanks most of all to my supervisor, Jon Grant, and my supervisory committee: Mike Dowd, Katja Fennel, Alex Hay, and Herb Vandermeulen. Their guidance and expertise was essential in allowing me to pursue the multidisciplinary aims of my research. I would also like to thank my external examiner, Dr. Susan Bell, for her participation and her expertise in seagrasses and landscape ecology. Special thanks also to my undergraduate supervisor at Gettysburg College, John Commito, who helped me discover my interest in science and gave me the first push in this direction.

My fellow students (and post-docs) in the Grant lab similarly were of great help and constant companions on the voyage. Thanks to Marie Archambault, Martha Baldwin, Lindsay Brager, Francisco Bravo, Mike Brown, Lin (Luke) Lu, Ramon Filgueira, Michelle Simone, and Tony Walker for your input and companionship through the years. Thanks also to Chris Taggart and his lab for adopting me and letting me attend the Christmas parties; I particularly enjoyed the laser tag. Although I enjoyed the company of a number of students in the Oceanography Department through the years, and couldn't possibly list them all, thanks especially to Darlene Childs, Adam Comeau, Remi Daigle, Kim Davies, Michelle Lloyd, Eric Oliver, Clark Richards, and Angelia Vanderlaan, and all the others who hopefully aren't upset if I've snubbed them.

I relied heavily on the good will of others for support in conducting the fieldwork for this thesis, and I owe much gratitude to all. In particular, thanks to Simon Courtenay,

Marc Skinner, Marie-Hélène Theirault, and Monica Boudreau for helping with boats and other infrastructure for my acoustic surveys, enduring the occasional equipment malfunctions and bad weather selflessly. Thanks also to the extremely helpful aquaculturists in Richibucto: Ola Daigles and Serge Gaudet, who helped me out with boats, and particularly Yrois Robichaud, who opened up his oyster lease and his property for me to use.

I also gained tremendous knowledge through my interactions with various academic and government researchers, both directly and indirectly. Special thanks to everyone associated with the DFO eelgrass working group: Guy Robichaud, Marc Ouellette, Al Hanson, Matt Mahoney, and Eric Tremblay, as well as several others already mentioned. Thanks also to the large and growing list of researchers with DFO, Parks Canada, Environment Canada, academia, et al. who have helped me in some way or other: Melisa Wong, Peter Lawton, Vladimir Kostylev, Chris McCarthy, Peter Cranford, Yi (Joe) Zhou, Pierre Legendre, Tim Webster, Pierre Goovaerts, Marie-Josée Fortin, and many others.

Of course, none of this could have been done without the help of my family and friends, who have supported me unconditionally and invariably. Additionally, thanks to Katie Porter for... everything. Finally, I would like acknowledge all members of the scientific community not listed above that contributed to my experiences through interactions in classes, workshops, meetings, and conferences, who greatly enriched my experience and education.

Chapter 1. Introduction

Coastal ecosystems are incredibly important, providing a wealth of resources and ecosystem services and serving key roles in global ecological function. They are also under immense pressures due to intensive coastal development and climate change leading to widespread declines. As a primary interface between humanity and the global ocean, the coasts are exposed to numerous direct and indirect anthropogenic stressors. Coastal populations are expanding at a high and accelerating rate, dramatically increasing the pressures on coastal resources. Recent estimates suggest that as much as 44% of the global human population lives within 150 km of the oceans, and population growth in these areas is accelerating (UN 2014). As a result, coastal habitats are threatened and declining, and continued provision of the numerous services provided by coastal resources are at risk (Lotze et al. 2006, Waycott et al. 2009).

Understanding the distribution of coastal habitats such as seagrass beds is a complex undertaking. The processes that regulate the spatial distribution of coastal habitats operate over a range of spatial and temporal scales. Collaborative and interdisciplinary approaches are needed to understand and protect these crucial areas. This thesis addresses issues associated with the spatial distribution of coastal habitats, combining elements of remote sensing, spatial statistics, and landscape ecology to increase understanding of the spatial dynamics of coastal marine habitats.

Below, I introduce and briefly review several of the main concepts and themes recurring throughout my thesis, with relevant history and background details to lay the foundation for the remainder of the manuscript.

1.1 Seagrass Ecology

Seagrasses are a group of marine angiosperms that are distributed over a near-global extent, occurring on 6 continents (Green & Short 2003, den Hartog & Kuo 2006). Seagrasses perform a wide range of functions in coastal ecosystems, and rank among the most valuable and productive habitats worldwide (Costanza et al. 1997). They provide a variety of important services including primary production, nutrient cycling, water filtration, attenuation of wave energy, carbon sequestration, sediment stabilization and erosion protection (Orth et al. 2006, Chen et al. 2007, Barbier et al. 2011). They function as autogenic ecosystem engineers, creating and maintaining environmental conditions that support a diverse assemblage of species (Jones et al. 1994). The biogenic structure of seagrass provides substrate for epiphytic species, nursery habitat for fish and invertebrates, and a direct source of food for grazing invertebrates, megafauna, and waterfowl (Valentine & Heck 1999, Hanson 2004, Borowitzka et al. 2006, Boström et al. 2006). Seagrasses are also an important source of nutrients exported as subsidies to neighboring ecosystems (Heck et al. 2008).

In Atlantic Canada, the seagrass community is comprised primarily of eelgrass (*Zostera marina* L.) and to a much lesser extent the salt-tolerant widgeon grass (*Ruppia maritima* L.). Eelgrass can be found along the coast of North America extending northwards from North Carolina, USA to Labrador, Canada, spanning a range greater than 20 degrees of latitude (Green & Short 2003). *Z. marina* is also found along the eastern Atlantic coastline as well as both sides of the Pacific (den Hartog & Kuo 2006). Other members of the *Zostera* genus are found in temperate coastal waters of both hemispheres. Eelgrass occurs in both intertidal and shallow-subtidal areas, particularly in

estuaries and coastal embayments with soft sediments and adequate protection from hydrodynamic stress. Eelgrass is widely distributed throughout the coastal areas of New Brunswick, Prince Edward Island, and Nova Scotia excepting the Bay of Fundy.

The importance of aquatic vegetation to coastal ecosystems has prompted diverse efforts to understand the factors that govern its growth and mortality. Seagrasses experienced a sharp decline beginning in the 1930s, believed to be due to the effects of the slime mold *Labyrinthula zosterae*, leading to a condition termed “wasting disease” (Moore & Short 2006). Following this episode, eelgrass was either locally exterminated or experienced only partial recovery, leading to widespread changes in the function of coastal ecosystems. More recently, declines in the extent and abundance of seagrasses have been detected over near-global extent (Orth et al. 2006, Waycott et al. 2009), including Atlantic Canada (Seymour et al. 2002, Garbary et al. 2014), due to several factors. Seagrasses are threatened by changes in environmental conditions over a range of spatial and temporal scales, and are vulnerable to cumulative effects from multiple stressors. In particular, seagrass declines have been linked to various anthropogenic pressures such as eutrophication, sedimentation, fisheries and aquaculture, pollution, invasive species, and direct and indirect destruction through coastal development (Lotze et al. 2006, Orth et al. 2006). Expected global-scale changes associated with climate change such as increasing temperatures and sea level rise will likely cause additional impacts in the near- and long-term future (Orth et al. 2006, Short et al. 2011).

The comprehensive value and keystone role played by seagrasses in marine ecosystems has led to their inclusion in various aspects of coastal management. In Canada, the value of eelgrass habitat has been formally recognized through the definition

of *Z. marina* as an ‘ecologically significant species’ (ESS) (DFO 2009), and its sensitivity and vulnerability has been evaluated for inclusion in habitat management programs (Vandermeulen 2005, Vandermeulen 2009, DFO 2011). The distribution and health of seagrass habitat can be used as an indicator of ecosystem health due to its need for high water quality (Dennison et al. 1993, Moore & Short 2006, Krause-Jensen et al. 2008, Martínez-Crego et al. 2008). Seagrasses are often used in habitat restoration as a means for restoring lost ecosystem services through compensatory mitigation (Fonseca et al. 2000, van Katwijk et al. 2009), and play an important role in marine spatial planning (MSP) and integrated coastal zone management (Foley et al. 2010).



Figure 1-1. Hierarchy of spatial scales represented in a seagrass landscape: (*left*) individual plant with leaf and rhizome structures, (*center*) a collection of plants forming a patch, and (*right*) landscape-scale mosaic of patches. All photos taken by J. Barrell at Eastern Passage, Nova Scotia, Canada.

1.1.1 Seagrass Spatial Structure

Seagrass habitat occurs naturally in configurations ranging from highly fragmented to continuous meadows (Duarte et al. 2006). The spatial structure of seagrass habitat can be conceptualized as a hierarchy of spatial scales ranging from individual shoots to patches to landscape-scale meadows (Figure 1-1). The spatial pattern of seagrass habitat is shaped by a number of spatially and temporally variable biotic and abiotic processes. Meadow structure is biologically mediated through intrinsic processes of seedling recruitment and clonal expansion through horizontal rhizome elongation (Duarte et al. 2006). External processes governing seagrass spatial structure include the hydrodynamic regime (Fonseca et al. 1983), sediment characteristics and geochemistry (Koch 2001, Bradley & Stolt 2006), light availability (Dennison et al. 1993, Hauxwell et al. 2006), bioturbation and grazing (Townsend and Fonseca 1998, Valentine & Heck 1999, Hughes et al. 2004, Rivers & Short 2007), and periodic disturbances from storms, ice scouring, and other natural or anthropogenic events (Bell et al. 2008).

The high economic and ecological value of seagrass and its sensitivity to disturbance has prompted efforts to understand and quantify its distribution and relationship with ecological processes. Threats to the health of seagrass ecosystems occur at a wide range of spatial scales, from molecular processes (e.g., disease) to global (e.g., climate change). Addressing these threats requires the consideration of seagrass pattern at multiple spatial scales and an interdisciplinary approach (Neckles et al. 2011). A necessary prerequisite of seagrass management is understanding of the natural spatial and temporal dynamics of seagrass distribution. Tools and methods for monitoring and predicting the distribution of seagrasses in Atlantic Canada are currently lacking, and

represent a critical priority for maintaining the integrity of coastal ecosystems and the services they provide.

1.2 Spatial Analysis and Landscape¹ Ecology

The study of spatial pattern has long been a central theme of ecology (Watt 1947, Hutchinson 1953, MacArthur & Wilson 1967, Legendre & Fortin 1989, Levin 1992, Legendre & Legendre 1998). Ecosystems are structured by biotic and abiotic processes, creating spatially heterogeneous habitat mosaics that influence ecological function over a range of spatial and temporal scales. The causes and consequences of this heterogeneity are fundamental to numerous ecological theories, and have thus been the focus of efforts to characterize and quantify spatial patterns in diverse sectors of ecology (Li & Reynolds 1995, Wagner & Fortin 2005). Efforts to understand the spatial ecology of marine habitats such as seagrass beds have lately been aided by technical and theoretical developments in spatial analysis, spatial statistics, and the field of landscape ecology.

Landscape ecology explicitly emphasizes the causes and consequences of environmental heterogeneity through an interdisciplinary approach to the quantification and modelling of spatial pattern in natural ecosystems (Turner et al. 2001). The fundamental principles of landscape ecology originated from the theory of island biogeography, where spatial characteristics of islands (e.g., size, geometry, spatial arrangement) directly and indirectly influence the ecological function of the habitat

¹ Alternate terminology is frequently applied to denote the “landscape” in a marine context, with varying usage in the literature (e.g., “seascape”, “benthoscape”). The author prefers the convention of “landscape” to emphasize linkages with the terrestrial discipline, and will do so throughout this manuscript.

(MacArthur & Wilson 1967). It emerged as a recognized scientific discipline in the 1980s, though the term had been coined several decades prior to describe the mosaic of land parcels visible from the rapidly-developing medium of aerial photography (Troll 1939). The establishment and expansion of landscape ecology was in large part fueled by improvements in remote sensing, computing power, and GPS technology, leading to extensive applications particularly in terrestrial environments (Turner et al. 2001).

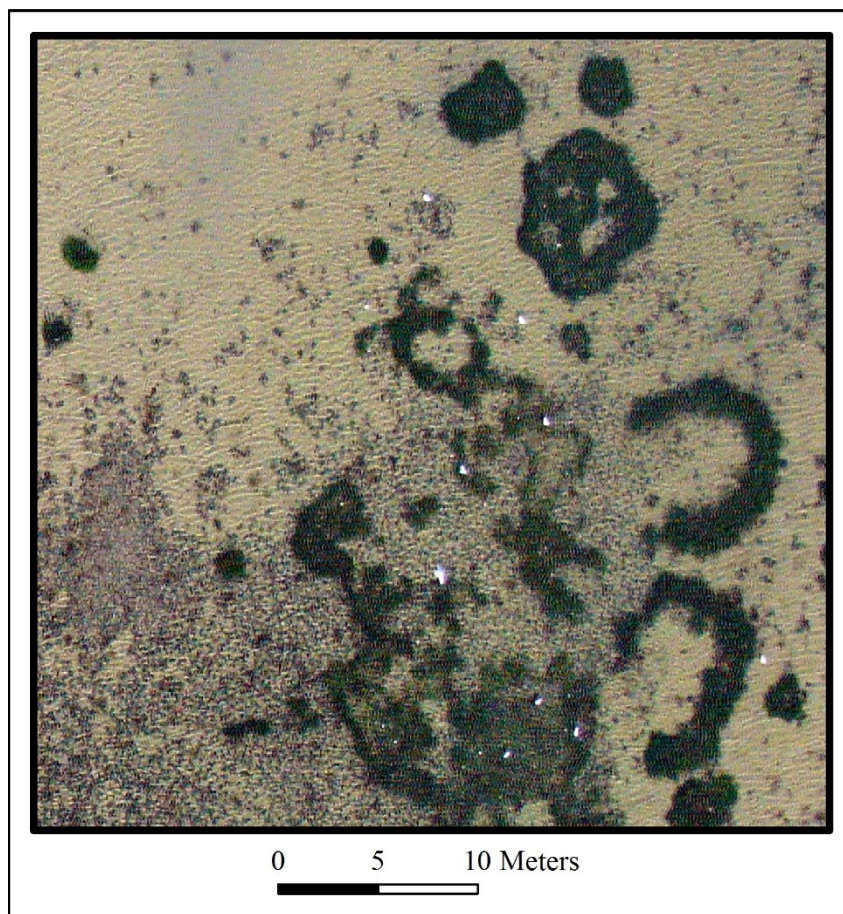


Figure 1-2. Aerial photograph showing patches of eelgrass and mussels distributed through a background matrix of soft sediments. Image collected from Eastern Passage, Nova Scotia, Canada (see Chapter 4).

The concept of the “landscape” in ecology has evolved from its origins in representing the broad-scale mosaic of natural and human habitats visible from aerial photography to a more flexible definition that can be applied to diverse systems (Turner et al. 2001, Turner 2005). The landscape can generally be defined as a spatially heterogeneous mosaic of patches. This heterogeneity can be defined over a broad range of spatial scales, depending on the characteristics of the organisms or ecological processes under study. Consideration of spatial scale (grain and extent) is a primary concern of landscape ecology, fundamental to both the theory and practice of spatial analysis in ecological systems (Wiens 1989, Levin 1992, Pickett & Cadenasso 1995, Wu & Hobbs 2002).

Recognition of the value of the landscape approach led to its extension to the marine environment in the 1990s, focusing primarily on patch-forming biogenic marine habitats such as corals, bivalves, and aquatic vegetation (Hinchey et al. 2008). The landscape approach was first formally applied to seagrasses in the 1990s (Robbins & Bell 1994) and has since expanded to encompass diverse aspects of seagrass spatial patterns, patch and gap dynamics, biotic interactions, and relationships with physical processes (Irlandi et al. 1995, Bell et al. 2006, Boström et al. 2006, Boström et al. 2011). The integrative approach of landscape ecology is well-suited to patch-forming seagrass habitat that varies over a hierarchy of spatial scales (Figure 1-1) (Bell et al. 2006). In the context of seagrasses, the landscape can be considered a heterogeneous mix of seagrass patches embedded in a background matrix of soft sediments, often coexisting with patches of other features such as bivalves (Figure 1-2).

1.2.1 *Quantification of Landscape Pattern*

Several types of spatial statistics and metrics are used for the quantification of spatial structure in seagrass habitats, often conducted within a geographic information system (GIS) using data collected through remote sensing (Fortin & Dale 2005). Spatial statistics are used to quantify the degree of spatial dependence present in a dataset, neatly encapsulated by Tobler's first law of geography: "...everything is related to everything else, but near things are more related than distant things" (Tobler 1970). Several approaches including geostatistical methods, global spatial statistics (e.g., Moran's *I*, Geary's *C*), and local spatial statistics (e.g., local indicators of spatial association; LISAs) have been applied for quantifying spatial dependence in ecological datasets (Goovaerts 1997, Legendre & Legendre 1998, Wagner & Fortin 2005, Kent et al. 2006, Getis 2008).

Landscape ecology commonly involves the use of spatial pattern metrics to quantify aspects of the composition, configuration, and complexity of patches in the landscape, often at multiple spatial scales (O'Neill et al. 1988, Turner 1989). Pattern metrics are now widely applied for establishing relationships between spatial pattern and ecological processes in diverse systems (Turner 2005). A variety of metrics can be implemented through powerful freeware programs such as FRAGSTATS (McGarigal et al. 2012). However, despite their widespread use, many problematic issues complicate the formulation and analysis of landscape metrics. Many metrics are sensitive to spatial scale and uncertainty (Wagner & Fortin 2005), and statistical interpretation is confounded by non-independence, the presence of spatial autocorrelation, and redundancy between indices (Legendre 1993, Li & Wu 2004, Turner 2005). Landscape metrics focus primarily on categorical or thematic maps of seagrass habitat despite difficulties in

establishing and interpreting patch boundaries in certain landscapes (Arnot et al. 2004, Wagner & Fortin 2005), and some landscapes exhibit continuous variation that is difficult to capture with a discrete patch-mosaic model (McGarigal et al. 2009). Improving the technical and theoretical rationale of landscape pattern analysis is recognized as an important area of future research (Li & Wu 2004, Turner 2005, Hoehstetter et al. 2008, Kupfer 2012).

Though landscape ecology has been effectively applied to many types of marine habitats, questions remain about the application of landscape principles to seagrasses and the marine environment (Sleeman et al. 2005, Bell et al. 2006, Wedding et al. 2011). Most landscape metrics were developed for use with terrestrial data and may require adaptation or reformulation for use in the marine context. A recent review of the flagship journal *Landscape Ecology* found that studies of coastal, marine, and freshwater habitats were extremely rare, comprising less than 4% of studies examined for the review (Newton et al. 2009). This paucity of studies highlights the need for further research into the causes and consequences of landscape pattern in the marine environment.

1.3 Remote Sensing of Coastal Habitats

Data representing marine habitats can be difficult to collect through direct observation or sampling due to the overlying water column, requiring costly and time-consuming efforts. Analysis of landscape pattern requires high-quality data at fine spatial resolution in order to capture patterns, often over a broad extent. The cost of direct sampling for covering large areas at fine resolution is generally prohibitive. As a result,

most studies of marine landscapes utilize spatial data captured through some form of remote sensing.

The type and scale of remote sensing can have dramatic consequences on the results of spatial and landscape analysis. Pattern is recognized to be spatial-scale dependent, with different patterns emerging depending upon the spatial scale of investigation (Turner et al. 1989, Wiens 1989). In particular, the spatial resolution of remote sensing has been shown to correlate strongly with the results of landscape metrics, necessitating careful consideration of scale when using remote sensing data to quantify pattern. The accuracy of remote sensing data also exerts a strong influence on the results of landscape pattern analysis and can be a major source of errors (Hess 1994, Shao & Wu 2008). Issues of accuracy, uncertainty, and unreported errors are considered a critical point of emphasis for new research in landscape ecology (Wu & Hobbs 2002).

For marine benthic habitats, remote sensing can be broadly categorized as either acoustic or optical. Acoustic sensors use pulses of sound to gather information on the seabed. Data from acoustic sensors are used to produce detailed maps of bathymetry as well as the geological and biological components of the seabed, providing a wealth of information for mapping and analyzing benthic habitats (Brown et al. 2011). Seagrasses exhibit strong acoustic reflectivity due to the presence of oxygen-filled lacunae that provide buoyancy to their leaves, aiding detection with acoustic methods. Many types of acoustic sensors have been applied to mapping vegetated marine habitats, including single-beam, sidescan, and multibeam sonars, as well as other types of acoustic instruments such as acoustic Doppler current profilers (ADCPs) (Duarte 1987, Pasqualini et al. 1998, Sabol et al. 2002, Warren & Peterson 2007).

In contrast to acoustics, optical remote sensing makes use of reflected light energy to infer the composition of the seabed, and can be collected either in-water or from aerial platforms. In-water optical remote sensing consists of underwater photography and videography, and is commonly used as a source of ground-reference data in studies of seagrass landscapes (McKenzie et al. 2002, McDonald et al. 2006). Aerial optical remote sensing includes several forms of imaging collected from airborne or spaceborne platforms including analog and digital photography as well as multi- and hyperspectral imaging and LiDAR (Dekker et al. 2006). The collection of analog aerial photography for mapping marine habitats has a long history (e.g., Edwards & Brown 1960), and remains a common source of spatial data in the modern era (McKenzie et al. 2001). However, particular care must be taken when using optical remote sensing in the marine environment due to the absorption of light in seawater and the confounding effects of water depth and clarity (Silva et al. 2008).

Acoustic and optical remote sensing produce inherently different conceptualizations of the seagrass landscape, requiring different processing and interpretation. Single-beam acoustic surveys are commonly conducted along transect tracks, sampling a subset of the study area and interpolating or extrapolating the results to create maps (e.g. Guan et al. 1999, Valley et al. 2005). In contrast, optical remote sensing provides synoptic data that requires image classification to delineate separate habitats. Aerial and acoustic methods also have distinct strengths and weaknesses depending on spatial scale, extent, and differences in site-specific conditions such as water clarity and depth.

With the proliferation of remote sensing techniques delivering spatial data representing seagrass landscapes, efforts to locate, quantify, and monitor the distribution of seagrasses have increased, offering many potential benefits for the management and understanding of these valuable habitats (Bell et al. 2006). However, many of these efforts have been hampered from a lack of integration between the disciplines of landscape ecology, spatial statistics, and remote sensing (Newton et al. 2009). Further investigation of landscape pattern through the lens of remote sensing holds much promise for elucidating the causes and consequences of heterogeneity in seagrass habitats and the marine environment.

1.4 Objectives and Outline

Scientific investigations of spatial ecology are rapidly evolving, driven in part by improvements in remote sensing and computing. Researchers now have greater access to high-resolution, broad extent spatial data than ever before, opening new avenues for studying spatial patterns at both very fine and very broad scales. These advances have highlighted the need for new and adapted statistical techniques and metrics for analyzing ecological patterns, particularly for the marine environment (Sleeman et al. 2005, Bell et al. 2006). Analysis of marine landscapes requires input from multiple disciplines including oceanography, biology, ecology, geography, geomatics, remote sensing, and statistics. Increasing collaboration among these fields promises to fuel new advances to benefit the management of coastal and marine landscapes (Newton et al. 2009, Boström et al. 2011).

Improved analysis of spatial pattern in seagrass habitat benefits conservation and management through multiple pathways. Knowledge of the amount of disturbance that can be accommodated by seagrass habitat would be beneficial for the evaluation of coastal development and habitat restoration projects (e.g., recovery potential). Knowledge of the spatial and temporal variability of seagrass habitat is also a necessary prerequisite for monitoring and change detection. Crucially, understanding of spatial scale and its effects on seagrass mapping and monitoring requires further attention. Knowledge of characteristic scales of patterning is necessary for estimating the uncertainty of remote sensing data and derived map products that are regularly used for management decisions, and for the sampling design of monitoring and other ecological investigations. Spatial scale takes on added importance with the increasing prevalence of high-resolution remote-sensing data allowing greater freedom in the spatial resolution of data and study design, and raising questions about comparisons with datasets derived from older methods. The selection of spatial scale has great implications, and should be undertaken with consideration of the ecological relevance for the intended application.

This thesis addresses the spatial arrangement of seagrass habitat through a combination of field data collection and spatial analysis. The works contained herein represent original and novel applications of spatial analysis to seagrasses and coastal marine habitats. Data for this thesis were collected from two study sites in Atlantic Canada: Richibucto, New Brunswick and Eastern Passage, Nova Scotia. Chapters 2-4 of this thesis are structured as stand-alone manuscripts, followed by a summary of findings and conclusions in Chapter 5. Additional technical details not included in the body of the document can be found in the Appendix.

Chapter 2, “Detecting hot and cold spots in a seagrass landscape using local indicators of spatial association”, examines the spatial structure of seagrass habitat at a study site in Richibucto, New Brunswick, Canada, through the analysis of single-beam acoustic data. Local spatial statistics (Getis-Ord G_i^*) and geostatistics are applied to extract spatial information from the acoustic dataset, with a multi-scale approach unique to acoustic seagrass habitat mapping. This approach allows for the quantification of pattern and the detection of boundaries in a spatially continuous seagrass bed. This chapter was recently published in the journal *Landscape Ecology* (Barrell & Grant 2013). All of the data collection, analysis, and writing was performed by the author of this thesis, with guidance and editing provided by the coauthor.

Chapter 3, “Evaluating the accuracy of seagrass landscape mapping through comparison of acoustic and satellite remote sensing data”, examines two seagrass beds in the same estuary as the previous chapter using a combination of acoustic and satellite remote sensing data. This paper compares the spatial representations produced by each dataset, contrasting their results to characterize the effects of remote sensing on map accuracy. For this chapter, the classified satellite image was obtained from colleagues at Environment Canada / Canadian Wildlife Service (Mahoney & Hanson 2007). All other data analysis and writing was performed by the author of this thesis. This paper is currently in preparation and will be submitted for publication in the near future.

Chapter 4, “Use of high-resolution low-altitude aerial photography for the characterization of eelgrass (*Zostera marina* L.) and blue mussel (*Mytilus edulis* L.) landscape structure at multiple spatial scales”, focuses on a multi-species biogenic landscape located at Eastern Passage, Nova Scotia, Canada. Aerial photography

encompassing the landscape was gathered from a helium balloon-mounted digital camera platform and analyzed using several landscape pattern metrics. This method allows for the collection of very high resolution data, aiding in the calculation and tracking of spatial landscape metrics through time. All data collection, analysis, and writing was done by the author of this thesis, with guidance and editing provided by the coauthor. This manuscript is currently under review.

Chapter 2. Detecting Hot and Cold Spots in a Seagrass Landscape Using Local Indicators of Spatial Association²

2.1 Introduction

Seagrasses are widely recognized as important features of coastal areas, acting as ecosystem engineers and providing a suite of ecosystem services that ranks among the most valuable worldwide (Costanza et al. 1997, Barbier et al. 2011). They provide a significant source of primary production, influence hydrodynamic and sedimentary regimes, regulate nutrient cycling, and provide habitat and substrate for a variety of species (Orth et al. 2006). They are also sensitive to environmental change and disturbance, with extensive declines reported globally resulting from stressors acting over multiple spatial and temporal scales (Waycott et al. 2009). In particular, seagrasses are vulnerable to direct physical disturbance and declining water quality resulting from watershed and coastal development. Despite recognition of the threats to seagrass ecosystems, conservation efforts have been limited by a lack of knowledge regarding their present extent and the ecological processes regulating their spatial distribution (Duarte 2002). Given the ecological importance of seagrass habitat, there is a strong need for methods to characterize and monitor its distribution, and to assess and predict the potential impacts of changing environmental conditions in coastal ecosystems.

² This chapter is a manuscript version of a paper published as: Barrell J, Grant J (2013) Detecting hot and cold spots in a seagrass landscape using local indicators of spatial association. *Landscape Ecology* 28:2005-2018. The final publication is available at Springer via <http://dx.doi.org/10.1007/s10980-013-9937-2>

Seagrasses form habitat mosaic patterns of varying configurations ranging from highly fragmented to continuous meadows over a continuum of spatial scales (Duarte et al. 2006). Their spatial arrangement can be expressed through the conceptual framework of landscape ecology, where a simplified landscape consists of a heterogeneous mosaic of seagrass patches embedded in a background matrix of unvegetated soft sediments (Robbins & Bell 1994, Turner et al. 2001). The landscape ecology framework commonly involves the use of quantitative spatial pattern metrics or indices to quantify important aspects of habitat spatial pattern such as patch size, shape, configuration, and composition (O'Neill et al. 1988). Though the extension of these techniques to the marine realm has been limited by difficulties in acquiring and processing data, recent advances in remote sensing technology and geographic information systems (GIS) have increased the ability of researchers to acquire spatially explicit data and apply quantitative spatial analyses to marine ecosystems (Hinchey et al. 2008, Boström et al. 2011).

The application of landscape analysis techniques to seagrass ecosystems is a recent occurrence (Robbins & Bell 1994), and it is as yet unknown which data models and statistical techniques best represent the spatial structure of seagrass landscapes (Sleeman et al. 2005, Bell et al. 2006). Recent reviews have highlighted the need for further research on seagrass landscapes from both theoretical and practical perspectives, particularly regarding its use for the assessment and monitoring of landscape change (Boström et al. 2011, Wedding et al. 2011). Beyond the marine context, the application of landscape ecology methods with ever-improving remote sensing platforms and

consideration of associated uncertainty and errors remains an active area of research (Wu & Hobbs 2002).

Data representing seagrass patch structure are primarily drawn from aircraft or satellite-based optical sensors (McKenzie et al. 2001, Dekker et al. 2006). These methods are relatively inexpensive compared to direct sampling and provide synoptic coverage and high-resolution data. However, aerial methods are influenced by water clarity and weather conditions, require extensive ground-truthing, and create binary or categorical maps of seagrass presence-absence that can be strongly affected by spatial scale and classification bias (Wagner & Fortin 2005). These categorical representations of landscape structure, consistent with the “patch-mosaic” or “patch-matrix” landscape models derived from island biogeography (MacArthur & Wilson 1967, Wedding et al. 2011), apply well to fragmented seagrass beds showing distinct patch structure and unambiguous boundaries. However, seagrasses often grow in what appears to be continuous coverage as designated by optical remote sensing. Meaningful within-patch spatial patterns exist in these areas that are difficult to resolve accurately using standard optical methods, particularly in turbid waters. In these cases, the patch-matrix model of landscape structure may be inappropriate, necessitating a different model for the depiction of landscape structure in continuous seagrass beds.

Hydroacoustic methods are an alternative approach for mapping seagrass spatial structure at a scale intermediate to direct physical sampling and optical remote sensing. Single-beam sonar has been shown in several studies to provide an effective, sensitive, and repeatable mapping technique for several species of aquatic macrophytes in both freshwater and marine systems (Sabol et al. 2002, Sabol et al. 2009). Aquatic vegetation

exhibits strong acoustic reflectivity due to the presence of oxygen and other dissolved gases present in plant tissues; this effect is particularly strong with seagrasses due to the presence of oxygen-filled lacunae (Sabol et al. 2002, Warren & Peterson 2007, Paul et al. 2011). This signature can be extracted from acoustic data to provide the high-resolution broad-extent data required for landscape analysis. Though acoustic methods can also be negatively impacted by some weather conditions (e.g. waves), these effects are minimal compared to aerial methods, and water clarity is not a limiting factor in the shallow waters preferred by seagrasses. Acoustic data can be acquired without the extensive labor required for direct sampling and without the high costs and operational constraints of aerial optical methods. Single-beam sonar can also provide accurate measures of water depth, canopy height, and percent cover, going beyond binary measures of presence-absence and improving the thematic resolution of output maps.

Despite the apparent advantages of acoustic techniques, quantitative studies of seagrass landscape structure using acoustic data are rare or nonexistent. Previous studies examining seagrass with single-beam sonar have focused on the production of maps through contouring or geostatistical interpolation procedures such as kriging (e.g. Guan et al. 1999, Valley et al. 2005). These maps provide synoptic broad-scale depiction of the seagrass bed, though the interpolation process tends to smooth the data, underestimating the spatial variability inherent in the landscape, particularly in patchy environments (Fortin & Dale 2005). These interpolated maps are often unable to delineate distinct patch boundaries, and as such are unable to provide data suitable for the application of many patch-focused indices common in terrestrial landscape ecology. The ability of acoustic methods to measure percent cover of aquatic vegetation at high resolution and

broad extent in turbid coastal waters should allow for the detection of heterogeneity and patch structure at a scale inaccessible to aerial methods. Nonetheless, this capability has not yet been demonstrated in the literature.

A variety of methods for the analysis of ecological spatial structure have been developed, each with specific goals and assumptions (Fortin & Dale 2005). Global spatial statistics (e.g. Moran's I , Geary's c) and related geostatistical methods such as variography and kriging are commonly applied techniques that estimate spatial autocorrelation over the entire study area. While useful in many systems, these approaches fail to capture local patterns by summing and averaging variability in the dataset as a function of distance without consideration of location (Fortin & Dale 2005). In most naturally occurring landscapes where several processes interact to create apparent structure, it is likely that the magnitude of each process varies over the study area resulting in distinct areas or patches (Legendre & Legendre 1998). These processes commonly occur over a wide range of spatial scales and interact non-linearly, complicating the interpretation of ecological relationships. Furthermore, these interactions violate the assumption of stationarity required for global measures of spatial autocorrelation, including assessment of significance.

In contrast to global measures, local spatial statistics are applied to examine local patterns in the intensity of spatial dependence. This group of methods (e.g. local Moran's I , local Geary's c , Getis-Ord G_i and G_i^*) are commonly referred to as local indicators of spatial association, or LISA (Anselin 1995). These statistics can be used to locate clusters of similar values higher or lower than the mean that represent local patterns of spatial dependence, commonly termed "hot spots" and "cold spots" respectively (Nelson

& Boots 2008). As a tool for exploratory spatial data analysis, these operators can be calculated at multiple local neighborhood sizes in order to assess the scale-dependence of detected patterns. Local spatial statistics have previously been applied to the quantification of terrestrial patterns derived from aerial remote sensing (Wulder & Boots 1998), the mapping of patterns in marine sediments (Harris & Stokesbury 2010), and detection of patch boundaries in simulated datasets (Philibert et al. 2008), but have not previously been applied to seagrass ecosystems.

The purpose of this study was to utilize remote sensing techniques with local spatial statistics to develop methods appropriate for detecting patch structure at a scale relevant to an estuarine seagrass bed. Single-beam acoustic data representing the seagrass landscape were collected, processed, and analyzed with the Getis-Ord G_i^* LISA statistic (Getis & Ord 1992). These clusters were then used to quantify localized patches of high and low cover and produce spatial maps of their distribution. This approach is intended to facilitate the assessment, monitoring, and management of these ecologically valuable and vulnerable ecosystems.

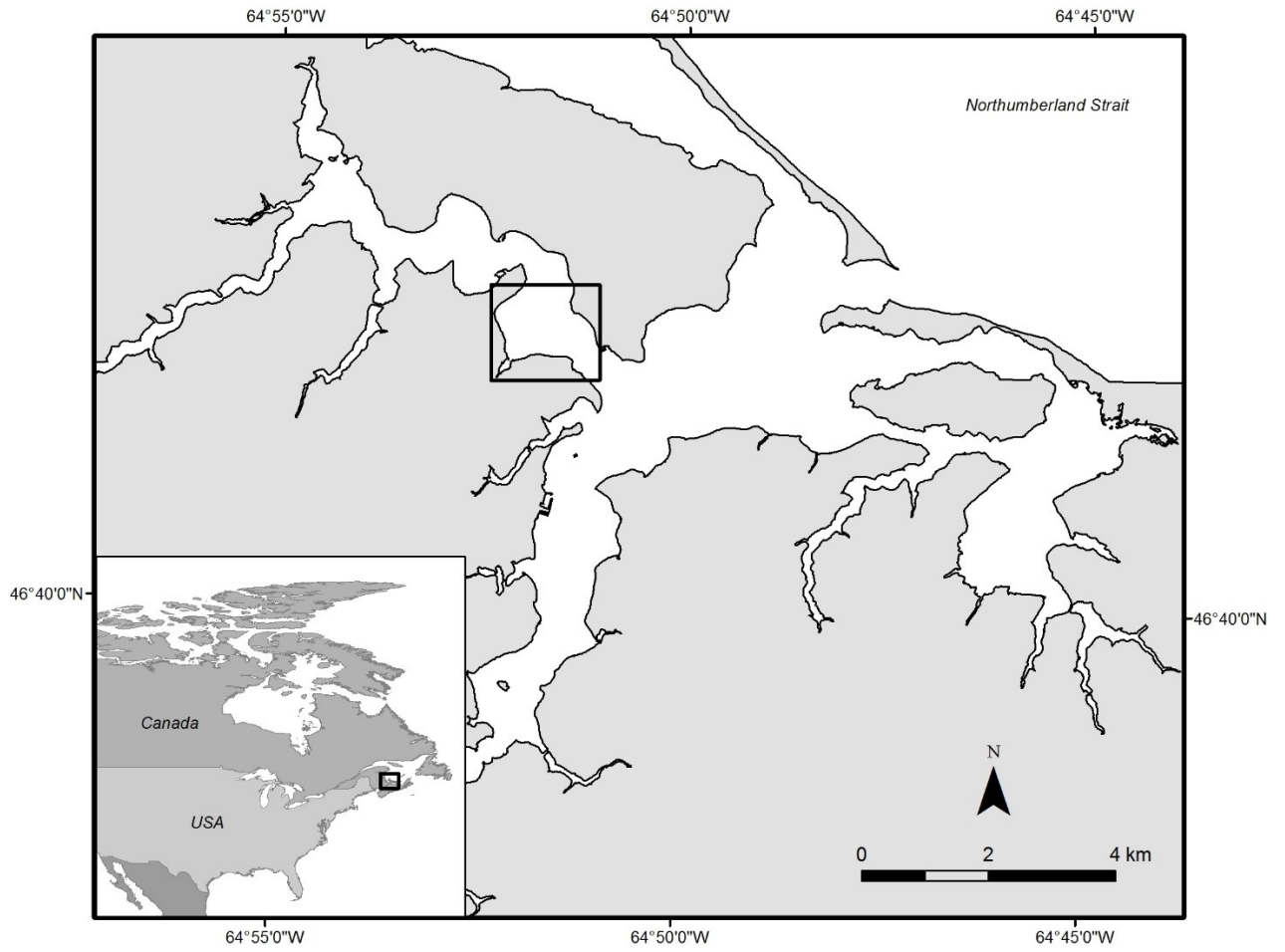


Figure 2-1. Map of the Richibucto estuary with the primary study location highlighted. (Inset) Location in eastern Canada.

2.2 Methods

2.2.1 Study Site and Acoustic Survey

The Richibucto estuary is located on the eastern coast of New Brunswick, Canada in the southern Gulf of St. Lawrence (64°51' W, 46°42' N)(Figure 2-1). It is a semi-enclosed barrier island system that is similar in characteristics to several other estuaries along the New Brunswick Gulf coastline. The estuary is fed by the Richibucto, Aldouane, and St. Charles Rivers, representing a primarily suburban, agricultural, and forested watershed. Oyster and mussel aquaculture occurs in moderate densities throughout the estuary.

The study site was located in a basin of the northwestern branch of the estuary, characterized by depths of 1-2 m outside of a narrow channel that reaches up to 7 m in depth. Tidal range at the site is approximately 1-2 m (Guyondet et al. 2005). A large peninsula that is part of the adjacent Kouchibouguac National Park shelters the study site from most wind-generated wave action. Eelgrass (*Zostera marina*) occurs subtidally throughout the estuary (excepting the channel), and areas where eelgrass is absent occur as bare sediment. The sediments consist mostly of muddy sand with relatively uniform grain size (Lu et al. 2008).

Acoustic data were collected using a vertically-oriented 430 kHz 6.2° beam angle transducer and BioSonics DE-X echosounder mounted on a small vessel. This high-frequency acoustic system is optimal for detecting aquatic vegetation with high accuracy (Sabot et al. 2002). The narrow beam angle results in a small footprint size, balancing resolution and spatial coverage along the sampled transect. Given the 6.2° beam angle, the circular footprint of a single ping at 1 m depth has a diameter of 11 cm (0.01 m²). To

avoid sonic saturation due to shallow depth, a power-reduction setting of -8.8 dB and pulse duration of 0.1 ms were used. The echosounder system generated acoustic pings at a rate of 5 Hz. All acoustic data were georeferenced with a JRC differential GPS (DGPS) with positional accuracy of approximately 3 m recording positions at a frequency of 1 Hz. The receiver was linked to DGPS reference station 332 in Port Escuminac, New Brunswick (64° 48' W, 47° 04' N).

The acoustic survey was conducted on 10 October 2007 at high tide in calm conditions. Data were collected on transects separated by 30-50 m where possible. The survey vessel was kept at a constant speed of 2 m s⁻¹ (7.2 km h⁻¹) to minimize noise and disruptive cavitation around the transducer face and to maintain consistent spatial coverage. Ground-truthing data for verification were collected with an underwater video camera deployed at several locations throughout the study site. The camera was used to observe the seafloor directly below the transducer for seagrass presence/absence and later compared to ping output reports for verification.

2.2.2 Data Processing and Analysis

Characteristics of the seagrass bed were extracted from raw acoustic data using BioSonics EcoSAV v1.2 software. The software is based on a heuristic algorithm designed by the US Army Corps of Engineers to extract distinctive features from each acoustic ping to determine the water depth, canopy height, and presence or absence of seagrass (Sabot et al. 2002). These values are then summarized for a collection of sequential pings and output as report points. Each output point contains measures of the percent cover of vegetation ('plant' pings divided by total pings per cycle), mean canopy

height for ‘plant’ pings, and mean water depth. The accuracy of the algorithm has been independently tested and verified for several species of macrophytes in diverse environments (Guan et al. 1999, Sabol et al. 2002, Valley et al. 2005).

The analysis procedure georeferences the acoustic data by summarizing all pings between two DGPS positions. With DGPS positions recorded at 1 Hz and a ping rate of 5 Hz, this results in one report every 2 seconds. Through the course of analysis it was observed that this would result in uneven ping counts per report point due to a slight offset between the ping rate and GPS time. The software settings were therefore adjusted in order to ensure that each report represented a consistent spatial data support of 15 pings. This provides a balance between consistent spatial coverage for each point and maximum geospatial accuracy. Minor adjustments were also made to the default analysis settings to account for the power reduction setting and ambient temperature and salinity conditions. To streamline data processing and prevent false detection of vegetation, a depth limit of 3 m was imposed, as no vegetation was observed below this depth in the study area.

Acoustic measurements of water depth and canopy height were corrected to account for changes in tidal height over the survey duration and the depth of the transducer face in the water column. The resulting data were output as XYZ comma-separated text files and converted into ESRI shapefile format for GIS analysis. The relationship between water depth and seagrass percent cover was explored using Pearson’s correlation.

Global spatial autocorrelation was assessed through the analysis of variograms using ArcGIS v10 (Geostatistical Analyst extension) and SpaceStat v2.1 software.

Variograms were modeled for a range of lag sizes to best represent the spatial structure of the site and the scale of sampling. Both isotropic and anisotropic variograms were examined to detect any directionality (anisotropy) in the dataset. A variogram map was created to provide a visual depiction of anisotropy in the landscape. The variogram map was constructed according to values derived from the variogram, with a lag size range of 2 - 200 m. Additionally, an interpolated map of percent cover was produced through ordinary kriging based on the isotropic variogram for visual comparison to Getis-Ord G_i^* results.

Local regions with percent cover values higher or lower than the overall mean were identified by calculating the Getis-Ord G_i^* statistic. G_i^* is a local spatial statistic that measures the ratio of the weighted local neighborhood sum to the overall dataset:

$$(Eq. 2-1) \quad G_i^*(d) = \frac{\sum_{j=1}^n W_{ij}(d)x_j}{\sum_{j=1}^n x_j}$$

Where d is neighborhood size, W_{ij} is the weight matrix of sample location i and its neighbor(s) j , and x is the quantitative variable of interest. The G_i^* statistic differs from the related Getis-Ord G_i in that the sample location itself (the ego) is included in each calculation ($i=j$). The equation produces a z-score where high values ($G_i^* \geq 2$) represent local clusters of high values relative to the whole area, also referred to as “hot spots”, while low values ($G_i^* \leq -2$) represent “cold spots”.

The neighborhood size and weights can be set to a constant search radius or can be variable to include the same number of neighbors in each calculation. The constant radius approach was taken in order to maintain consistent spatial resolution. The weight matrix W_{ij} was defined so that all points falling within the neighborhood radius distance were given an equal weight of one, while all points outside that radius were given a weight of zero. The G_i^* statistic was initially calculated for five neighborhood search radii (10, 20, 30, 40, and 50 m) in order to determine the optimal analysis scale and to visualize the effects of altering spatial scale on the statistic. Neighboring point weights were standardized within each search area. The expected value of G_i^* under the assumption of complete spatial randomness depends on the number of neighboring points, but has been shown to approximate a normal distribution when $n \geq 8$ neighbors (Ord & Getis 1995). The number of neighboring points within the search radius were tallied for each point in order to meet this criterion (i.e. the number of j around each i , for each of the 5 distance classes).

Significance testing was conducted through a Monte Carlo randomization procedure ($n = 999$ simulations) with a null hypothesis of complete spatial randomness. The Simes correction (Simes 1986) was applied to adjust p -values to account for multiple comparisons, as each sample location i is included in the neighborhood calculation for several neighboring points (Boots 2002). The Simes correction is less conservative than the similar Bonferroni procedure, allowing the detection of significance in the presence of highly correlated test statistics. Notably, there are difficulties associated with the assessment of statistical significance with the presence of multiple testing and global spatial autocorrelation. Accordingly, local spatial statistics were used in the context of

exploratory spatial data analysis as per suggestions in the literature (Boots 2002, Fortin & Dale 2005).

Formulation of seagrass patch polygons from punctual hot and cold spots was conducted with ArcGIS v10 software. Buffer rings of a size matching each neighborhood search radius were drawn around each statistically significant cluster location. Groups of buffer rings of the same class were merged into polygons representing a contiguous neighborhood zone for both hot and cold spots. Overlapping zones were identified to indicate boundaries or areas of rapid change between high and low seagrass cover. Data values of the points falling within these polygons were then compiled and summarized to describe the seagrass characteristics within each class of polygon.

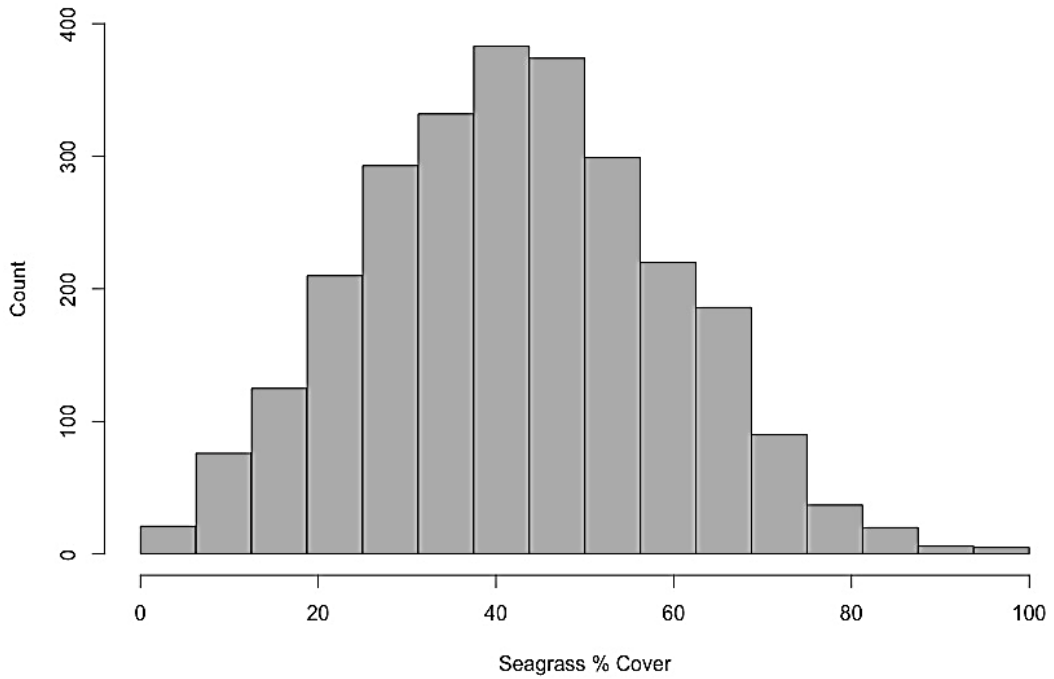
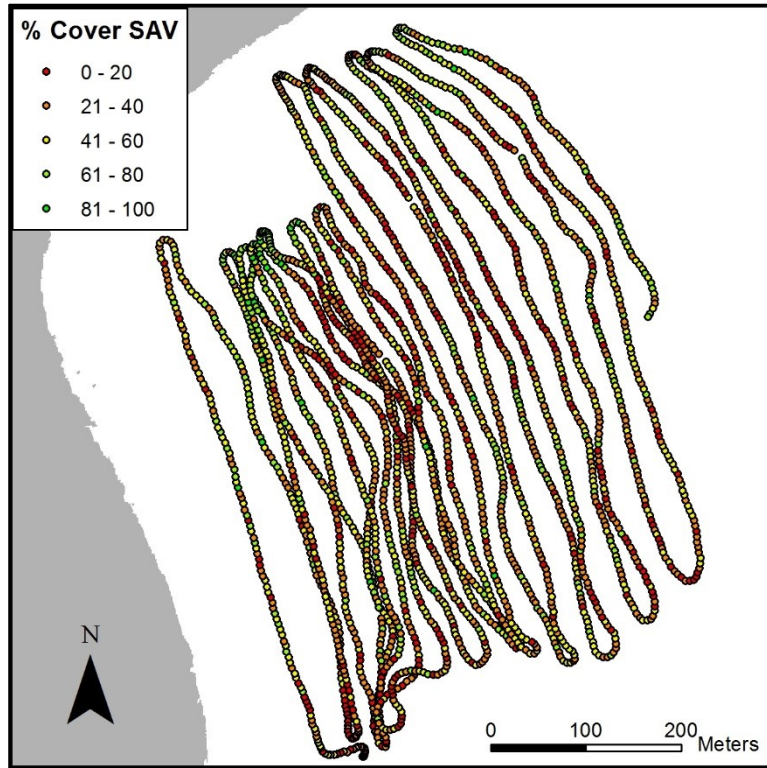


Figure 2-2. (Above) Acoustic data tracks, showing the distribution of percent cover values. (Below) Histogram of the distribution of percent cover values.

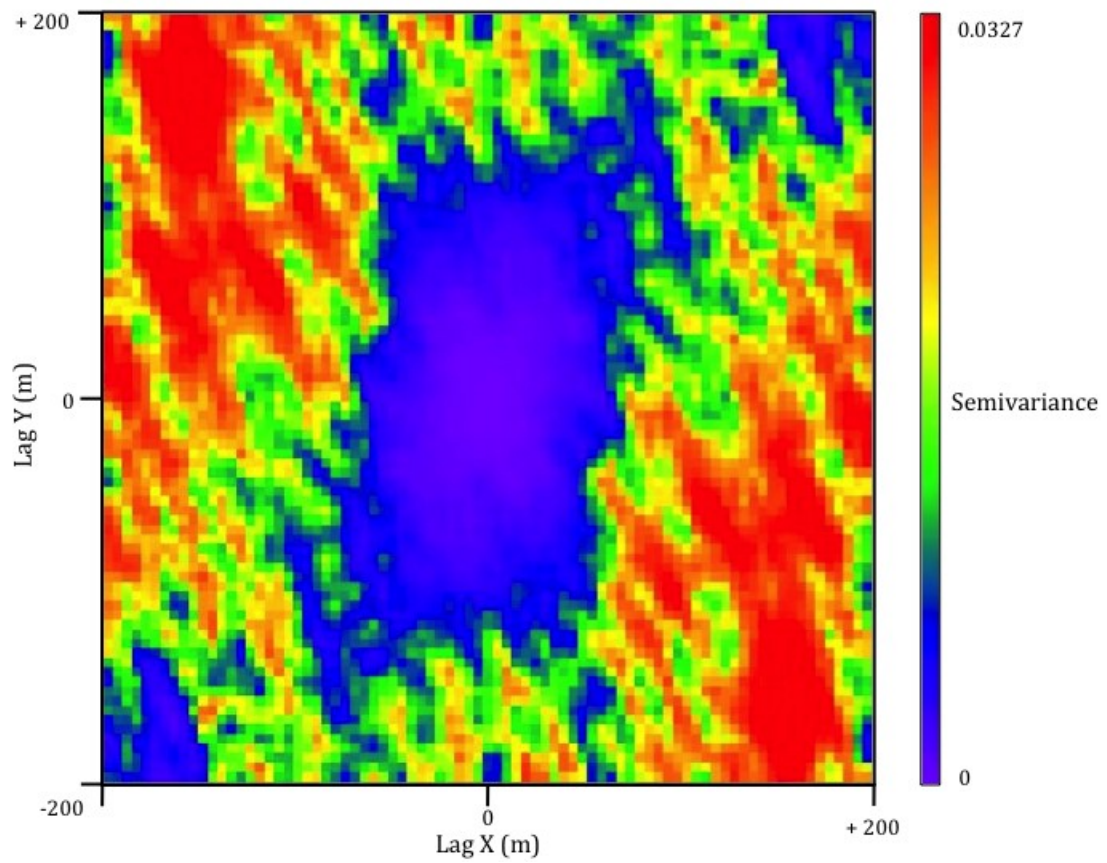


Figure 2-3. Variogram map depicting anisotropy in the dataset with a lag size range from 2 -200 m.

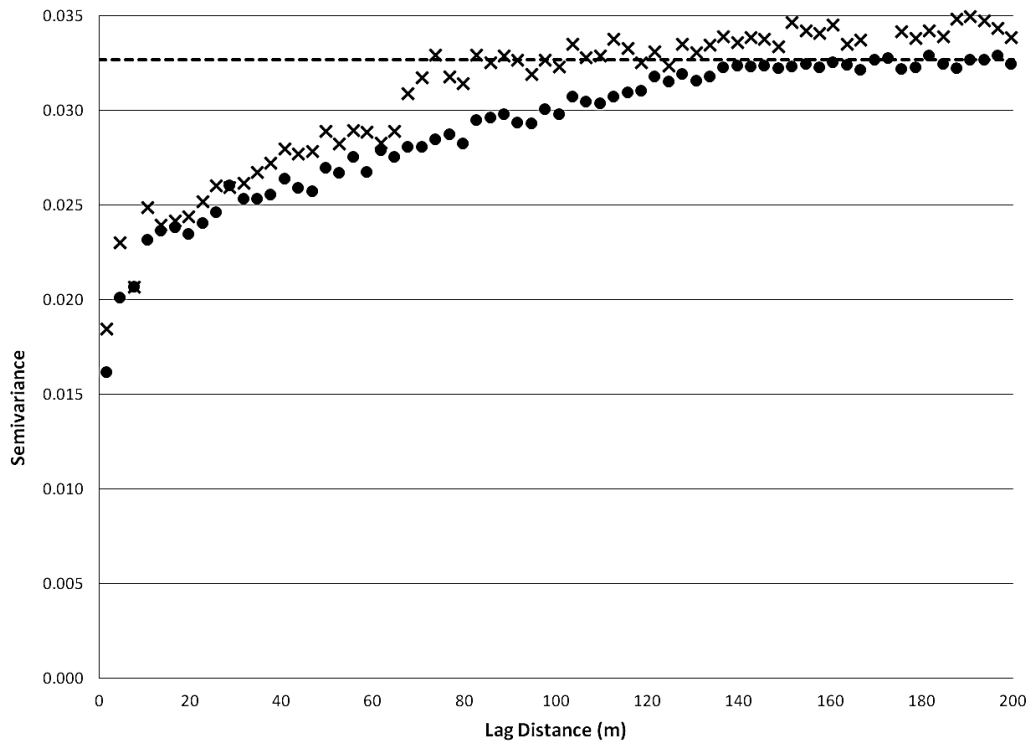
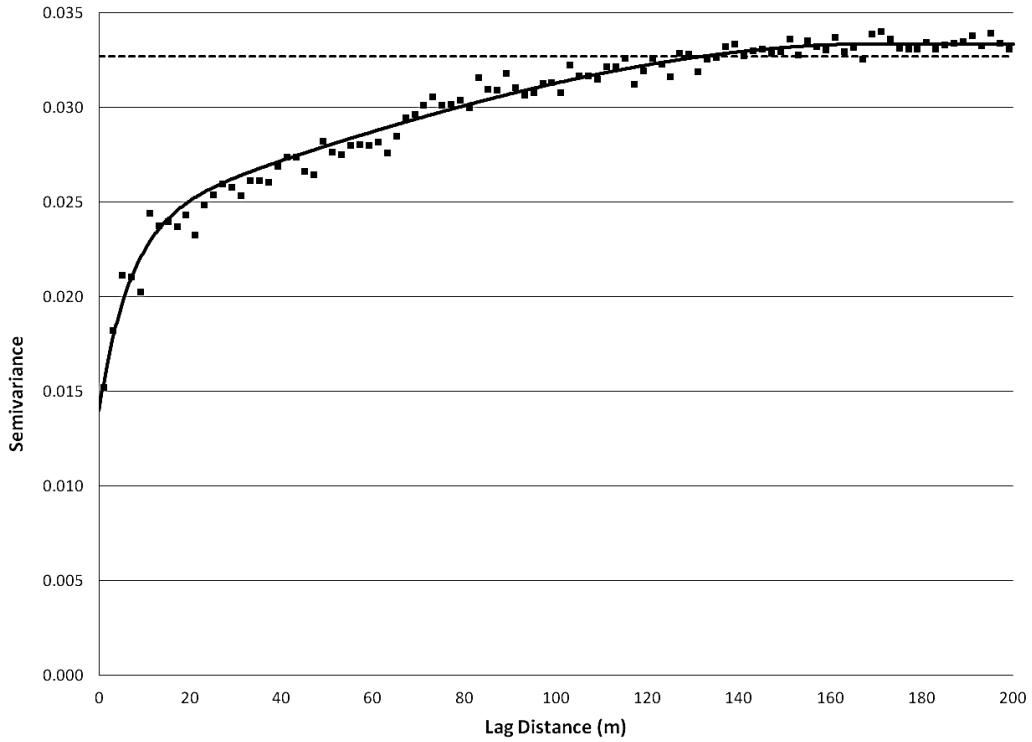


Figure 2-4. (Above) Modeled omnidirectional variogram. (Below) anisotropic empirical variograms representing the east-west (crosses) and north-south (points) axes.

2.3 Results

2.3.1 Acoustic Survey

The acoustic survey produced a total of 2677 output points over a total transect length of 14.7 km, sub-sampling an extent of 29.7 ha (Figure 2-2). Mean seagrass cover was $41.8 \pm 18.1\%$ (SD). The distribution of percent cover values was approximately normal. Notably, only 21/2677 points (<1%) registered a value of 0% cover, indicating that at least a small quantity of seagrass was present throughout nearly the entire study area. Water depth was relatively uniform with a mean depth of 1.39 ± 0.12 m (SD). No notable relationship was found between water depth and percent cover over the surveyed area (Pearson's $R = 0.124$). Compared to the ground-reference video data, the acoustic survey was 100% accurate in discriminating SAV from bare sediments (see Appendix A).

2.3.2 Geostatistical Analysis

Geostatistical procedures were initially used to assess spatial autocorrelation structure and anisotropy in the dataset. A variogram map was produced to graphically depict any directional trend indicating the presence of anisotropy in the dataset (Figure 2-3). The variogram map is a geometric representation of semivariance in the dataset, with directionality preserved so that each pixel represents the sum of all data pairs at that direction and distance from the center of the map. Minimum semivariance was found in approximately the north-south direction, indicating the presence of anisotropy. This was reflected in observed differences between the omnidirectional and anisotropic variograms (Figure 2-4).

The omnidirectional variogram of seagrass percent cover was modeled to show a range of 143 m, a sill equivalent to the variance of the dataset at 0.0327, and a nugget effect of 0.014 (42.8% of variance), representing measurement errors and any variation occurring at a spatial scale less than that of distance between sampling points (Figure 2-4). The bi-directional anisotropic variogram reflects the directionality visible in the variogram map, with the north-south axis curve exhibiting a smaller sill and shorter range than the east-west axis. This pattern is consistent with zonal anisotropy (Goovaerts 1997).

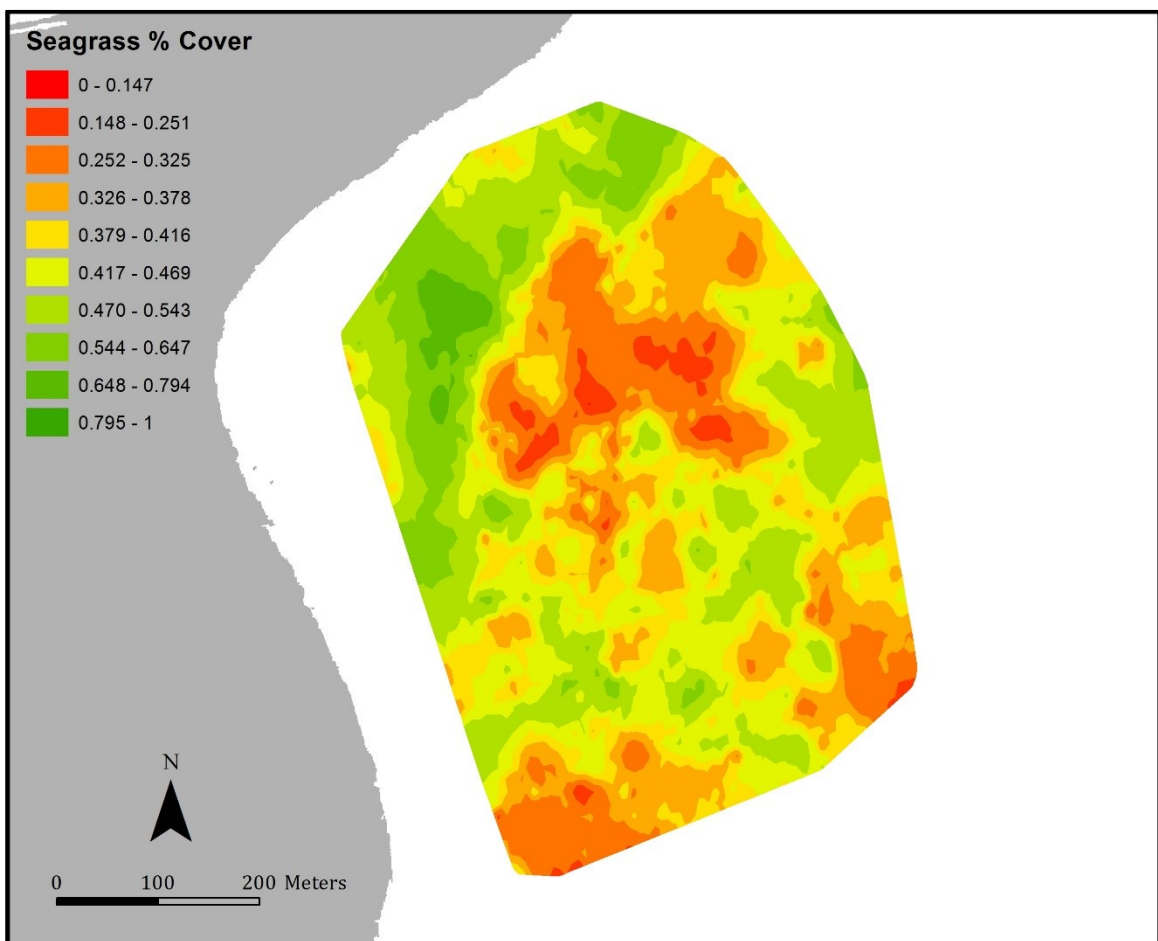


Figure 2-5. Map of seagrass percent cover interpolated using ordinary kriging.

The percent cover dataset was interpolated to produce a smoothed surface through ordinary kriging implemented with ArcGIS Geostatistical Analyst (Figure 2-5). The resulting map shows a contoured representation of seagrass cover within the study area. This map does not facilitate the application of patch-focused landscape analysis, as boundaries are not discernible. However, it is possible to see distinct patterns, and note that the anisotropy indicated through variography is likely due to locally clustered patches of high cover in the northwest corner of the study area and low cover throughout the central, southern and eastern regions.

Neighborhood radius	Mean # neighbors (minimum)	Significant hot spots (proportion total)	Significant cold spots (proportion total)
10 m	6.8 (3)	135 (0.05)	126 (0.05)
20 m	19.5 (7)	236 (0.09)	282 (0.11)
30 m	33.2 (9)	274 (0.10)	330 (0.12)
40 m	46.8 (13)	220 (0.08)	261 (0.10)
50 m	61 (17)	167 (0.06)	152 (0.06)

Table 2-1. Results of G_i^* at five search radii indicating the number and proportion of points identified as hot or cold spots, and the mean and minimum number of neighboring points found around each hot or cold spot.

2.3.3 *Local Spatial Statistics*

The Getis-Ord G_i^* statistic identified acoustic report points representing significant hot and cold spots, or regions of locally high and low mean percent cover respectively, at each of the five spatial scales examined. Between 10 – 22% of the dataset points ($n = 2677$) were identified as significant hot or cold spots at each scale

(Table 2-1). The largest number significant hot and cold spots were found at a search radius of 30 m.

The mean number of neighbors for each significant point (i.e. the number of j for each i) grew with increasing neighborhood radius (Table 2-1). At a search radius of 10 m, the mean number of neighbors was insufficient to meet the assumption of normality ($n \geq 8$) as recommended by Ord & Getis (1995). At a search radius of 20 m, the mean number of neighbors exceeded this threshold, but the minimum did not. Accordingly, subsequent analysis focused on the 30, 40, and 50 m neighborhood radius sizes to ensure that this assumption was treated consistently.

Neighborhood radius	Type	# Patches	Neighborhood count	Nbhd. mean % cover (St. Dev.)	Hot-cold difference
30 m	Hot spot	6	881	0.523 (0.167)	0.207
	Cold spot	4	892	0.316 (0.162)	
40 m	Hot spot	5	1103	0.499 (0.169)	0.16
	Cold spot	3	1095	0.339 (0.171)	
50 m	Hot spot	5	1187	0.486 (0.168)	0.138
	Cold spot	4	1013	0.348 (0.169)	

Table 2-2. Neighborhood values for the G_i^* analysis at each of 3 spatial scales along with average seagrass percent cover and the number of discrete “patches” formed via buffering procedures.

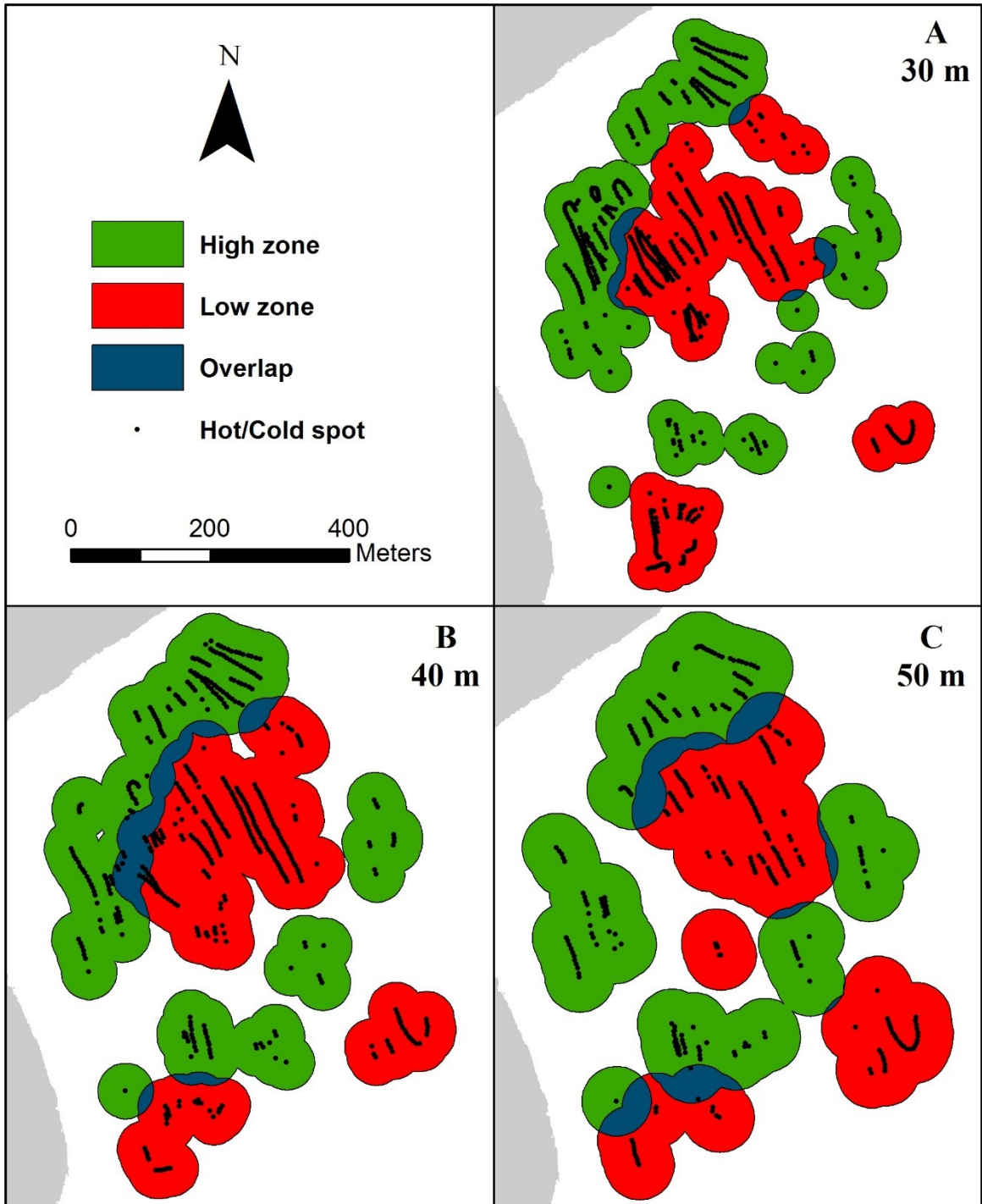


Figure 2-6. Zones of high and low seagrass cover as derived from G_i^* analysis for (A) 30 m, (B) 40 m, and (C) 50 m neighborhood search radii. Overlap zones are indicated in blue.

Neighborhood statistics indicated that percent cover in hot spots was consistently higher than in cold spots (Table 2-2). This difference decreased with increasing neighborhood size as the patches aggregated into larger areas and encompassed a larger number of neighboring points. The within-patch variance remained relatively uniform at each scale, and was smallest at the 30m neighborhood radius.

Patches representing contiguous neighborhoods of hot and cold spots at each spatial scale produced a visual pattern that was similar to the interpolated map, with a region of high percent cover in the northwest, a large central patch of low percent cover, and smaller variable patches throughout the remainder (Figure 2-6). This distributional pattern, and the total number of hot and cold patches, remained mostly consistent regardless of the neighborhood radius definition.

Zones of overlap occurred between the neighborhoods of hot and cold spots at each spatial scale. These regions correspond to areas of rapid change in seagrass cover that can be considered analogous to patch boundaries or ecotones. The amount of overlap area increased with neighborhood size. A small number of significant points fell within the overlap areas at two of the three analysis scales (15 points at 40 m scale; 2 points at 50 m scale). For these points, the neighborhood encompasses both hot and cold spots and likely indicates an especially sharp gradient of change. These points also may indicate that the neighborhood size is too large, suggesting that the optimal spatial scale for detecting pattern is less than 40 meters.

2.4 Discussion

2.4.1 G_i^* Considerations

The use of local spatial statistics in this study provided information on local spatial heterogeneity not captured at the scales commonly used for monitoring, and explicitly described pattern at multiple spatial scales as defined by the neighborhood search radius. Of the three spatial scales considered, the 30 m neighborhood radius appears to best characterize the local variability within the study area (Figure 2-6a). Analysis at this scale detected the largest proportion of significant hot and cold spots, represented the largest difference in neighborhood percent cover (52.3% in hot spots vs. 31.6% in cold spots), and resulted in the lowest within-patch variance. This scale also produced the smallest area of overlap between hot and cold neighborhoods, and resulted in no significant points occurring in overlap zones. However, all three spatial scales produced maps with similar numbers and distributional patterns of hot and cold spots, highlighting the robust nature of the technique.

When conducting multi-scale analysis, it is important to differentiate between scales of observation and analysis (Qi & Wu 2004). The scale of observation can be adjusted through manipulating the spacing and orientation of survey tracks, boat speed, or software data collection settings. In contrast, the analysis scale can be adjusted by changing the neighborhood size when calculating G_i^* . The interaction between observation scale (i.e. transect spacing) and analysis scale (neighborhood radius) in seagrass beds is not well understood, as site-specific factors can result in variation over very short distances.

Global measures of spatial association generally require assumptions and prior knowledge of habitat structure that is often unavailable prior to study design. Further, it is often not possible to determine a single ‘correct’ scale when the magnitude and directionality of variation changes over relatively small extents, as in this study (i.e., Figure 2-3). A major strength of the LISA approach is the ability to detect localized patterns and define characteristic scales of variation in complex systems without prior knowledge of habitat structure. This allows the detection of distinct regions regardless of spatial scale without requiring the assumptions of global methods, and broadens the applicability of the method to many different types of seagrass beds.

Analysis of the proximity of high and low clusters detected by local spatial statistics can provide information on the locations of boundaries separating distinct within-patch regimes. Areas of overlap in the neighborhoods around high and low cluster points may be of particular interest, indicating zones of rapid change in seagrass cover (Figure 2-6). These areas may be considered analogous to boundaries between distinct regions, or ecotones: transitional zones between ecological communities (Hufkens et al. 2009). The detection and analysis of boundaries is an important part of landscape ecology, and has been widely applied in terrestrial systems. In the context of aquatic vegetation, prior research has focused on how boundaries affect fauna, particularly in patchy areas with clearly defined boundaries. In contrast, the overlap areas detected in this study represent 2D boundary zones between distinct areas within an extent of mostly continuous seagrass cover. Boundary characteristics such as width, magnitude of change, position, and orientation could be quantified and studied in the landscape context. Better

understanding of how to detect and analyze boundaries in seagrass habitat has previously been recognized as an important area of future research (Bell et al. 2006).

In a few instances, a small number of hot or cold spots were found within overlapping boundary areas (Figure 2-6). This most likely indicates an especially sharp gradient of change; for these hot and cold spots, adjacent neighborhoods are determined to be significantly dissimilar despite sharing a large number of data points between both ‘hot’ and ‘cold’ neighborhood zones. The presence of overlap implies that the analysis scale (neighborhood radius) is too large to detect structure in these areas. Depending on the sharpness of the boundary, these areas may or may not have been detected with aerial imaging.

Notably, hot and cold spots are defined according to the structure of the sampled area, as they are calculated relative to the site mean. Accordingly, the interpretation of “hot” and “cold” is site-specific and requires additional contextual considerations when comparing disparate locations. For example, a cold spot in a highly fragmented or patchy bed may contain little to no seagrass, while in a dense continuous meadow an area identified as “cold” may still contain substantial plant biomass, though at a level below the site mean.

2.4.2 Implications for Landscape Analysis

The ability to detect and quantify landscape pattern is strongly influenced by the spatial scales of mapping and analysis relative to the features of interest (Wiens 1989, Wedding et al. 2011). Landscape indices are highly sensitive to scale and are at risk for scale mismatch, where landscape elements can be obscured or misrepresented if

examined at an inappropriate scale (Qi & Wu 2004). Recognition of these issues and analysis of the associated errors and uncertainties is crucial when applying the results of landscape analysis.

While many landscape studies of seagrass ecosystems have attempted to quantify spatial patterns of patch structure, these have been primarily based on categorical thematic maps derived from aerial remote sensing data (Wedding et al. 2011). The analysis of aerial imagery has long been the standard method for mapping aquatic macrophytes, offering a relatively low-cost and repeatable method for surveying large areas (McKenzie et al. 2001). However, the classification of aerial imagery of marine environments is fraught with uncertainty, and errors can propagate through to the results of landscape analyses (Shao & Wu 2008). Aerial sensors can be negatively affected by weather conditions, and are subject to confounding effects from water depth and clarity that can be further exacerbated by classification bias. Although aerial photography and some satellite sensors are able to achieve sub-meter spatial resolution, these methods have limited thematic resolution, or ability to discern between different patch classes. In effect, image classification reduces the landscape to a binary map of seagrass presence/absence, potentially resulting in significant data loss and classification errors. The presence/absence threshold for detection of seagrass in a given pixel for is also unknown. These errors are often ignored or unreported despite the widespread use and increasing availability of remote sensing data of seagrass beds. Accordingly, issues associated with accuracy and unidentified error are recognized as a main research priority in the field of landscape ecology (Wu & Hobbs 2002).

Acoustic survey methods hold a major advantage over aerial remote sensing in their ability to quantify seagrass cover at and below the patch scale. Image analysis is able to achieve high accuracy when differentiating between gross vegetated and unvegetated areas, but is less able to detect transition zones or within-patch patterns. The use of local spatial statistics in conjunction with acoustic data in this study demonstrated a method for detecting clusters of anomalously high and low values in what would otherwise be classified as a patch or area of continuous cover, quantifying an aspect of seagrass spatial structure inaccessible to aerial remote sensing. These areas may be of particular interest to habitat managers, as the ability to detect within-patch changes prior to visually apparent fragmentation could be very valuable to conservation efforts. This approach also allows for the identification of areas of interest for future studies, as well as conservation and restoration efforts, such as local regions of exceptionally high or low cover, or boundary zones that may be of great importance for faunal interactions (Boström et al. 2006).

Most prior studies using single-beam sonar to map seagrasses have used the output to interpolate continuous broad-scale maps representing SAV distribution at landscape scale (e.g. Guan et al. 1999, Valley et al. 2005). These representations have proven useful for monitoring long-term change, but are much less effective for quantifying spatial structure at and below the patch level. Interpolation in these cases is used to predict or estimate seagrass cover in unsampled locations, and is by nature a smoothing process that overestimates low and underestimates high values. In contrast to these broad-scale mapping exercises, this study demonstrates the use of acoustic data to detect and quantify local spatial patterns at the patch level in a manner consistent with a

landscape model of heterogeneity. The quantification of characteristic scales of variability at the patch level is critical for monitoring the disturbance and fragmentation of valuable seagrass habitat. Patch scale has many important implications for both the persistence and loss-gain dynamics of seagrass itself (Fonseca et al. 2002, Duarte et al. 2006), and for the ecosystem services it provides to diverse faunal communities (Boström et al. 2006). The methods outlined here are able to detect changes in habitat distribution and configuration beyond simple loss and gain, adding a valuable extra dimension to the study and management of seagrasses and marine habitat in general.

Not all types of marine data are suitable for analysis within the dominant patch-matrix paradigm of landscape structure, where the landscape consists of a mosaic of discrete patches with clear boundaries dispersed throughout a background matrix. When boundaries are not readily apparent, such as in beds that appear continuous to remote sensing, it is difficult to apply common landscape metrics that utilize spatial patch characteristics such as area and perimeter. However, as this study demonstrated, there is still spatial structure in these areas that can be quantified to increase our understanding of seagrass structure and the mechanisms that create and maintain it. Although the patch-matrix model has proven to be of great value in diverse ecosystems both terrestrial and marine, it is unable to describe continuous variation without significant loss of information (McGarigal et al. 2009). Recent work has begun to describe ways of quantifying continuous heterogeneity outside of the patch-matrix paradigm, such as through surface metrics designed for 3D landscape patterns such as those found in topographical analysis (Hoechstetter et al. 2008, McGarigal et al. 2009). Although not pursued in the current study, acoustic seagrass detection can also measure the canopy

height of vegetation, providing further information on habitat structure and indicating the potential to extend analysis of within-patch variability to three dimensions (Sabot et al. 2002, Valley et al. 2005). This 3D approach may be particularly valuable for elucidating fine-scale patterns in habitat as experienced by fauna. Further modifications to the traditional landscape model, such as in the current study, serve to increase understanding of marine landscape dynamics in areas that do not neatly fit the common framework derived from terrestrial landscape ecology.

Seagrass maps derived from aerial remote sensing overlook local spatial heterogeneity through the process of boundary delineation and patch classification, leading to significant uncertainties and errors. In contrast, acoustic methods provide data at much finer resolution representing the quantitative variation of seagrass cover through space. Analysis of these data through methods such as those described in the present study allow for the quantification of continuous heterogeneity, improving the ability of researchers to describe real-world landscapes. This helps to merge the interrelated concepts of boundary and landscape analysis, allowing for further insights into seagrass landscape structure. Methods for the quantification of structure are required to fuse the continuous and discrete models of landscape structure and allow for comparisons between different sites and bed types (Wagner & Fortin 2005). Integration of diverse sectors of spatial analysis (e.g. landscape metrics, geostatistics, GIS, spatial modeling), will lead to greater understanding of the spatial dynamics of ecological landscapes.

2.4.3 *Conclusions*

The application of the Getis-Ord G_i^* LISA statistic to acoustic survey data detected distinct patterns in seagrass distribution within a continuous bed. These results demonstrate the ability of the technique to identify local zones of high or low seagrass cover relative to the mean and an improved way to extract spatial data through remote sensing of seagrass landscapes, especially in areas that would otherwise be described as “continuous”. Beyond maps of seagrass presence or absence, this method allows for the measurement of heterogeneity at multiple spatial scales, providing important information for the design of specific studies, such as the impacts of patch arrangement on faunal interactions (e.g., the use of habitat by slow-moving or sessile organisms such as bivalves vs. highly mobile fish), or the impacts of local vs. broad-scale stressors. This approach can help gain a better understanding of the factors and processes that govern seagrass patterns and persistence, with a mind to improving predictive abilities, restoration, and management decisions through statistical modeling or predictive vegetation mapping. Increased understanding of the scale-dependence of seagrass patterns will also assist in the comparisons among and between sites located in different geographic regions, and to deal with scaling issues associated with extrapolating trends from small-scale studies to larger extents.

The information produced through local spatial statistics can be used to help guide the spatial scale of future mapping and monitoring efforts. A fine-scale, small extent acoustic survey such as that conducted here could be used as an exploratory tool to determine the baseline spatial structure and characteristic patch size of a site prior to a more intensive mapping effort. Initial acoustic surveys could complement broad-scale

mapping and monitoring by identifying high-priority areas of high or low cover, and as ground-truthing or accuracy assessment for broad-scale aerial remote sensing methods. It also can describe fragmentation and other changes in the arrangement of seagrass throughout a study area that would not be reflected in simple measures of percent cover. These results can be used for the further application of landscape ecology concepts to seagrass habitat and the marine environment in general, and contribute to further understanding of the spatial dynamics of these ecosystems.

Chapter 3. Evaluating the Accuracy of Seagrass Landscape Mapping through Comparison of Acoustic and Satellite Remote Sensing Data

3.1 Introduction

Seagrass meadows are widely recognized for their valuable contributions to ecological function and provision of ecosystem services in coastal environments (Costanza et al. 1997). Seagrasses provide a significant source of primary production supporting a diverse assemblage of species. In Atlantic Canada, the seagrass species eelgrass (*Zostera marina* L.) acts as an ecosystem engineer (Jones et al. 1994) in the coastal zone by providing physical substrate as habitat for many species and by altering hydrodynamics, sedimentary conditions, and nutrient cycling where it occurs (Bradley & Stolt 2006, Berkenbusch & Rowden 2007, Chen et al. 2007, Vandermeulen 2009). In addition to their apparent ecological value, seagrasses are also sensitive to disturbance, with extensive declines reported worldwide attributed to both anthropogenic and natural causes such as coastal development and eutrophication (Orth et al. 2006, Waycott et al. 2009). As a result of their value and sensitivity, seagrasses are often used as indicators of ecosystem health and as a monitoring and assessment tool for the management and protection of coastal habitat (Dennison et al. 1993, Neckles et al. 2012). In Canada, eelgrass has been recognized as an ‘ecologically significant species’ (ESS) by the Department of Fisheries and Oceans (DFO 2009), and its sensitivity to stressors has been evaluated for inclusion in habitat management programs and policies (Vandermeulen 2005, Vandermeulen et al. 2006, DFO 2012).

Effective mapping and monitoring of seagrass ecosystems is recognized as a crucial component of the management and protection of coastal landscapes and the ecosystem services they provide (Duarte 2002, Bell et al. 2006, Neckles et al. 2012). Seagrasses naturally form habitat mosaic patterns of varying configurations ranging from highly fragmented to continuous meadows (Duarte et al. 2006). Their spatial arrangement can be expressed through the conceptual framework of landscape ecology, where a typical “landscape” consists of a heterogeneous mosaic of seagrass patches embedded in a background matrix of soft sediments (Robbins & Bell 1994, Turner et al. 2001). Increased recognition of the ecological value and vulnerability of seagrasses has led to a proliferation of studies investigating the landscape pattern of seagrass beds (Bell et al. 2006, Boström et al. 2011, Wedding et al. 2011).

Accurate maps representing the spatial distribution of seagrasses are a prerequisite for effective ecosystem monitoring (Neckles et al. 2012), change detection (Roelfsema et al. 2013), understanding species-environment relationships (Boström et al. 2006), and predictive modeling with respect to the processes that structure the landscape (Bell et al. 2006). However, many questions remain regarding the accuracy of mapping and the application of statistical tools and indices for seagrasses and marine landscapes in general (Sleeman et al. 2005, Bell et al. 2006, Wedding et al. 2011).

Maps of seagrass distribution are most commonly produced through the manual or automated classification of imagery drawn from aerial photography or satellite remote sensing (McKenzie et al. 2001, Dekker et al. 2006). Compared to direct sampling, remote sensing offers a cost-effective and repeatable approach providing high-resolution data with synoptic coverage. Aerial photography has been the primary source of seagrass

imagery for several decades, though satellite-based sensors are quickly becoming a major source of data at landscape or regional scales (Dekker et al. 2006). Recent improvements in the spatial and spectral resolution of satellite remote sensing platforms and declining costs have led to a growing number of studies using high-resolution satellite imagery for the detection and monitoring of seagrass habitat (e.g., Mumby & Edwards 2002, Fornes et al. 2006, Urbański et al. 2009, Knudby & Nordlund 2011).

Several studies have highlighted the need to account for sources of error when using remote-sensing data to map and quantify landscape pattern (Lunetta et al. 1991, Hess 1994, Li & Wu 2004, Shao & Wu 2008, Boyd & Foody 2011). Most studies of landscape pattern are conducted using maps derived from the classification of optical remote-sensing data, but the image classification procedure is subject to numerous errors that can propagate through landscape analysis (Shao & Wu 2008). Spatial scale (resolution & extent) has been shown to influence the results of landscape studies, creating uncertainty in the measurement of pattern and in any subsequent analysis (Turner et al. 1989, Wu & Hobbs 2002). Spatial resolution also affects the ability of remote-sensing to distinguish between landscape features (e.g., the smallest detectable patch is directly proportional to the pixel size) (Qi & Wu 1996). Landscape analysis focuses largely on patch/gap dynamics, necessitating accurate measures of the location and shape of patch boundaries. In some cases, sharp boundaries are relatively easy to delineate from aerial imagery. However, boundaries may be complex and difficult to capture through optical methods, and this difficulty is compounded if spatial resolution is too coarse (Arnot et al. 2004). This can contribute to classification errors, particularly in

fragmented seagrass meadows with many small patches, creating a large proportion of “mixed pixels” that are difficult to interpret (Fisher 1997).

Maps produced through image classification are also limited by their thematic resolution, defined as the number of categories or classes that they depict. In contrast to terrestrial applications, the absorption of light in seawater limits the amount of spectral information that can be used in classification of marine benthic habitats (Dekker et al. 2006), often resulting in binary maps of seagrass presence or absence, equivalent to a thematic resolution of only two categories. These maps are useful for the calculation of landscape metrics, but they reduce the landscape into discrete patch units that are assumed to be homogeneous with abrupt, “hard” boundaries. These sharp boundaries imply certainty or accuracy, though this is rarely evaluated or stated explicitly in mapping studies (Arnot et al. 2004, Philibert et al. 2008). The degree of uncertainty introduced through classification is a function of the spatial and thematic characteristics of the data and classification scheme, and could be expected to differ when considering beds with differing spatial patterns (Barrell & Grant 2013).

In contrast to optical methods, acoustic methods detect aquatic vegetation with pulses of sound from a boat-mounted transducer. Many acoustic sensors have been used to detect aquatic vegetation, including side-scan (e.g., Pasqualini et al. 1998) and single-beam sonars (e.g., Sabol et al. 2002, 2009). Acoustic methods are less affected by water clarity, and thus in many cases are more effective than optical methods for mapping seagrasses in turbid coastal waters. Acoustic methods are also able to detect aspects of spatial heterogeneity at local scales inaccessible to optical methods, while still covering a large extent relative to direct observation methods (Barrell & Grant 2013). Seagrass beds

have been studied at the bed-scale using acoustics in many contexts (Guan et al. 1999, Valley et al. 2005), but acoustic data does not readily lend itself to the formation of categorical maps, and thus has not been much explored in the context of landscape analysis.

Acoustic and aerial remote sensing measure fundamentally different aspects of seagrass landscape structure, and may offer value in different applications. Aerial remote-sensing data produce categorical maps with sharp boundaries well-suited for landscape analysis of discrete patches. In contrast, acoustic surveys produce continuous data representing seagrass percent cover (Sabol et al. 2002, 2009, Barrell & Grant 2013). The effects of the contrast between discrete and continuous data models on the accuracy of seagrass maps are not well understood. Though both aerial and acoustic remote sensing methods have been widely applied to the mapping of seagrasses, comparative studies are lacking.

In the field of remote sensing, map classification accuracy is commonly evaluated against reference data using an error matrix, also often referred to as a confusion matrix or contingency table (Congalton 1991, Congalton & Green 2009). In a typical error matrix (e.g., see Table 3-1), the predictions of the remote sensing classification are compared to reference data to identify agreement (true positives and true absences), errors of omission (false negatives), and errors of commission (false positives). Numerous metrics can then be derived from the error matrix for assessing map accuracy. Though reference data is often assumed to be error-free, this assumption is often violated, particularly when both the prediction and reference datasets are derived from different types remote sensing (Foody 2010). It is not currently known if acoustic data can be used

as reference data for satellite seagrass maps. Aside from the implications for accuracy assessment, there is potentially utility in using the error matrix to investigate the comparative performance of satellite and acoustic remote sensing of seagrass beds.

Although continuous acoustic percent cover data is itself valuable for detecting patterns in seagrass beds (e.g., Sabol et al. 2002, Barrell & Grant 2013), this output is not directly comparable to presence-absence maps produced by aerial remote sensing. Comparison requires the application of a decision threshold to classify the continuous acoustic dataset into binary format. This is analogous to converting probability of occurrence to presence-absence in species distribution modeling for evaluating model performance and prediction errors (Fielding & Bell 1997). There are many possible approaches to threshold selection, largely depending on the goals of the application. The threshold can be established subjectively, for example at an arbitrary value of 0.5, or can be selected to maximize summary statistics such as overall accuracy or kappa. Alternatively, the threshold can be selected to maximize the prediction success rate for either presences or absences, or so that presences and absences have an equal chance of being predicted correctly. Similarly, the use of receiver operating characteristic (ROC) curves represents another common approach for evaluating the performance of binary classification using information derived from the error matrix (Fielding & Bell 1997). Several recent studies have investigated the effects of threshold selection through multiple criteria with the goal of maximizing prediction accuracy as measured by metrics derived from the error matrix (Liu et al. 2005, Jiménez-Valverde & Lobo 2007, Freeman & Moisen 2008).

In this study, issues of accuracy in seagrass mapping were addressed through the comparison of thematic maps derived from satellite remote sensing with acoustic data. A map of seagrass distribution produced through classification of Quickbird satellite imagery was acquired from Environment Canada (Mahoney & Hanson 2007) and evaluated against independent acoustic survey data using an error matrix to identify differences between the two techniques. Multiple binary classification thresholds were examined with the following goals:

- 1) Estimate the accuracy of satellite remote sensing for seagrass mapping through comparison to acoustic data,
- 2) Compare the performance of satellite and acoustic classifications between seagrass beds with differing landscape structure, and
- 3) Assess the implications of thematic accuracy and uncertainty on studies of landscape pattern in the marine environment.

Despite their fundamental differences, acoustic and satellite remote sensing have been independently demonstrated to produce accurate maps of seagrasses in many contexts (Sabot et al. 2002, 2009, Mahoney & Hanson 2007, Barrell & Grant 2013). With respect to comparing remote sensing techniques, evaluating the effects of threshold selection on binary classification performance allowed insight into the differences between the two methods, and was not intended to identify the ‘best’ threshold for maximizing classification accuracy. Reducing the acoustic dataset to a binary representation inevitably results in some loss of data, and may result in a lack of

agreement between the satellite map and acoustic data. It therefore was expected that maps derived from satellite and acoustic remote sensing would exhibit a high degree of correlation, and any lack of agreement would result primarily from the binary classification of the continuous acoustic dataset. Other potential sources of disagreement include spatial uncertainty (i.e., georeferencing and GPS errors), classification errors, systematic errors related to the sensors, and environmental effects such as water clarity and the local composition of the seagrass community.

3.2 Methods

3.2.1 Study Site

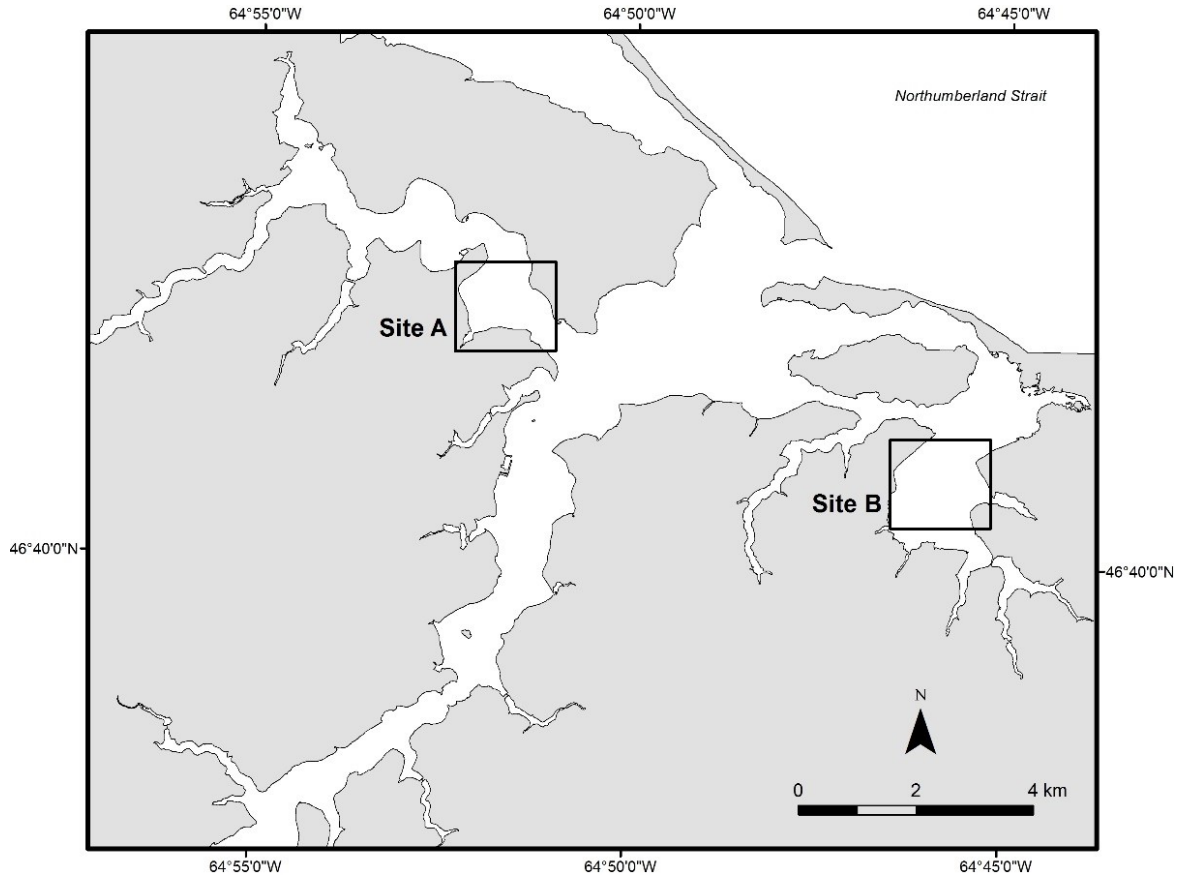


Figure 3-1. Map of the study locations Site A and Site B within the Richibucto estuary, New Brunswick, Canada.

The study was conducted in the Richibucto estuary, New Brunswick, Canada (64°51' W, 46°42' N) (Figure 3-1). The estuary consists of a semi-enclosed barrier island system similar in physical characteristics to several nearby estuaries along the Gulf of St. Lawrence coastline. Eelgrass occurs at varying densities in most areas with suitable

depth and substrate conditions. The estuary is fed by the Richibucto, Aldouane, and St. Charles Rivers, representing a mainly suburban, agricultural, and forested watershed. Aquaculture of the Eastern oyster (*Crassostrea virginica*) occurs in moderate densities at several locations within the estuary. The tidal range is approximately 1-2 m (Guyondet et al. 2005).

Focus was given to two locations within the estuary. Site A was located in a basin of the northwestern branch of the estuary (Figure 3-1). This basin is characterized by depths of 1-2 m outside of a narrow channel that reaches up to 7 m in depth. The land to the north of site A is part of Kouchibouguac National Park, and is used very infrequently outside of limited non-motorized recreational activities. A few small oyster and mussel aquaculture sites are located in this portion of this estuary. The eelgrass community at site A is widespread, ranging from high to intermediate density (Barrell & Grant 2013). Sediments in this area are mainly muddy sand with relatively uniform grain size (Lu et al. 2008).

Site B was located in a basin of the eastern part of the estuary locally referred to as Baie du Village (Figure 3-1). This area is on average slightly deeper than site A (~2-3 m) and does not have any significant riverine sources of freshwater input. Oyster and mussel aquaculture occurs in this part of the estuary at a higher density than at site A, and limited access to some areas for the acoustic survey. This area also contains a seafood processing plant with effluent feeding into the estuary.

3.2.2 *Image Acquisition and Classification*

The image acquisition and classification procedure of this research was performed by Matthew Mahoney and Al Hanson of Environment Canada/Canadian Wildlife Service as part of a collaboration with a Fisheries and Oceans working group on eelgrass mapping, of which the author is a participant (Mahoney & Hanson 2007). Only the final map product was used for comparison to acoustic data. Production of this map product is summarized below.

New Quickbird satellite imagery covering the full extent of the Richibucto estuary (70 km²) was acquired at low tide on 27 August 2007 (Mahoney & Hanson 2007). Both multispectral and panchromatic products were acquired. Multispectral imagery at 2.4 m spatial resolution consisted of four bands: blue (430-545 nm), green (466-620 nm), red (590-710 nm), and near-infrared (715-918 nm). The panchromatic image consisted of a single band (405-1053 nm) at 0.6 m spatial resolution. The raw multispectral and panchromatic images were combined through pan-sharpening to create a multispectral image with 0.6 m spatial resolution.

Prior to classification, dry land and the navigation channel were manually identified and excluded from further analysis with the assumption of eelgrass absence in these locations. The remainder of the image was segmented into distinct regions and classified using an object-based image analysis (OBIA) procedure with Definiens eCognition software into four categories: eelgrass present, eelgrass absent, aquaculture, and intertidal mudflat (see Mahoney et al. 2007). Only the categories of eelgrass presence and absence were considered for the present study, forming a binary classification of seagrass distribution throughout the Richibucto estuary.

Ground reference data for image classification were collected with a towed video camera survey conducted 2-5 July 2007, encompassing 8.82 hours of video over a total transect length of 33km (Vandermeulen 2013). Areas of dense cover and eelgrass absence were recorded over a 3m transect “window” of video with the goal of classifying for presence-absence; areas of intermediate cover were excluded. Ground reference points were then allocated with 60% used for training the OBIA algorithm and 40% reserved for the purposes of accuracy assessment.

3.2.3 Acoustic Survey and Analysis

Acoustic data representing seagrass landscape structure were collected using a BioSonics DE-X 430 kHz, 6.2° single beam sonar unit. Sites A and B were extensively sampled within the Richibucto estuary on 10-11 October 2007. All surveys were conducted during calm conditions within 2 hours of a low tide. Each survey was designed with tracks separated by approximately 30m where possible, while allowing for deviations around obstacles such as shoals and aquaculture gear. Vessel speed was kept constant at 7 km h⁻¹ to minimize noise and maintain consistent spatial resolution of the output data. Ping data were recorded at a rate of 5 Hz. Position was recorded using a JRC differential GPS (DGPS) receiver referenced to the Point Escuminac, New Brunswick DGPS beacon located at a distance of approximately 41 km (64° 48' W, 47° 04' N), achieving an estimated ≤ 2 m horizontal accuracy.

Characteristics of the seagrass habitat were extracted from raw ping data using the heuristic algorithm within BioSonics EcoSAV v1.2 software (Sabot et al. 2002). The

effectiveness of this method has been verified for diverse species of macrophytes in both fresh and salt water (Guan et al. 1999, Sabol et al. 2002, Valley et al. 2005, Sabol et al. 2009, Barrell & Grant 2013). The algorithm examines each individual ping and extracts information on seagrass presence/absence, canopy height (if present), and water depth. Successive pings are then summarized into one cycle of 10-15 pings and exported for analysis with geographic information systems (GIS) software. The resulting output points were separated by 4-6 m in the along-transect direction. For this study, focus was given to the output variable of percent cover, defined as the proportion of ‘plant’ pings divided by the total number of pings per cycle.

Some data points at site A were manually removed prior to analysis to account for the effect of crossing the channel. Additional manual editing was conducted to remove any points falling within aquaculture leases, and to remove extra points where boat was stationary.

3.2.4 Error Matrix and Threshold Formulation

Comparisons between the acoustic and optical datasets were performed using ArcGIS v10.1 software. Multiple presence/absence thresholds were applied to the continuous acoustic percent cover dataset for conversion to a binary classification scheme. Thresholds were established at increments of 10% cover from 0 - 100%, notated as $t_0 - t_{100}$. Percent cover values in the acoustic dataset at or below the threshold percent were assigned a value of “0” for absence, notated as A_0 , while all points at or above the threshold were assigned a value of “1” for presence (A_1). The acoustic output points

were then overlaid on the classified map and assigned values of either “2” or “4” for eelgrass presence (S_1) and absence (S_0), respectively. These acoustic and satellite values were then summed together to produce a unique integer value for each possible outcome. This procedure was then repeated for each threshold $t_0 - t_{100}$.

At each threshold, there were four possible outcomes in the comparison: 1) presence in both datasets (S_1A_1); 2) absence in both datasets (S_0A_0); 3) satellite presence and acoustic absence (S_1A_0); and 4) satellite absence with acoustic presence (S_0A_1). These outcomes are represented by the error matrix, depicting classification accuracy through comparison between observed ground reference data and the value predicted by remote sensing (Table 3-1). For this study, the acoustic dataset was effectively treated as ground reference data for the validation of predictions made by the classification scheme. In this context, S_1A_1 represents the true positives (TP) and S_0A_0 represents true negatives (TN) where both datasets agree; S_1A_0 represents the false positives (FP), also known as errors of commission; and S_0A_1 represents the false negatives (FN), or errors of omission. One error matrix was produced for each threshold value at both study sites.

Satellite classification (Prediction)	Acoustic data (Reference)	
	<i>Present</i>	<i>Absent</i>
<i>Present</i>	S_1A_1 (TP)	S_1A_0 (FP)
<i>Absent</i>	S_0A_1 (FN)	S_0A_0 (TN)

Table 3-1. Error matrix representing the possible outcomes in the comparison between acoustic and satellite datasets.

Various statistics and ratios can be derived from the error matrix, and details of these measures and their calculation are found in the relevant literature (e.g., Congalton & Green 2009). Emphasis was placed on trends in overall accuracy, prevalence, sensitivity, specificity, positive predictive value (PPV), and negative predictive value (NPV) (Table 3-2). It is useful to note that all of these metrics are highly correlated, as each is derived from some combination of the 4 possible outcomes of the error matrix (i.e., TP, TN, FP, FN).

Each statistic was calculated for both sites A and B at threshold values $t_0 - t_{100}$ and expressed as a proportion from 0 - 1. Due to the development of error matrix analysis in multiple fields (e.g., diagnostic testing, remote sensing, species distribution modelling), many terms are interrelated or used interchangeably, occasionally leading to confusion. In this study, the terminology generally follows that of diagnostic testing, forgoing the common terminology of remote sensing and cartography to focus on the statistical aspects of comparing two sensors with a binary classification scheme. For example, in the remote sensing literature, sensitivity and specificity are referred to as the “producer’s accuracy”, while NPV and PPV represent the “user’s accuracy” for their respective categories. In this study, the acoustic dataset is treated as the reference (or “ground-truth”) data, and the classified pixel value as a prediction, though it is generally acknowledged that some error is always present in reference data as well (Foody 2010).

The kappa statistic was also calculated in order to compare satellite and acoustic methods. Kappa corrects the estimate of overall accuracy by accounting for correlations occurring by random chance, and is commonly applied to remote sensing classifications

(Congalton 1991, Congalton & Green 2009). Kappa (κ) was calculated according to the following formula:

$$(Eq. 3-1) \quad \kappa = \frac{\left(\frac{TP+TN}{n}\right) - \left(\frac{(TP+FP)(TP+FN) + (FN+TN)(FP+TN)}{n^2}\right)}{1 - \frac{(TP+FP)(TP+FN) + (FN+TN)(FP+TN)}{n^2}}$$

Where n represents the total number of samples and TP, FP, TN, and FN represent true positives, false positives, true negatives, and false negatives, respectively (Table 3-1). Kappa estimates the agreement of two binary classifications relative to random chance, ranging from 1 (perfect agreement) to 0 (random agreement) to -1 (systematic disagreement below that expected by random chance) (Congalton 1991, Congalton & Green 2009).

In addition to the error matrix comparisons, the raw acoustic percent cover dataset was also directly compared to the classified map. All acoustic points falling in the respective categories of presence or absence at each site were grouped together and summary statistics were calculated for each class.

<i>Metric</i>	<i>Value</i>	<i>Description</i>
Overall Accuracy	$(TP + TN) / n$	Proportion of all predictions that were correct
Prevalence	$(TP + FN) / n$	Proportion of observations (acoustic points) classified as presence
Sensitivity	$TP / (TP + FN)$	Proportion of correctly predicted presences
Specificity	$TN / (TN + FP)$	Proportion of correctly predicted absences
Positive Predictive Value (PPV)	$TP / (TP + FP)$	Proportion of positive predictions that are true positives
Negative Predictive Value (NPV)	$TN / (TN + FN)$	Proportion of negative predictions that are true negatives

Table 3-2. Description of metrics derived from the error matrix along with the calculation used for their derivation.

3.3 Results

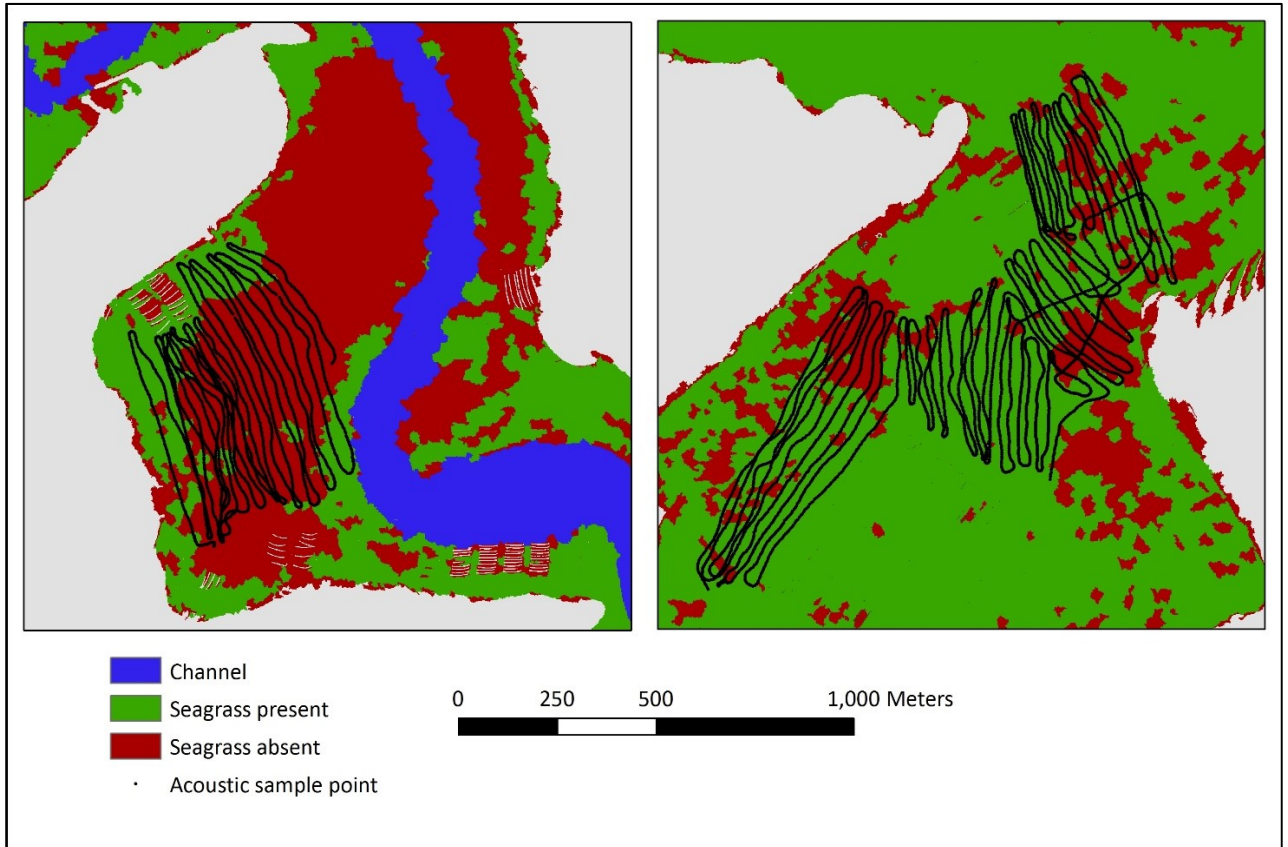


Figure 3-2. Classified map of sites A (*left*) and B (*right*) with the location of sampled acoustic points overlaid.

3.3.1 Image Classification

The OBIA classification produced a binary categorical raster map of eelgrass presence and absence throughout the estuary (Figure 3-2). The classification scheme based on eelgrass presence-absence resulted in an accuracy of 72.3% when compared to the video transect reference data across the entire study area (Mahoney & Hanson 2007). When analyzed with a fuzzy classification method, accuracy increased to 81.5%.

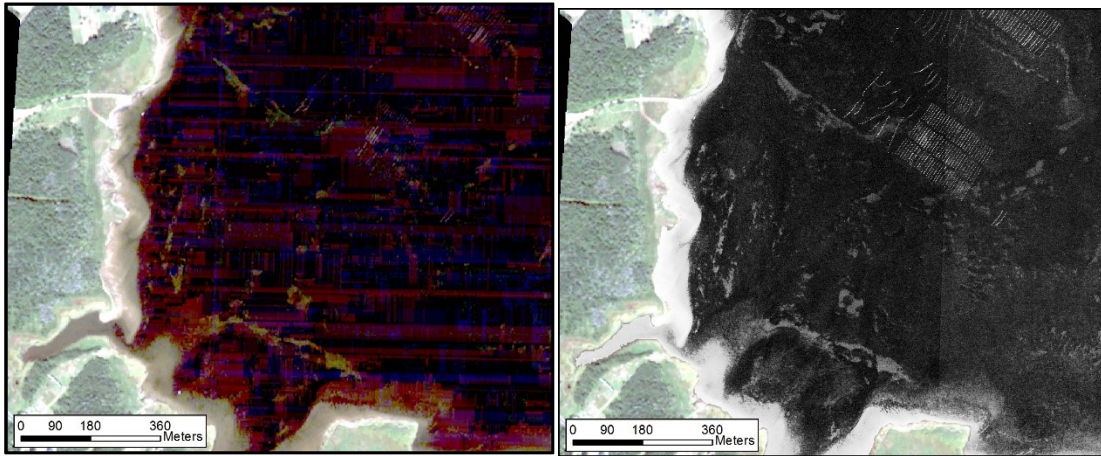


Figure 3-3. Spectral banding at site B affected the 2.4 m resolution multispectral imagery (*left*) more strongly than the 0.6 m resolution panchromatic image (*right*).

The raw imagery was subject to a spectral banding issue that affected a large proportion of the image (Figure 3-3). This is caused by a systematic problem at the level of the satellite sensor and could not be managed from an end-user perspective; it generally occurred in large groups of conjoined pixels that exhibit very low reflectance. The occurrence of this distortion was minimal at site A and likely did not influence classification. However, the effect was much more prevalent at site B, though it was still possible to visibly discern eelgrass patches from the raw multispectral image.

3.3.2 *Acoustic Survey Results*

The acoustic survey of site A covered an extent of 29.7 ha over 14.7 km transect length with mean seagrass percent cover of $41.8 \pm 18.1\%$ (SD) (Figure 3-4). At least a small amount of vegetation was detected essentially throughout the entire study area,

with only 21 out of 2677 report points (0.78%) indicating 0% cover. Water depth was relatively constant with a mean depth of 1.39 ± 0.12 m (SD).

At site B, the acoustic survey covered an area of 53.2 ha over transect length of 26.4 km (Figure 3-5). Mean percent cover of seagrass was more variable than at site A: $33.2 \pm 24.5\%$ (SD). Areas lacking seagrass were much more prevalent than at site A, with 0% cover detected at 626 of the 4932 survey points (12.7%), indicating a patchy heterogeneous landscape structure. Water depth was slightly deeper at 2.00 ± 0.21 m (SD) throughout the study area.

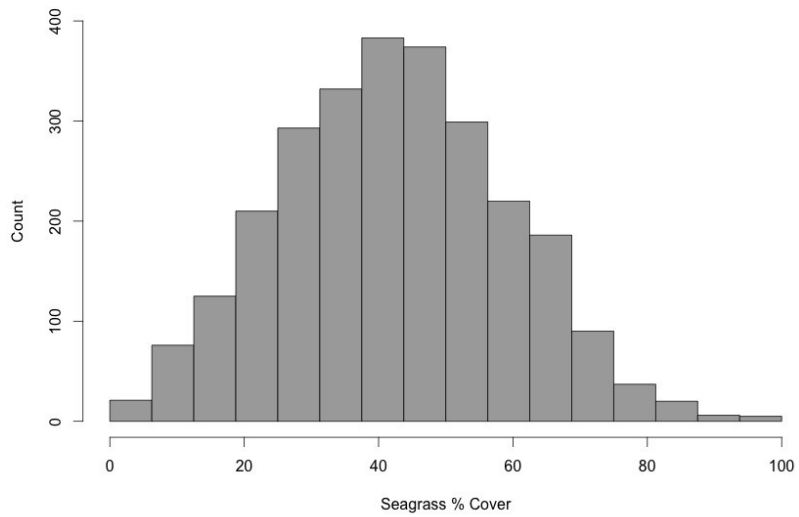
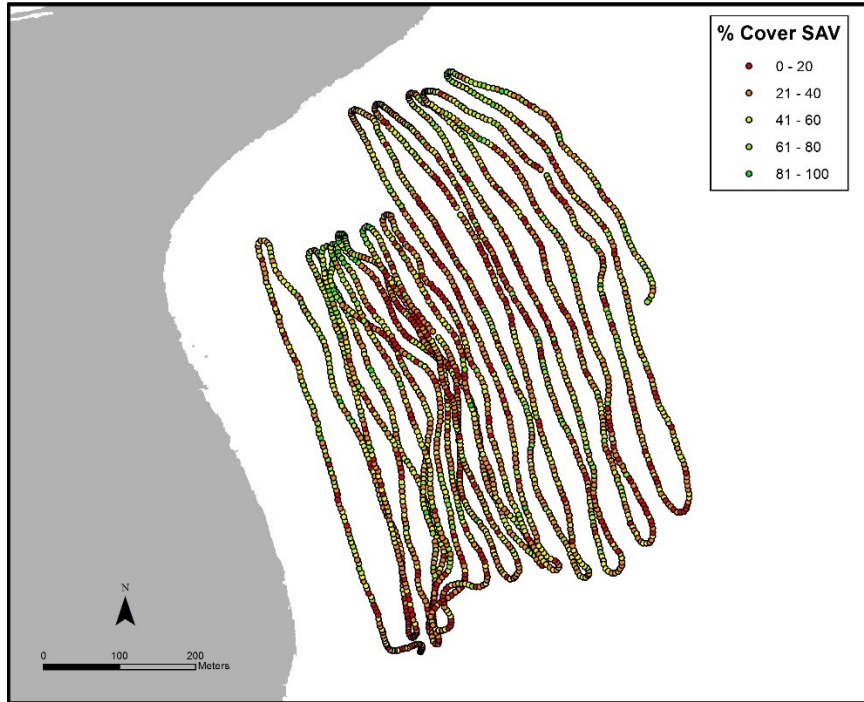


Figure 3-4. (above) Acoustic track map of site A from the October 2007 survey depicting percent cover of eelgrass; (below) histogram of seagrass percent cover at site A; mean $41.8 \pm 18.1\%$ (SD), $n = 2677$ points.

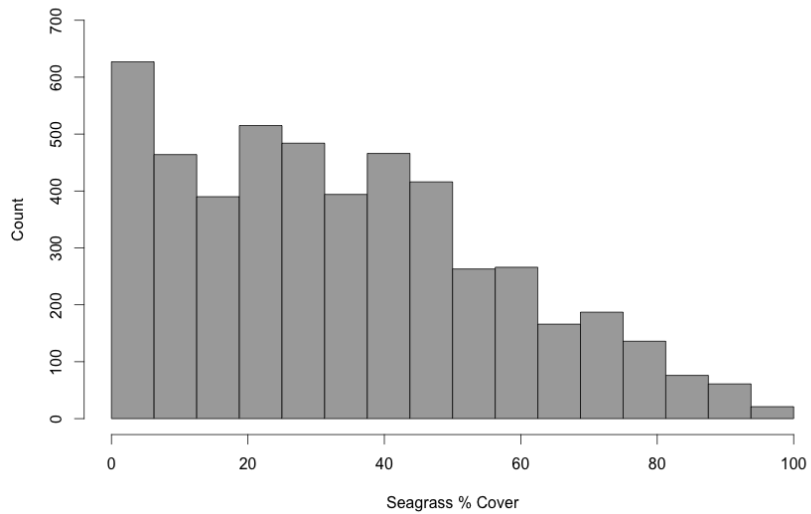
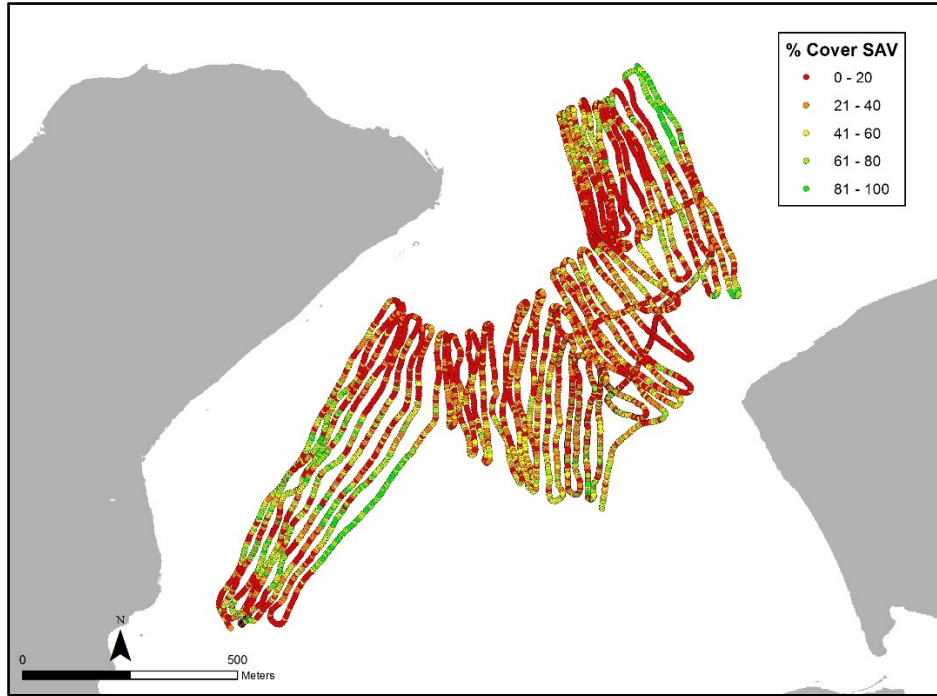


Figure 3-5. (above) Acoustic track map of site B from October 2007 showing percent cover of seagrass. (below) Histogram of seagrass percent cover at site B; $33.2 \pm 24.5\%$ (SD), $n = 4932$ points.

In the optically classified map of site A, acoustic points falling in areas classified as seagrass showed a mean of 49.4% cover, and areas classified as lacking seagrass were found to have a mean of 38.7% cover, representing a difference of 10.7% cover between the presence-absence categories. Of the 2677 acoustic points at site A, 29.3% occurred within areas classified optically as seagrass and 70.7% fell into areas classified optically as bare (Figure 3-2). At site B, seagrass presence areas were acoustically measured at a mean of 36.2% cover and bare areas at 24.3% cover for a differential of 11.9% cover. Of the 4932 acoustic points at site B, 74.4% occurred in areas classified optically as seagrass while 25.6% were classified optically as bare (Figure 3-2). Notably, the classification predicted lower seagrass cover at site A relative to site B (29.3% vs. 74.4% respectively), in contrast to the acoustic results that showed higher cover at site A than site B (41.8% vs. 33.2%). This highlights the general disagreement between the two remote sensing datasets.

3.3.3 Error Matrix Analysis

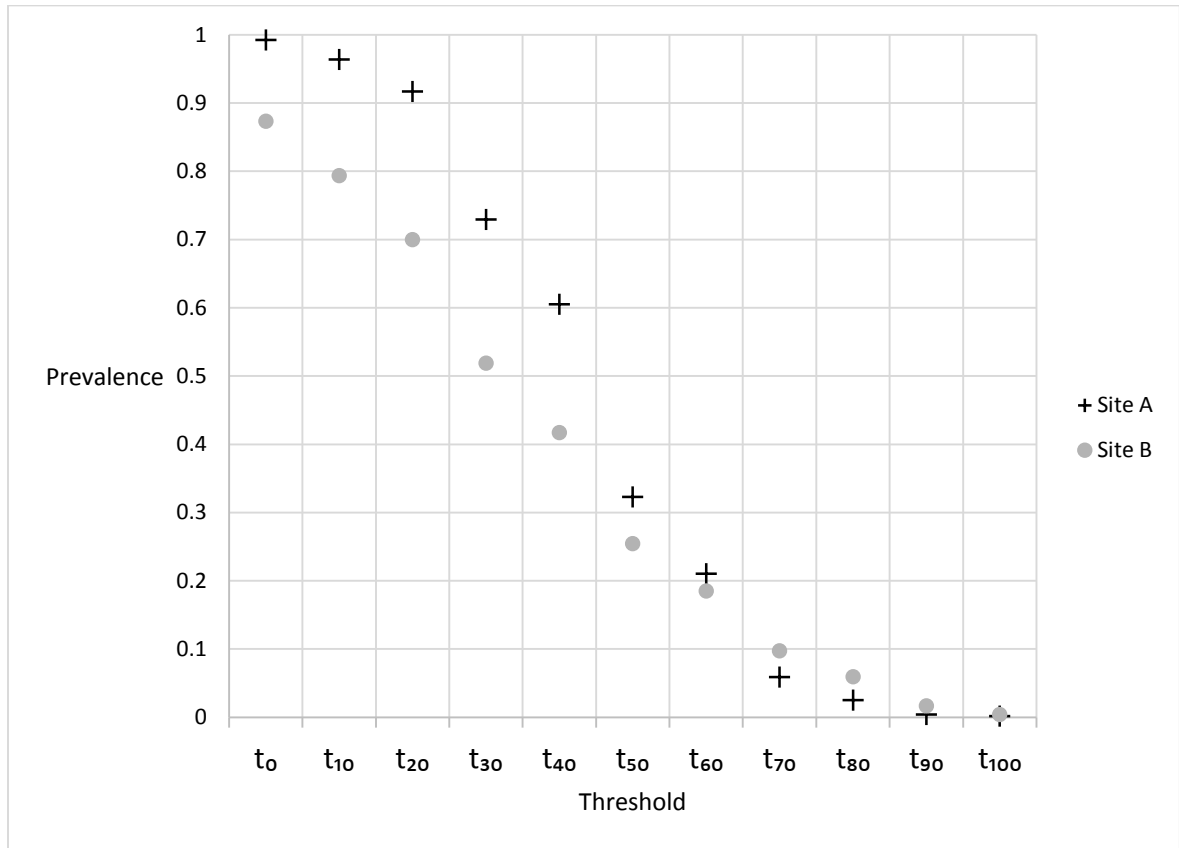


Figure 3-6. Prevalence of seagrass presence determined from the acoustic percent cover dataset at each examined threshold $t_0 - t_{100}$ for sites A and B.

Prevalence was seen to decline with increasing threshold at sites A and B (Figure 3-6). This matches the expected pattern as each increase in threshold corresponds to a decreasing number of points assigned to the category of seagrass presence. The differential in prevalence between sites A and B at t_0 represents the greater occurrence of zeroes at site B; 12.7% of points at site B were classified as absent, while only 0.78% of points at site A were disqualified at this most inclusive threshold. Prevalence approached zero at t_{100} , as only the small number of acoustic points with 100% cover were classified as present at this threshold.

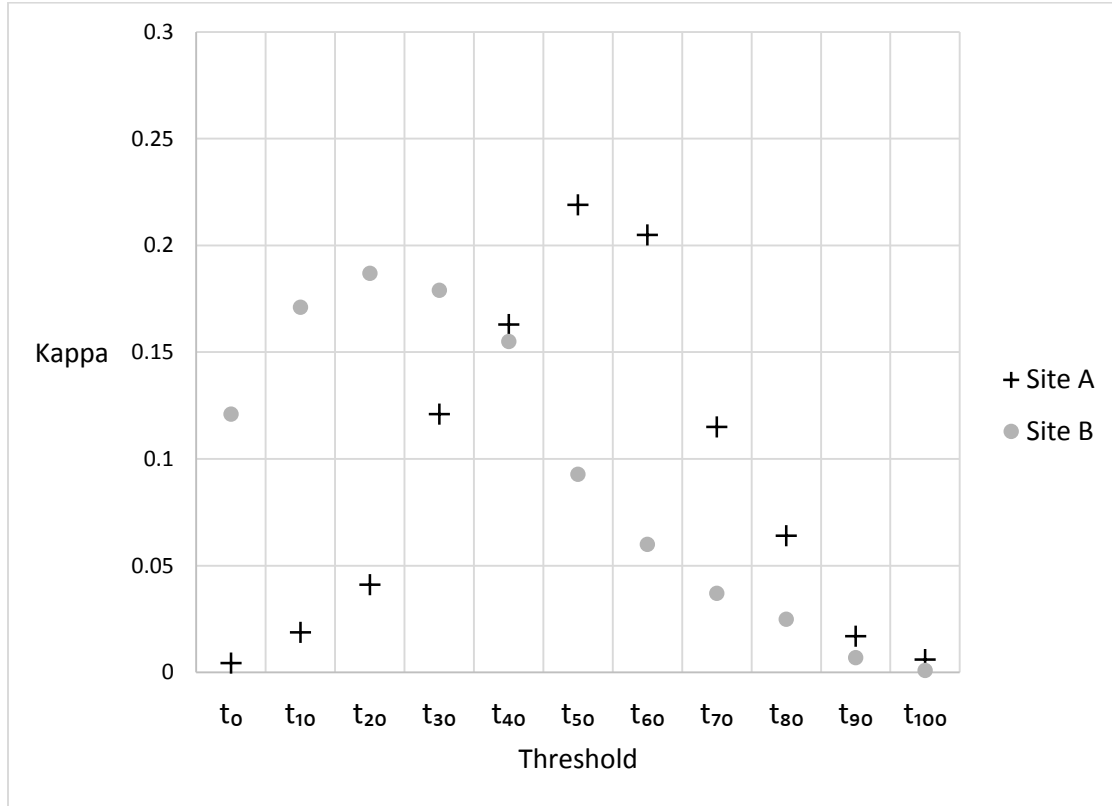


Figure 3-7. Results of the kappa statistic at each threshold from t_0 - t_{100} for sites A and B. Kappa measures the agreement of two binary classifications relative to random chance, ranging from 1 (perfect agreement) to 0 (random agreement) to -1 (systematic disagreement below that expected by random chance).

Results of the kappa statistic showed the agreement between the acoustic and satellite data at each threshold relative to the expected agreement due to random chance (Figure 3-7). All observed values of kappa represented “poor” to “fair” agreement (Landis & Koch 1977). Agreement was found to be relatively poor at every threshold at both sites A and B. At site A, kappa was maximum at t_{50} , decreasing to near zero at high and low thresholds. The maximum kappa at site B occurred at t_{20} , with a minimum at t_{100} .

Analysis of the error matrix depicted distinctly different trends in overall accuracy between sites A and B (Figure 3-8). These observed differences in overall accuracy were caused by the mismatch between predicted seagrass cover in the classified map and the observed acoustic dataset. At site A, overall accuracy was lowest at t_0 (29.9%) and increased with threshold value before leveling out near its maximum value (71.9%) at t_{70} . Overall accuracy at site A is lowest at t_0 due to disagreement between the observed prevalence at this threshold (~99%) and the classification in which only 29.3% of points occurred in areas of predicted seagrass presence. Overall accuracy improved as increasingly strict threshold values decreased prevalence to more closely match the predictions of the classified satellite dataset. In contrast, site B exhibited highest overall accuracy at t_0 (72.1%) and decreased at higher thresholds to the minimal value at t_{100} (25.9%). At site B, 74.4% of the acoustic points fell within areas of predicted seagrass presence. This led to maximum overall accuracy at t_0 where prevalence (87.3%) was highest. Overall accuracy declined at higher thresholds as prevalence decreased.

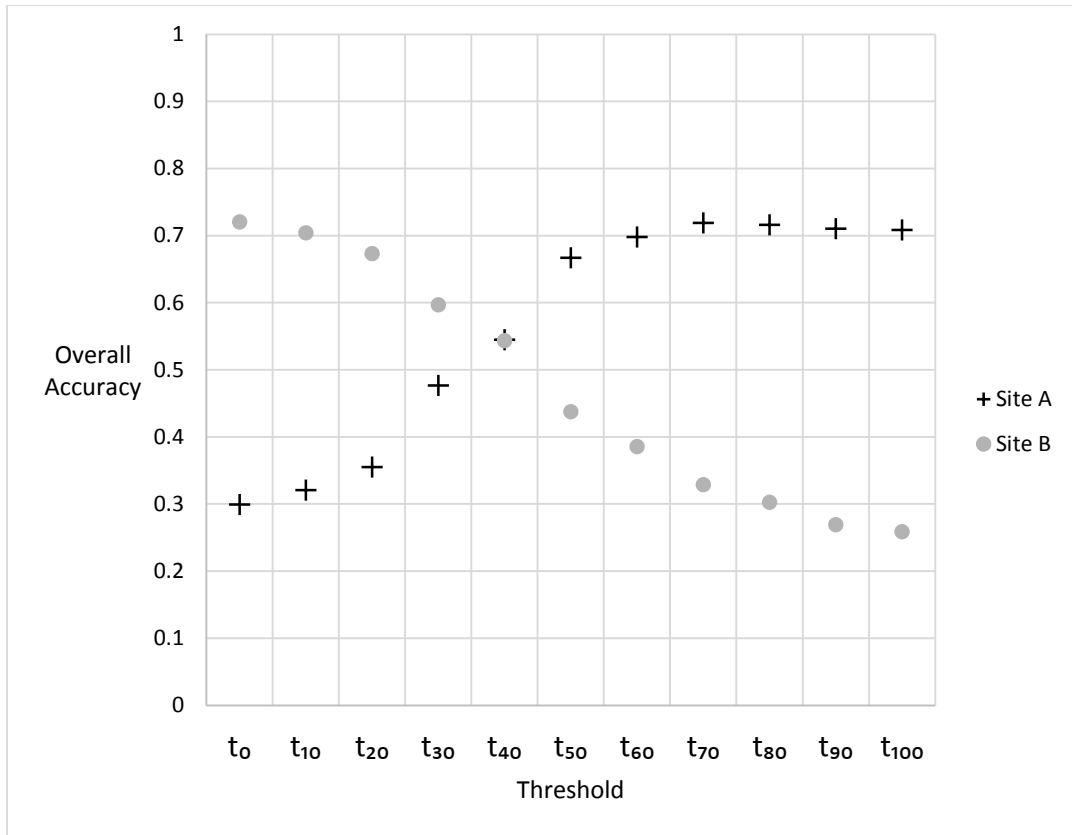


Figure 3-8. Trends in overall accuracy for sites A & B at each threshold value of seagrass percent cover ($t_0 - t_{100}$).

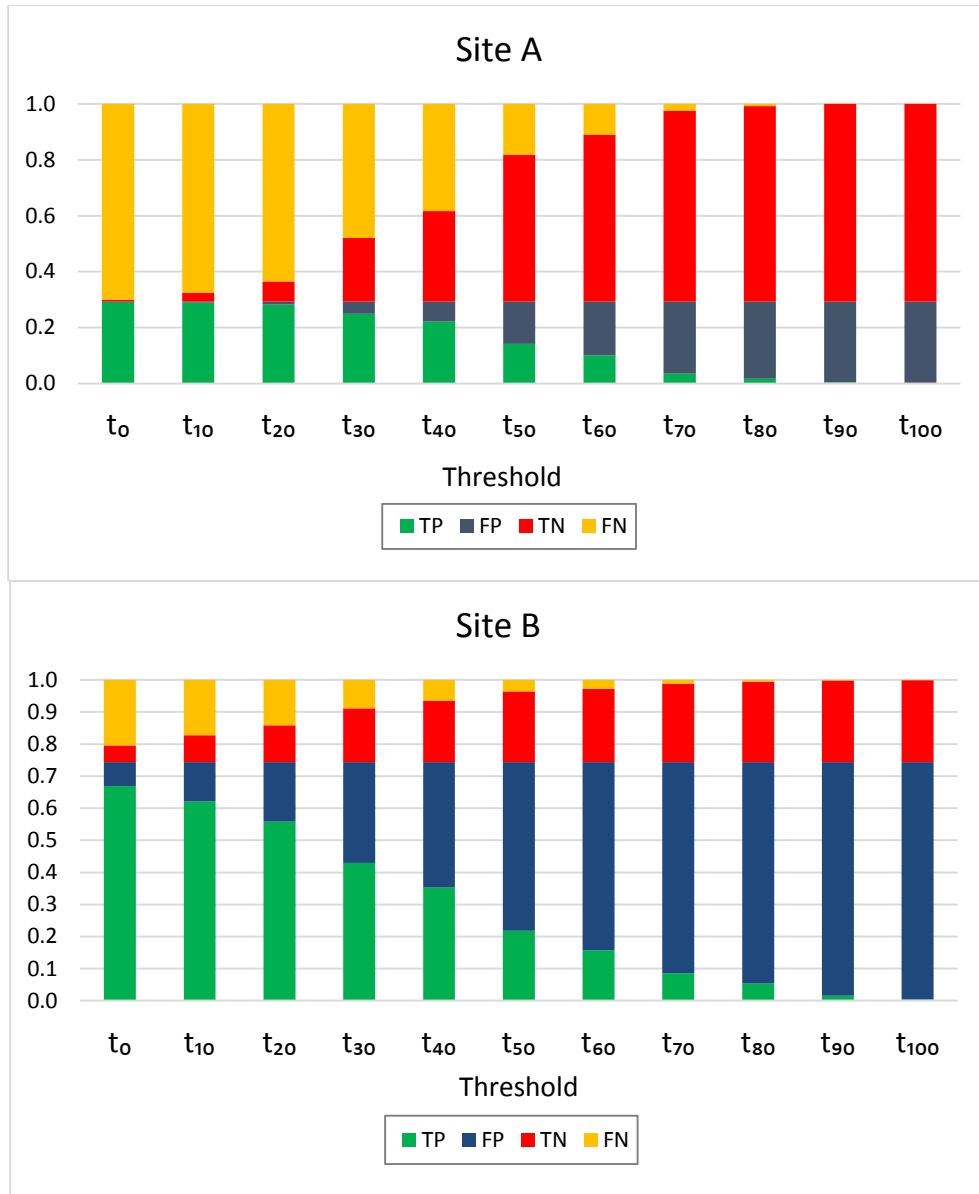


Figure 3-9. At each percent cover threshold, the proportion of points determined to be true positives (TP), true negatives (TN), false positives (FP), and false negatives (FN) for sites A (*above*) and B (*below*). The sum of TP and TN is equivalent to the overall accuracy, while the sum of FP and FN represents the misclassification rate. The ratio of classified positives (TP + FP) to classified negatives (TN + FN) is predetermined by the number of points falling in respective categories in the classified map.

Classification errors at site A were predominantly due to false negatives at lower thresholds, decreasing at higher thresholds with a corresponding increase in false positives (Figure 3-9). A similar pattern was found at site B, though false positives comprised a relatively larger proportion of classification errors, particularly at higher thresholds due to the higher predicted cover of the classified map at site A relative to site B. As a general pattern at both sites, increasing the acoustic threshold corresponded to an absolute decrease in true positives and false negatives and an increase in false positives and true negatives.

The balance between seagrass presence and absence predictions is predetermined by the number of acoustic points falling in each category of the classified map. The number of points classified as presence (TP + FP) and absence (TN + FN) are therefore fixed for each site by the predictions of the classified map (Figure 3-9). At site A, points classified as presence (TP + FP) account for 29.3% of the total, compared to 74.4% at site B. Due to this discrepancy, overall accuracy at site A was affected more by NPV than PPV, whereas site B was more strongly affected by PPV than NPV due to the higher proportion of points classified as presence (Figure 3-10).

Similar relationships between PPV and NPV were found at sites A and B, with maximum PPV and minimum NPV at t_0 , while minimum PPV and maximum NPV occurred at t_{100} (Figure 3-10). At t_0 only points with 0% cover were considered absent, leading to maximum numbers of TPs and FNs at both sites. Increasing the threshold resulted in lower observed prevalence leading to a relative increase in FPs and TNs, causing the observed drop in PPV and rise in NPV.

At site A, the classification scheme exhibited higher specificity than sensitivity at low threshold values, with maximum specificity and minimum sensitivity at t_0 (Figure 3-11). Specificity declined with successive thresholds to a minimum value at t_{100} while sensitivity increased up to its maximum at t_{90} . High prevalence at low thresholds led to a high proportion of false negatives relative to true negatives, reflected by the very low NPV, causing low sensitivity despite high PPV. Sensitivity increased moderately at successive thresholds as the decline in true positives was outpaced by the decline in false negatives.

In contrast to site A, site B showed higher sensitivity than specificity at each threshold interval (Figure 3-11). Presence as determined by the acoustic dataset was correctly identified for greater than 76% of points at all thresholds. High prevalence at low thresholds resulted in a large number of true positives, and false negatives were limited by the classification in which 74.4% of points were predicted as presence. This also led to a large number of false positives resulting from the discrepancy between the classification and the raw acoustic data. Specificity was found to be relatively low, declining after a maximum at t_0 due to the influence of false positives.

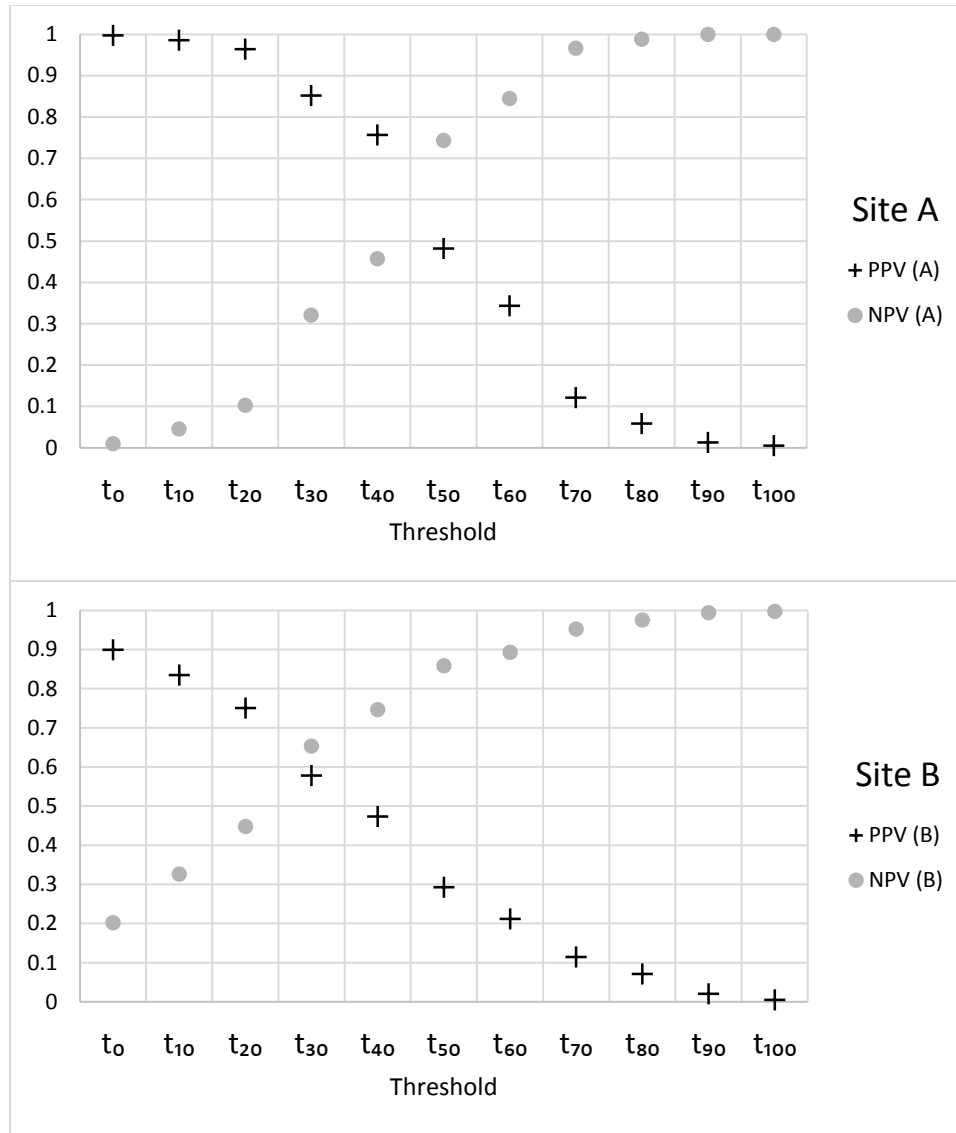


Figure 3-10. Trends in positive predictive value (PPV) and negative predictive value (NPV) at sites A (*above*) and B (*below*) through threshold values of percent cover from 0 – 100% (t₀ – t₁₀₀).

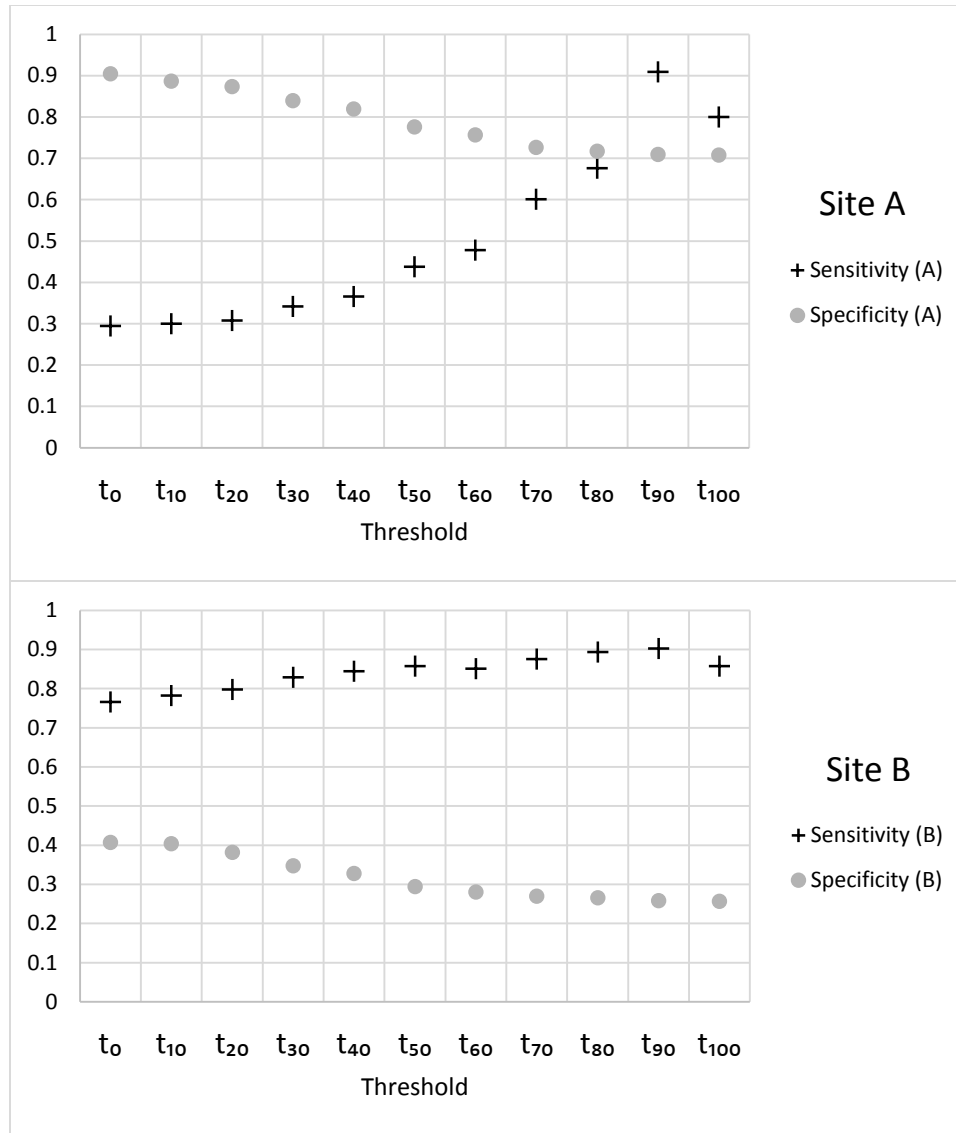


Figure 3-11. Sensitivity (correctly predicted presences) and specificity (correctly predicted absences) of the classification scheme for sites A (*above*) and B (*below*) at threshold values of percent cover from 0 – 100% ($t_0 - t_{100}$).

3.4 Discussion

3.4.1 Comparison of acoustic and satellite data

Contrary to expectations, the acoustic and satellite datasets did not produce highly similar estimates of seagrass percent cover at any threshold. This is most clearly illustrated by kappa (Figure 3-7). The maximum value achieved at either site was 0.219 at site A (t_{50}), representing at best “fair” agreement (Landis & Koch 1977). This low level of inter-observer agreement indicates that, in the current study, acoustic data cannot be used as suitable ground reference data to assess the classification accuracy of satellite remote sensing. However, dissecting the apparent disagreement helps to illustrate the differences between acoustic and optical methods, suggesting when it is appropriate to apply either technique. At site A, the satellite classification underestimated the distribution of seagrass relative to the acoustic survey with only 29.3% of the acoustic points falling into areas classified as seagrass, in contrast to the acoustic estimate of 41.8% cover overall. An opposite result was apparent at site B, where 74.4% of acoustic points fell in areas classified as seagrass compared to the acoustic estimate of 33.2% cover. This discrepancy explained many of the observed differences in error matrix metrics between sites A and B.

One major issue associated with evaluating binary classification performance is the sensitivity of common metrics (e.g., overall accuracy, kappa) to prevalence (Fielding & Bell 1997, Manel et al. 2001, Liu et al. 2005, Allouche et al. 2006, Freeman & Moisen 2008). For example, Fielding & Bell (1997) describe a hypothetical example where if prevalence was 5%, it would be possible to achieve overall accuracy of 95% if all cases were simply classified as negative. This has particular relevance for the selection of a

binary classification threshold. In this study, prevalence was a function of the applied threshold relative to the site-specific distribution of acoustic percent cover values. At both sites, increasing the threshold effectively decreased prevalence and reclassified acoustic points from present to absent (Figure 3-6). Maximum kappa at both sites occurred when the applied threshold resulted in the closest match between acoustic prevalence and the satellite classification.

This dependence on prevalence explains the contrasting overall accuracy curves for sites A and B (Figure 3-8). At site A, the acoustic survey found an approximately normal distribution of percent cover values with a very low proportion of zeroes (0.78%). Overall accuracy was at its minimum at t_0 (29.9%), where prevalence was maximum (99.2%) as all non-zero acoustic points were classified as presences, contrasting with the comparatively low estimate of the satellite classification (predicted 29.3% presence) and leading to a large number of false negatives. The observed improvement in overall accuracy at higher thresholds is driven by a reduction in false negatives and improving NPV that outweighs the corresponding decrease in PPV (Figure 3-10). Maximum overall accuracy was achieved when prevalence was reduced to the level of the satellite classification.

At site B, in contrast to site A, overall accuracy was maximized at t_0 where the threshold established presence for all acoustic points except those with a value of zero percent cover. This result was driven by agreement between the satellite classification (predicted 74.4% presence) and correspondingly high prevalence in the acoustic dataset (87.3%). Prevalence at t_0 was lower than at site A due to the comparatively large presence of zeroes in the acoustic dataset (12.7%). Although the majority of these were

misclassified, 40.7% were correctly classified as true negatives (Figure 3-10), adding to the high overall accuracy measured at t_0 .

These results highlight the difficulty of comparing remote sensing methods with different data models. Satellite remote sensing does not provide an effective predictive model of seagrass percent cover as measured by acoustics, and satellite classification accuracy assessment should not be evaluated with continuous acoustic data. However, the observed lack of agreement does not decisively suggest that either method is more or less “correct” than the other. Although both methods are able to produce objectively accurate maps when evaluated with independent reference data (e.g. Mahoney & Hanson 2007, Appendix A), the lack of strong agreement belies inherent accuracy issues underpinning both methods. Relative to the acoustic dataset, the satellite classification under- and overestimated seagrass cover at sites A and B, respectively. This emphasizes the finding that site-specific differences in prevalence are crucial for understanding classification accuracy in seagrass ecosystems. The potential for largely under- or over-estimating seagrass abundance from applying bay-scale classification to multiple spatial regimes with different prevalence is a risk that should be accounted for in all monitoring and management activities associated with seagrasses.

3.4.2 Factors affecting classification accuracy

The discrepancy between acoustic and satellite maps of seagrass distribution may have been affected by other factors aside from the binary classification scheme. As discussed above, characteristics of the seagrass bed such as prevalence can influence the

ability of remote sensing to detect vegetation. The spatial scale of patchiness inherent to the seagrass bed interacts with the spatial resolution of remote sensing as represented by its fundamental unit, the pixel. The ability to resolve seagrasses from aerial imagery is dependent on the size of the sampling unit (i.e., pixel) relative to the patch. If a patch is smaller than the sampling unit, it results in the “mixed-pixel problem”, where one pixel spans multiple classes of land cover, confounding the classification scheme and leading to errors (Fisher 1997, Lu & Weng 2007). Mixed pixels can also occur at patch boundaries when the pixel sits astride adjacent vegetated and bare areas. As a result, the proportion of mixed pixels is effectively a function of the size, shape, and configuration of seagrass patches in the landscape. As patch size increases relative to the sampling unit, the proportion of mixed pixels decreases, theoretically improving classification accuracy and the ability to resolve pattern (Lu & Weng 2007).

Image classification performance is also influenced by factors associated with the optical sensors used by the satellite platform. In subtidal marine ecosystems, light is quickly attenuated as a function of its wavelength and water depth, limiting the amount of information that can be extracted. This constraint is exacerbated in mixed pixels, when the spectral information collected by the satellite sensor represents components from more than one feature. The radiometric, spectral, and spatial resolution of the sensor together define the minimum resolvable unit, essentially the smallest amount of seagrass required to trigger a determination of seagrass presence. Though the smallest possible spatial representation would be equal to one pixel, it is not generally clear what quantity or density of seagrass within a pixel (i.e., the “purity” of a mixed pixel) constitutes the

minimum resolvable unit of seagrass for satellite remote sensing, and how this quantity varies with factors such as water depth, vegetation density, and substrate type.

In contrast to the regular (i.e., square) pixel produced by satellite remote sensing, the acoustic data analyzed in this study used an irregularly shaped sampling unit produced by averaging several acoustic pings over a linear distance of 4-6 m. Though the spatial area represented by one acoustic point and one satellite pixel are roughly comparable, it is likely that the ability to detect very small amounts of eelgrass differs between the two methods. The pixel size of the satellite imagery (5.76 m²) is most likely too coarse for detecting very small amounts of seagrass. However, the acoustic system is theoretically able to detect as little as a single blade of eelgrass with a single ping, as the area of a single ping footprint in 1 m depth is comparatively much smaller (ca. 0.01 m²). Averaged over a 10 ping cycle, this single blade would theoretically result in a measure of 10% cover, representing a minimum resolvable unit smaller than can be achieved with satellite remote sensing.

The differential sensitivity to small amounts of seagrass suggests a plausible explanation for the poor agreement between satellite and acoustic datasets. For example, at site A the acoustic survey detected at least a low level of seagrass cover throughout virtually the entire survey area. Acoustic points representing areas of sparse eelgrass below the minimum resolvable unit of the satellite classification scheme resulted in a large number of false negatives, particularly at low thresholds. Future research should be conducted to evaluate the minimum resolvable unit of seagrass that can be detected through satellite remote sensing.

Despite poor overall agreement, the acoustic percent cover dataset quantified differences between areas of presence and absence in the satellite map. The difference in percent cover between areas of predicted presence and absence was 10.7% at site A and 11.9% at site B. This suggests that the effective minimum resolvable unit is not an absolute value, but instead may be determined in terms of contrast with the surrounding landscape. Previous studies have explored the ability of acoustic methods to detect patterns within “continuous” seagrass beds (Barrell & Grant 2013, Chapter 2 of this thesis). The indeterminacy of boundaries may be a major source of error and uncertainty particularly in continuous seagrass beds (Barrell & Grant 2013). Detection of boundaries from remote sensing can be challenging when thematic resolution is limited compared to variation in the landscape (Arnot et al. 2004). The binary classification scheme that underpins the error matrix assumes the presence of sharp discontinuities between areas of presence and absence. In locations such as site A, forcing binary classification on a continuously varying landscape results in the high misclassification rate observed in this study.

The classified satellite map of site B depicted the seagrass bed with large areas of mostly continuous cover fragmented by several small gaps with visually apparent boundaries (Figure 3-2). The classification qualitatively showed stronger agreement with the acoustic dataset in the southwest of the surveyed area where patch-gap boundaries were most evident, but detected many false positive errors throughout the rest of the landscape. Agreement between satellite and acoustic datasets may have been stronger if analysis was confined to a subset of the surveyed area where confidence in satellite classification performance was higher. The spectral banding problem inherent to the

satellite data may have been responsible for some of these errors, as a visual inspection of site B showed many of the heavily banded areas misclassified as seagrass (Figure 3-3).

The satellite classification also notably misclassified a large oyster aquaculture operation at site B as seagrass, highlighting the potential effects of systematic errors associated with remote sensing. Similarly, the lack of agreement may have been influenced by spatial uncertainty in the satellite and/or acoustic datasets due to georeferencing or GPS errors. Additionally, the sharp boundaries present at site B could potentially exacerbate any positional or georeferencing errors caused by mismatch between the satellite and acoustic datasets (Arnot et al. 2004).

Characteristics of the satellite classification approach also may have influenced the results, as image classification is subject to a number of errors associated with interpreter bias (Lu & Weng 2007, Shao & Wu 2008). Aside from unintentional classification errors, the motivation for conducting the original satellite classification of Richibucto likely influenced the output map. Object-based image analysis focuses on detecting user-defined “objects” with particular spatial characteristics. The goal of the satellite classification was to map seagrass at the bay-scale, and was focused on broad trends of seagrass presence-absence (Mahoney & Hanson 2007). Spatial scale mismatch between the OBIA classification algorithm and the patch-scale focus of the acoustic survey likely contributed to the lack of agreement between the two datasets. Additionally, the gap between image acquisition and the acoustic survey (~1.5 months) may have resulted in a temporal mismatch if substantial changes in landscape structure occurred over the ensuing time period, though there were no major storm events or anthropogenic disturbances known to occur over the elapsed time span.

3.4.3 Conclusions

In this study, acoustic and satellite remote sensing datasets representing seagrass distribution did not exhibit strong agreement when compared using the error matrix and derived metrics. These results suggest that accuracy assessment of satellite-derived seagrass maps using acoustic reference data is problematic. Acoustic surveys measure seagrass percent cover with a continuous data model, in contrast to the categorical presence-absence representation produced through the classification of satellite imagery. The observed lack of agreement may be the result of applying binary classification to the continuous acoustic percent cover dataset, as well as site-specific differences in the prevalence of seagrass, environmental conditions, systematic errors with remote sensing, and spatial uncertainty in the output data.

The comparison of acoustic and satellite datasets presented here illustrates the variable performance of satellite classification in areas with differing landscape structure. In particular, estimates of seagrass distribution produced from satellite data vary as a function of the local prevalence and patchiness of seagrass. While both acoustic and satellite methods measure a comparable spatial footprint, acoustic remote sensing is more sensitive to small amounts of seagrass, revealing potential over- and underestimates in broad-scale satellite maps covering multiple spatial regimes. These results have important implications for the mapping and monitoring of seagrass ecosystems. Despite recognition of the sensitivity of habitat maps to error, studies investigating the magnitude of uncertainty in landscape analysis are relatively rare (Newton et al. 2009). Remote sensing and assessment of classification accuracy should be conducted with consideration

of potential mismatches between the goals of the application, the structure of the area under study, and the sensitivity of the remote sensing approach.

Chapter 4. Use of High-Resolution Low-Altitude Aerial Photography for the Characterization of Eelgrass (*Zostera marina* L.) and Blue Mussel (*Mytilus edulis* L.) Landscape Structure at Multiple Spatial Scales

4.1 Introduction

Study of spatial heterogeneity and the arrangement of habitats has long been a primary focus of marine ecology (e.g., Paine & Levin 1981). Understanding the relationship between spatial patterns and ecological processes is critical for the effective management of marine and coastal resources and the valuable ecosystem services they provide, with implications for conservation, marine spatial planning, and habitat restoration (Bell et al. 1997, Hinchey et al. 2008). The discipline of landscape ecology addresses the causes and ecological consequences of heterogeneity through quantitative analysis of the ‘landscape’, a heterogeneous mosaic of patches that can be defined over a broad range of spatial scales (Turner 2005). Landscape ecology is characterized by the use of metrics for quantifying the size, shape, and configuration of ecological phenomena such as habitat patches through space (O’Neill et al. 1988, Turner et al. 2001).

Landscape metrics are used to calculate these spatial characteristics at the level of the individual patch, class (i.e., all patches of a particular type), and the entire landscape.

This approach, while widespread in terrestrial ecology, is increasingly being applied to biogenic marine features such as coral reefs, seagrasses, and bivalves (Boström et al. 2011).

Several challenges are associated with the application of landscape techniques to marine and coastal environments (Hinchey et al. 2008, Boström et al. 2011). The range of habitats present in marine landscapes is small relative to the terrestrial context, particularly in temperate waters. At mid-latitudes, landscapes consist largely of bare sediments or rocks, aquatic vegetation (i.e., seagrasses & macroalgae), and shellfish beds. These areas are highly dynamic through time and space, necessitating high-quality fine-resolution spatial data over a relatively broad extent in order to capture pattern at relevant spatial scales. In subtidal areas, the overlying water column obscures the detection of bottom structure, particularly in turbid waters. For this reason, marine landscape ecology is well developed for habitats in clear tropical waters such as coral reefs (e.g., Mumby et al. 2008), but is less common in turbid temperate environments such as those prevalent in parts of Atlantic Canada.

Among common intertidal and shallow subtidal habitats in Atlantic Canada, the seagrass species eelgrass (*Zostera marina* L.) stands out as a particularly important component of the coastal environment, acting as an ecosystem engineer through modification of the physical and chemical environment (Jones et al. 1994, DFO 2009). Eelgrass provides a suite of ecosystem services such as primary production, shoreline protection, and nutrient cycling, ranking among the most valuable habitats worldwide (Costanza et al. 1997). Eelgrass habitats are also highly susceptible to disturbance and have declined in global extent over the last several decades due in large part to anthropogenic pressures (Orth et al. 2006, Waycott et al. 2009). Awareness of the value and sensitivity of seagrass habitat has led to diverse approaches to understand and model the processes driving seagrass dynamics, though efforts have been hampered in part by a

lack of accurate maps and spatial data representing the extent and distribution of seagrasses at fine spatial scales (Duarte 2002, Bell et al. 2006). Compared to most other marine habitats, seagrass landscapes have been relatively well-studied and have a long history as a focal species for landscape analysis (Robbins & Bell 1994).

Bivalves represent a second major source of biogenic structure in intertidal and shallow subtidal ecosystems. Bivalve shellfish naturally form aggregate communities, or reefs, that function as ecosystem engineers and support diverse ecological functions in the coastal environment (Gutiérrez et al. 2003, Coen et al. 2007). Species such as the blue mussel (*Mytilus edulis*) and Eastern oyster (*Crassostrea virginica*) contribute ecosystem services such as water filtration, wave attenuation, and shoreline protection in addition to their value through commercial and recreational fisheries and aquaculture. Bivalves, along with seagrasses, are often the subject of intensive restoration efforts (Coen & Luckenbach 2000, van Katwijk et al. 2009), and play important roles in coastal management and marine spatial planning. Though bivalve patterns on rocky intertidal substrate are comparatively well-studied (e.g., Paine & Levin 1981, Guichard et al. 2003), relatively little is known about patterns in soft-sediment habitats (Crawford et al. 2006). In Atlantic Canada, blue mussels are found on both hard and soft substrates, often coexisting with eelgrass in soft-sediment areas as discrete patches juxtaposed with or interspersed throughout the vegetative understory.

Seagrasses and bivalves share many commonalities when considered from a landscape perspective. Seagrasses occur as mosaics of fragmented or near-continuous meadows that can be conceptualized over a hierarchy of spatial scales ranging from individual plants to landscape-scale meadows (Bell et al. 2006, Duarte et al. 2006).

Similarly, bivalve reef structure has been characterized over multiple spatial scales ranging from individuals to dense reef agglomerations (Kostylev & Erlandsson 2001, Crawford et al. 2006). Bivalves and seagrasses are both structured by processes operating across multiple spatial and temporal scales and are greatly affected by hydrodynamics and water quality. Both also have wide-ranging impacts on the local ecosystem, affecting water movement, sedimentation, turbidity, faunal communities, and nutrient cycling where they occur.

Marine landscapes are typically studied with emphasis on a focal patch type following the patch-matrix model of landscape ecology where patches are distributed through a background of soft sediments (Boström et al. 2011). This results in a binary landscape of target patches (e.g., seagrass) embedded in a background matrix (e.g., soft sediments). This model has been applied to seagrass ecosystems for study of diverse aspects of landscape structure such as gap dynamics, faunal interactions, ecosystem monitoring, and predictive modeling (Bell et al. 2006). However, coastal habitats also frequently occur as larger habitat mosaics including multiple substrate types and additional biogenic components. The spatial arrangement of multi-component mosaics influences several aspects of ecosystem function through interactions between disparate habitats. For example, seagrasses affect adjacent habitats through the export of nutrient subsidies (Heck et al. 2008), and the presence of multiple landscape components can increase habitat quality for faunal species (Micheli & Peterson 1999, Grabowski et al. 2005). Seagrasses in particular exhibit complex interactions when paired with bivalves in coastal landscapes, with potential advantages and disadvantages to the relationship for

both species (e.g. Reusch et al. 1994, Reusch & Chapman 1995, Peterson & Heck 2001, Vinther et al. 2008).

The application of landscape techniques to the marine environment is still a relatively recent occurrence, and questions remain as to which statistics and technical approaches best represent the spatial dynamics of coastal landscape mosaics as opposed to the terrestrial environment (Bell et al. 2006, Hinchey et al. 2008, Barrell & Grant 2013). Despite the acknowledged importance of landscape context, marine patch-mosaic landscapes have been largely understudied due to difficulties in collecting and analyzing spatial data along the coastal margins. However, improvements in remote sensing, spatial statistics, and geographic information systems (GIS) may help to further the application of this approach to the marine environment (Boström et al. 2011, Wedding et al. 2011).

The primary source of spatial data for investigations of coastal landscape structure is optical imagery sourced from aircraft or satellite-based remote sensing (McKenzie et al. 2001). These methods provide synoptic and continuous data at high spatial resolution while minimizing the time and labor required for collecting data through alternative methods (i.e., physical, acoustic, or video-survey techniques). Optical methods have also been greatly improved due to recent advances in remote sensing and computing power and a corresponding decrease in cost (Dekker et al. 2006). The spatial resolution of modern imaging satellites (e.g., QuickBird, WorldView-2) has improved into the sub-meter range, allowing for the discernment of relatively fine-scale landscape features obscured at coarser resolution. These advances in remote sensing and geographic information systems (GIS) have increased the availability of high-resolution data and

improved the ability of researchers to conduct quantitative analyses of landscape structure in the marine environment (Hinchey et al. 2008, Boström et al. 2011).

Aside from the evident strengths of optical remote sensing as a source of spatial data, several shortcomings limit its effectiveness. These shortcomings commonly occur in the acquisition, classification, and analysis stages. The acquisition of aerial imagery is affected in various ways by weather and environmental conditions; cloud cover, wind-generated waves and ripples, sun glint, tidal height, and turbidity can all obscure image quality and complicate the timing of acquisition (McKenzie et al. 2001, Dekker et al. 2006). Image classification is subject to algorithmic or interpreter error, requires high-quality ground-reference data, and is sensitive to spatial scale mismatch (Qi & Wu 1996, Wagner & Fortin 2005), causing errors that can propagate through the calculation of landscape metrics (Shao & Wu 2008). Despite these drawbacks, aerial mapping of coastal and marine landscapes has been successfully applied at multiple spatial scales over a broad range of species and environments (Dekker et al. 2006).

The effect of spatial scale is a particularly important concern with respect to multi-component landscape mosaics where components vary over disparate spatial scales. For example, analysis of satellite imagery at fixed 2.4 m resolution will perform better in a landscape with large multi-pixel patches than a landscape with average patch size below the spatial resolution of remote sensing. For this reason, satellite remote sensing is much more commonly applied to seagrasses than to bivalves that typically exhibit spatial structure at finer scales. Studies of fine-scale mussel landscape patterns commonly use very high-resolution photography covering the extent of a sample quadrat (e.g., 1 m²), though these studies are mostly limited to intertidal mussel habitats (Crawford et al.

2006, Meager et al. 2011). Less commonly, low-altitude aerial photography from airborne kite or balloon platforms can be used to collect data at spatial resolution and extent intermediate to airborne and quadrat-scale photography (e.g. Guichard et al. 2000, Bryson et al. 2013). Low-altitude aerial photography is particularly valuable in coastal ecosystems because it can capture data across intertidal and shallow subtidal areas. This broadens the scope for multi-scale analysis of complex landscapes including both macrophyte and bivalve habitats, and improves the ability of landscape metrics to detect and quantify mosaic patterns along the nearshore coastal margins (Bryson et al. 2013). Additionally, relatively inexpensive low-altitude aerial methods allow for greater temporal resolution and the ability to detect landscape change.

In this study, an intertidal landscape mosaic of mussel and eelgrass patches in Halifax Harbor was observed using low-altitude aerial photography from a helium balloon-mounted digital camera platform. Although this is an industrial harbor with large areas of hardened shoreline and limited intertidal soft-sediment areas, a complex mosaic nonetheless has formed in Eastern Passage, a sandy intertidal area of the outer harbor. Imagery representing seagrass-bivalve landscape structure was captured, classified, and analyzed using multiple metrics of landscape composition and configuration at both the patch- and landscape-scale. Newly collected patch-scale imagery was also compared to a previous dataset in order to track temporal changes in seagrass patch metrics. This study leverages novel remote sensing technology to acquire high resolution imagery for the characterization and tracking of landscape metrics and to describe this unique bivalve-macrophyte landscape occurring in close proximity to a highly developed urban area.

4.2 Methods

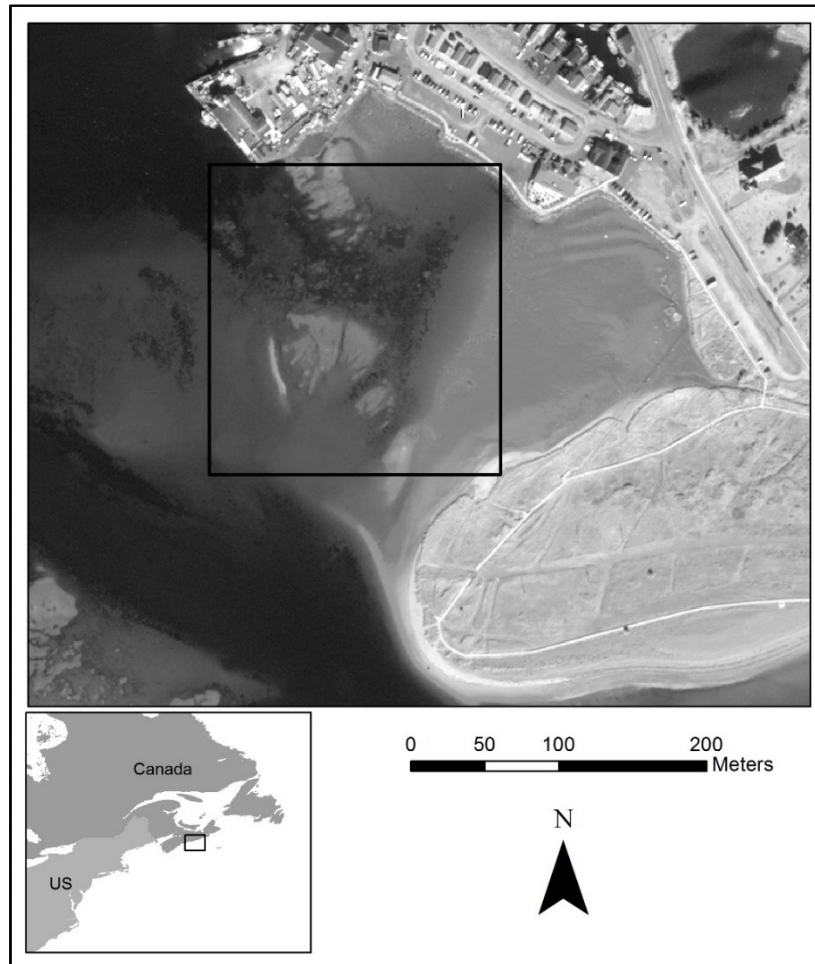


Figure 4-1. (*above*) Outline of the landscape of interest; (*below*) approximate location of the study site in Eastern Passage, Nova Scotia, Canada ($63^{\circ} 29.7' W$, $44^{\circ} 36.5' N$). Imagery source: QuickBird satellite.

4.2.1 Data Collection

The study site was located at McCormacks Beach near Eastern Passage, Nova Scotia, Canada, at the mouth of Halifax Harbor ($63^{\circ} 29.7' W$, $44^{\circ} 36.5' N$). The site is a moderately sized tidal flat sheltered by nearby Lawlors Island and McNabs Island (Figure 4-1). The flat is bordered by a recreational provincial park in the southeast and an

operational fishing wharf in the northwest. Relatively high human population density occurs in close proximity to the Eastern Passage area, suggesting at least a moderate level of human disturbance affecting water quality of the surrounding area. At very low tides, a large emergent reef of blue mussels (*Mytilus edulis* L.) is visually apparent in addition to isolated patches of eelgrass. Blue mussel patches were observed both separate from and within eelgrass patches.

Fieldwork was conducted on 20 October 2010 near the afternoon low tide of 0.57 m. Ground control points (GCPs) consisting of 3' x 4' (0.914 m x 1.22 m) "X" shapes formed by white corrugated plastic boards were first placed and georeferenced by GPS prior to the aerial photography. Five GCPs were marked, in addition to other distinctive landmarks such as rocks visible from the balloon camera. Additionally, the camera operators on the ground carried GPS units to function as supplementary GCPs when included in the image frame.

Low-altitude aerial photographs were collected using a digital camera suspended from a tethered helium-filled balloon. This system allows the photographer to rotate, tilt, zoom, and trigger the camera remotely from a ground unit. Images can also be monitored real-time from the ground station to ensure target area coverage. The camera used was a 7.2 megapixel Sony DSC-V3 with pixel dimensions of 3072 (width) by 2304 (height). A Garmin eTrex Vista HCx GPS unit equipped with barometric pressure sensor was attached to the camera platform to record the precise location of each image. The GPS was set to record positions at high frequency for later syncing with imagery through the time stamp. Downward-facing photographs were collected in RAW format, allowing the highest level of detail and flexibility in post-processing. The camera was also configured

with shutter speed priority in order to prevent blurring resultant from wind or other platform instabilities. Images were collected continuously at multiple altitudes, reaching a maximum elevation of 133 m above sea level.

Additional images collected at the same site two years previously were also analyzed for comparison and to estimate patch expansion through time. This imagery was collected on 8 July 2008, approximately 27 months prior to the primary dataset, using the same camera and helium balloon system. This imagery was not originally intended to encompass both the seagrass and mussel beds, and thus did not cover the entire extent and was used only for patch-scale comparison of eelgrass patches within a subset of the landscape.

4.2.2 Data Processing & Image Classification

Images initially captured in proprietary RAW format were converted to TIFF (Tagged Image File Format) for further processing and analysis. Distortion due to the camera lens was removed and the resulting images were imported into ArcGIS v10.1 for georeferencing using GCP positions. The referenced and processed images were then classified with an ISODATA unsupervised classification algorithm. The number of classes was initially set to a larger-than-expected number and reduced through aggregation until three target classes representing seagrass, mussels, and bare sediment remained. Patches were then formed by the joining of contiguous cells of the same class as defined by the 8 nearest neighbors, with cell adjacency established for diagonal cells as well as immediate edge-to-edge neighbors.

Level	Metric	Units	Description
<i>Patch</i>	Patch area	m^2	Area occupied by each patch, not including any internal gaps
	Patch perimeter	m	Length of patch perimeter, including internal gaps
	Percent interior gap	%	Patch interior gaps expressed as % of patch area, providing an estimate of patch density
	Radius of gyration	m	Mean distance between each patch cell and patch centroid, estimating patch areal extent and density
	Perimeter to area ratio	-	Ratio of patch perimeter (m) to patch area (m^2)
	Shape index	-	Shape complexity compared to a standard square
	Related circumscribing circle	-	Ratio of patch area to smallest circumscribing circle area, estimating patch elongation and density
	Circumscribing circle radius	m	Radius length of smallest circumscribing circle, estimating patch linear extent
<i>Class</i>	Percentage of landscape	%	Percent of landscape occupied by each class
	Number of patches	-	Total number of patches for each class
	Mean patch area	m^2	Mean patch area of each class, not including gaps
	Patch density	m^{-2}	Number of patches per square meter for each class
	Largest patch index (class)	%	Percent of landscape occupied by largest patch for each class
	Clumpiness index	-	Measure of patch dispersion, ranging from -1 (most disaggregated) to 1 (most clumped)
<i>Landscape</i>	Landscape area	m^2	Total area of the entire landscape
	Largest patch index (landscape)	%	Percent of landscape occupied by largest patch of all classes

Table 4-1. Landscape metrics used for characterizing configuration and composition of the landscape at three levels: patch, class (comprising all patches of each category), and landscape. Metrics are either defined in the literature (i.e., McGarigal et al. 2012) or adapted from similar metrics.

4.2.3 Landscape- and Patch-Scale Analysis

Landscape configuration and composition were quantified from the classified images using multiple metrics of landscape structure. Landscape metrics were applied

using the FRAGSTATS software utility (McGarigal et al. 2012) in conjunction with ArcGIS v10.1. Patch-scale analysis focused on eight patch-level metrics, while landscape-scale analysis included two landscape-level and six class-level metrics (Table 4-1). Collectively, these metrics described multiple aspects of the composition, size, shape, and aggregation of patches within the landscape. Detailed descriptions of each metric can be found in the FRAGSTATS documentation and other published literature (McGarigal et al. 2012). Cell adjacency was defined for all metrics by the 8 nearest neighboring cells, same as in the image classification procedure.

The landscape-scale analysis focused on class and landscape level metrics from a single classified image (taken 20 October 2010) to describe the arrangement of both bivalves and macrophytes. Though multiple images of the landscape were analyzed, a single image was selected for the application of landscape metrics to avoid any confounding inconsistencies between images. The selected image offered the best balance between spatial resolution and spatial extent, encompassed sufficient GCPs to ensure accurate georeferencing, and contained minimal distortions from sun glare. For the seagrass classification, a threshold minimum mapping unit (MMU) of 350 contiguous pixels ($\sim 0.7 \text{ m}^2$) was applied to maintain focus on larger patches, in part due to potential confusion between bivalves and macrophytes resulting in the misclassification of very small patches. No MMU was applied to the bivalve class.

In contrast to the landscape-level, patch-scale metrics focused strictly on a subset of four seagrass patches to view the changes in metric values between the two sampling dates (8 July 2008 to 20 October 2010). The images chosen for patch-scale analysis covered approximately the same spatial extent and were taken at similar altitudes to

minimize differences in spatial resolution. These images were then cropped down to the selected subset area for comparison and analysis. Various metrics describing patch characteristics as well as the configuration of gaps internal to each patch were calculated (Table 4-1).

4.3 Results

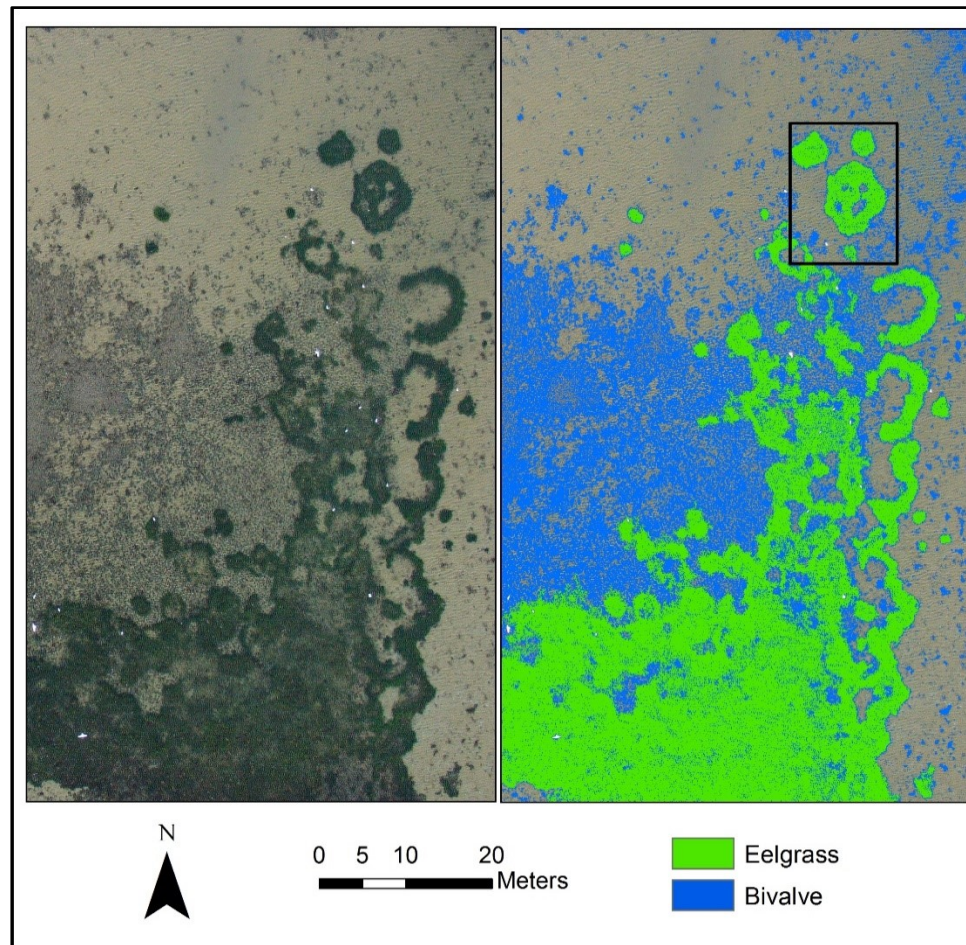


Figure 4-2. Map showing the raw unclassified imagery (*left*) with classified bivalve and eelgrass patches superimposed (*right*). The area of interest for patch-scale analysis is outlined at right. The spatial resolution of the imagery is 0.045 m.

4.3.1 Landscape-Scale Analysis

Analysis at the landscape scale included metrics operating over the entire mosaic and at the class level (i.e., eelgrass and mussel categories). The primary photo used for landscape-scale analysis was taken at an altitude of 121 meters, resulting in a spatial resolution (pixel edge length) of 0.045 m (4.5 cm) and a pixel area of 20.25 cm².

Classification produced a categorical map of eelgrass and bivalve patches interspersed throughout a background matrix of soft sediments (Figure 4-2).

The entire landscape encompassed an area of 4881 m², of which 27.9% was classified as eelgrass, 25.1% as bivalve, and the remaining balance (47%) as background sediments. Seagrass and bivalve classes were comprised of 29 and 29732 patches with mean patch area of 47.1 m² and 0.041 m², respectively. Correspondingly, patch density was much higher for the bivalve class (6.1 m⁻²) compared to seagrass (0.0059 m⁻²). The largest patch index (LPI) for the entire landscape was 23.9%, representing the large contiguous area of seagrass in the lower third of the image. At the class level, LPI for the bivalve category was 12.6%, and LPI for seagrass was 23.9%, resulting from the same patch as at the landscape level.

At the class level, the clumpiness index indicated relatively high patch aggregation for both eelgrass (0.881) and mussel (0.6566) classes. This metric is calculated from a categorical adjacency matrix measuring the proportion of similar or dissimilar cells neighboring each pixel. The index measures the deviation from a random distribution of cells, ranging from -1 (maximum disaggregation) to 0 (random) to 1 (maximum aggregation). The eelgrass class was highly aggregated, occurring primarily as large patches with a high proportion of like adjacencies. Eelgrass occurred primarily in the eastern and southern regions of the landscape and was largely absent from the mussel-dominated western area. Mussels are clumped to a lesser degree, reflecting the relatively smaller mean patch size and wider dispersion throughout the entire landscape.

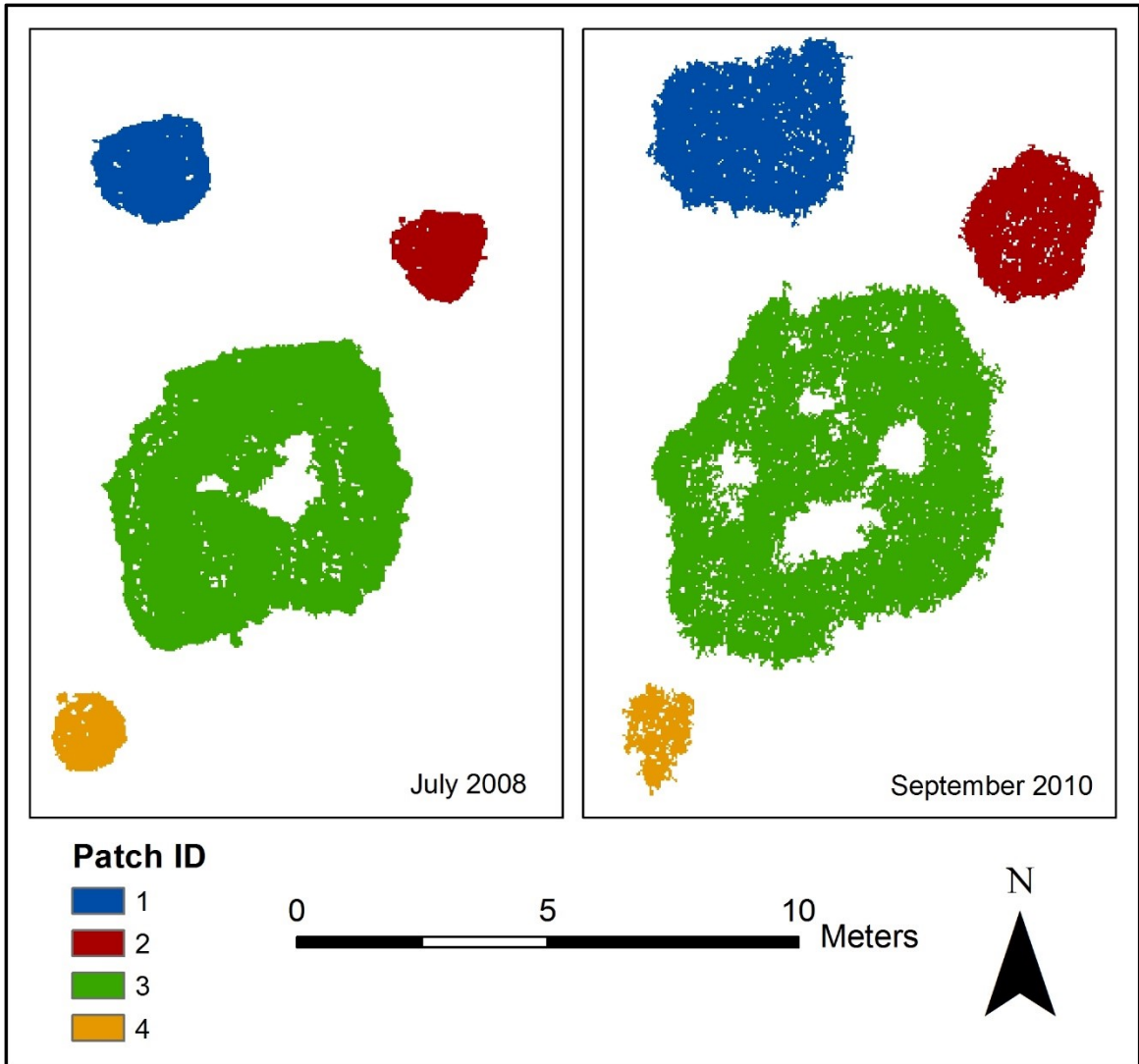


Figure 4-3. Depiction of the temporal change in four selected patches from imagery collected on 8 July 2008 (*left*) to 20 September 2010 (*right*). The spatial resolution (i.e., pixel edge length) of the 2008 and 2010 images are 0.0353 m and 0.0368 m respectively.

4.3.2 Patch-Scale Analysis of Eelgrass

Patch scale analysis focused exclusively on a multi-temporal analysis of four eelgrass patches representing a subset of the larger landscape (Figure 4-3). Each of the four patches in the subset area persisted as distinct entities over the 26 months between sampling dates. The selected image from 2008 was taken at an altitude of 103.3 m,

resulting in spatial resolution of 0.0353 m (3.53 cm) and pixel area of 12.5 cm². The 2010 image was taken at 108.8 m, corresponding to 0.0368 m (3.68 cm) resolution and pixel area of 13.5 cm².

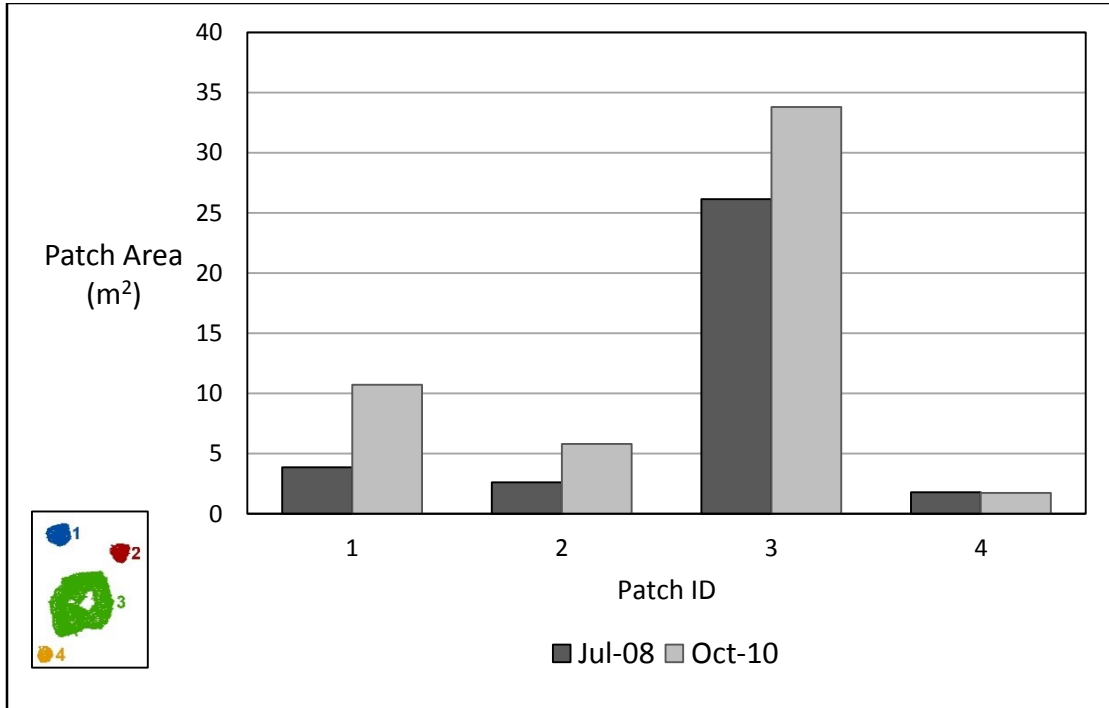


Figure 4-4. Change in patch area (m²) for four patches from July 2008 to October 2010. Does not include internal gap areas. (*Inset*) Relative patch location by patch ID.

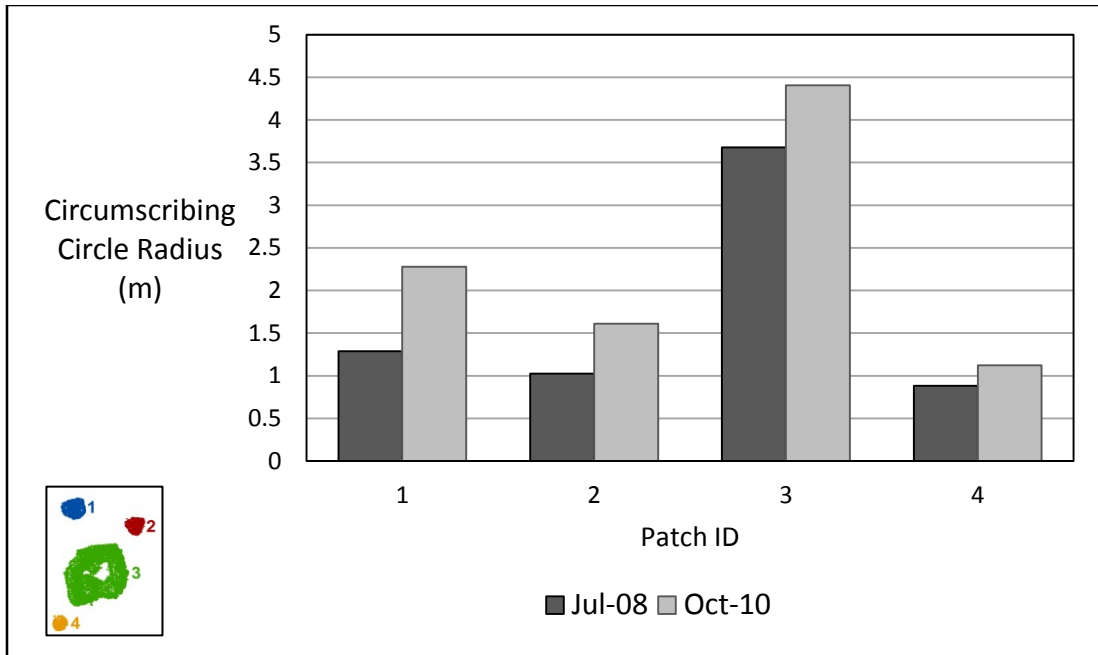


Figure 4-5. Change in circumscribing circle radius over the sampling period, measuring the radius of the smallest circumscribing circle for each patch. This metric estimates the maximum lateral expansion or retraction for each patch, and provides an estimate of patch linear extent. (*Inset*) Relative patch location by patch ID.

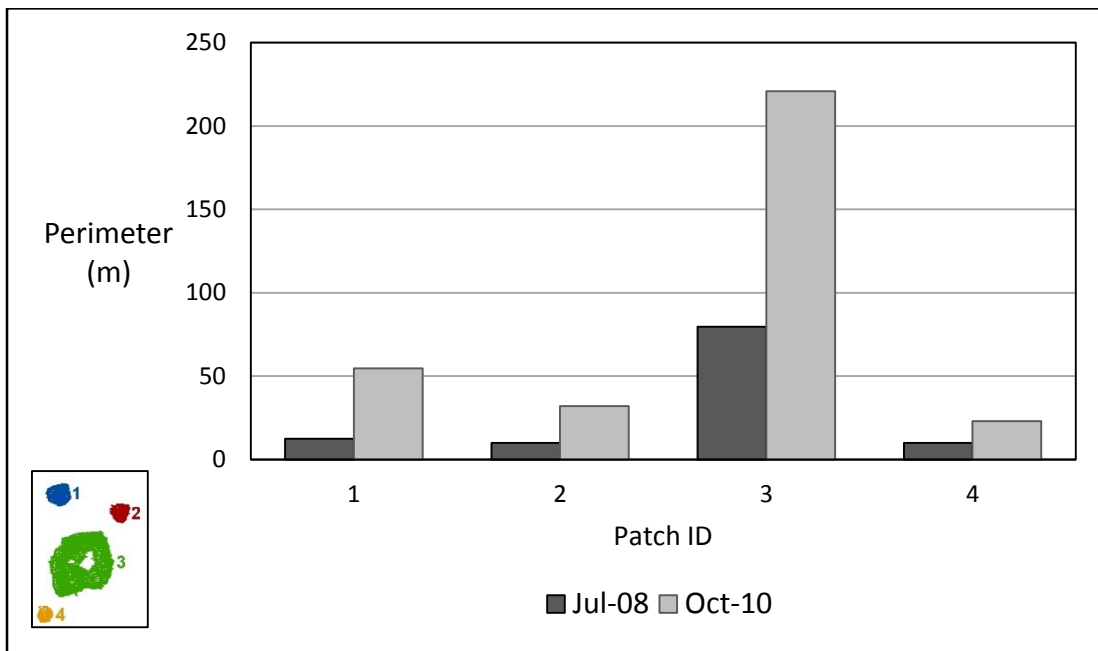


Figure 4-6. Change in patch perimeter length (m) for four patches between the sampling dates, including internal perimeter associated with patch gaps (*Inset*) Relative patch location by patch ID.

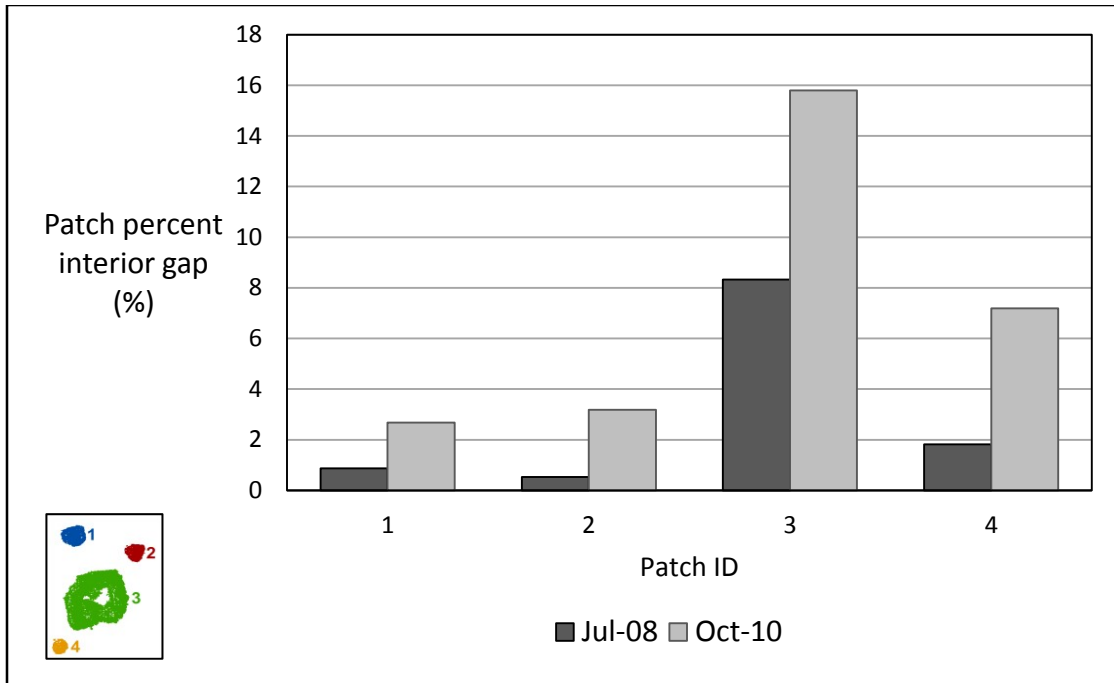


Figure 4-7. Change in interior patch gaps over the study period, expressed as a percentage of total patch area. (*Inset*) Relative patch location by patch ID.

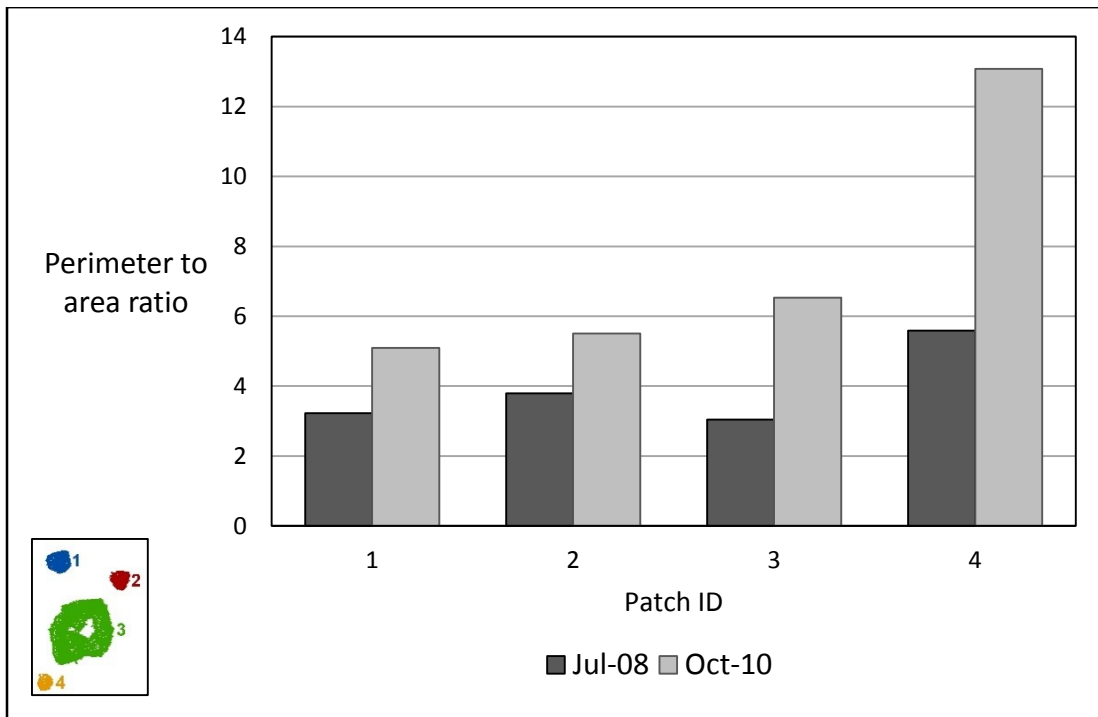


Figure 4-8. Change in perimeter-to-area ratio for each patch between the sample dates. This metric provides an estimate of patch shape complexity. (*Inset*) Relative patch location by patch ID.

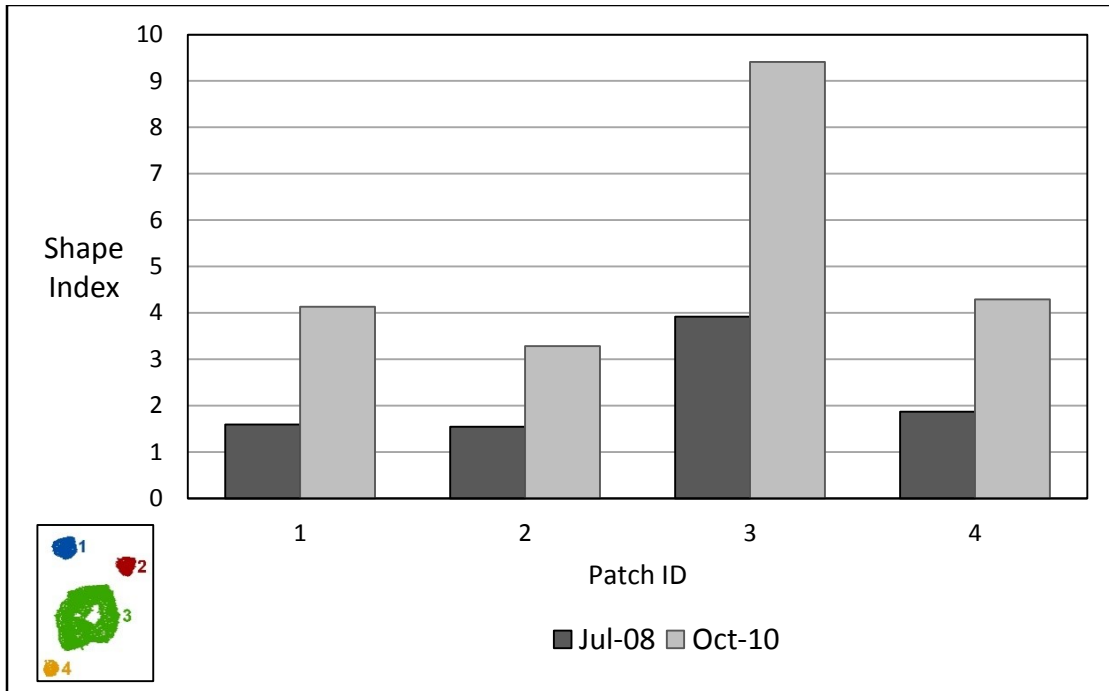


Figure 4-9. Change in shape index over the sampling period, estimating complexity relative to a standardized square shape. (*Inset*) Relative patch location by patch ID.

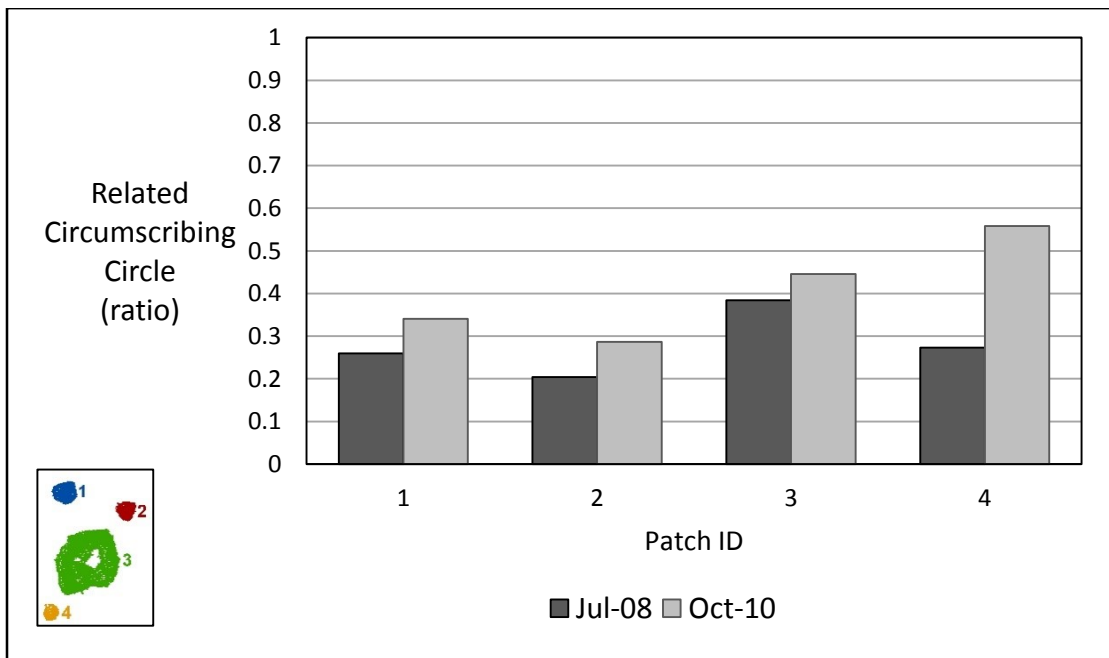


Figure 4-10. Change in the related circumscribing circle metric over the sample period. This metric measures the area of a patch relative to the area of its smallest circumscribing circle, providing estimates of patch density and elongation. (*Inset*) Relative patch location by patch ID.

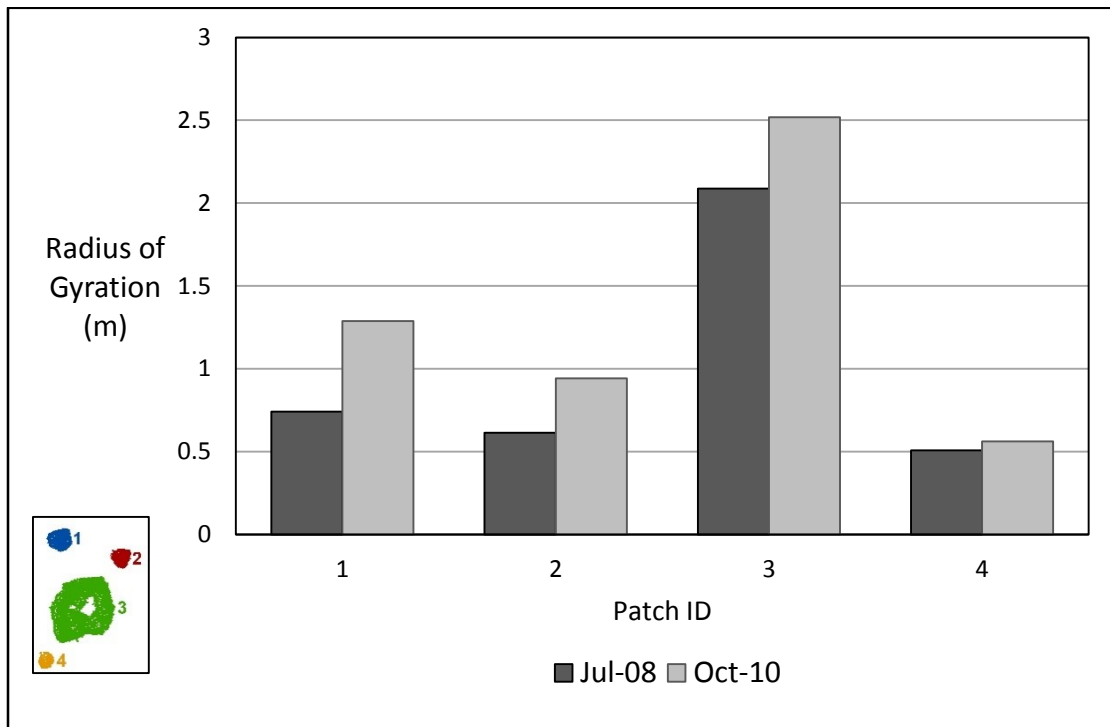


Figure 4-11. Change in the radius of gyration metric for each patch, calculated as the mean distance from each cell of the patch to the patch centroid. This metric estimates the weighted areal extent of each patch as well as patch elongation. (*Inset*) Relative patch location by patch ID.

Collectively, the four patches increased their total area from 34.4 m² to 52.1 m² over the study period. Three of the patches increased in area over the time period, while patch four registered a slight areal decline (Figure 4-4). Patch linear extent as measured by the radius of the smallest circumscribing circle showed an increase for all four patches, with the largest growth (0.99 m) occurring at patch 1 (Figure 4-5). This indicates that all four patches experienced lateral expansion in at least one dimension over the time period despite the overall reduction in area for patch 4. Adjusted for the 26 month period between sampling, the mean patch radius expansion rate observed for all

four patches was 0.29 ± 0.14 (SD) m y^{-1} , and the maximum rate at patch 1 reached 0.46 m y^{-1} .

All four patches experienced increases in perimeter length with the largest rise occurring at patch 3 (Figure 4-6). These increases were driven by patch expansion as well as the growth of interior gap areas creating “interior perimeter” as patches thinned (Figure 4-7). Patch 3 experienced the greatest change with internal gap area increasing from 8.3% to 15.8% of total patch area. This was also the largest rise in absolute terms with an additional 3.16 m^2 of gap area appearing over the time span, indicating a substantial decrease in patch density.

Patch shape metrics indicated increasing complexity over the time period of the study. Perimeter to area ratio increased for all four patches with the largest rise observed at patch 4 (Figure 4-8). This was driven in large part by the widening of interior gaps creating internal perimeter, as well as increasing complexity of the external borders. Due to the scale-dependence of perimeter to area ratio, the shape index was also calculated. This metric corrects for scale-dependence through reference to a standard square shape equal in area to the patch so that a square produces a value of one, and increases with rising complexity (McGarigal et al. 2012). Following this correction, all four patches still exhibited increasing complexity over the span of the study, though the largest increase was observed at patch 3 (Figure 4-9).

The related circumscribing circle metric provides another measure of patch elongation as well as density, based on the ratio of patch area to the area of the smallest circumscribing circle. Low values generally represent regular circular shapes, though highly convoluted patches may still have low value if they are relatively compact.

Higher values indicate increasing patch elongation. This metric increased for all four patches over the study period with the largest rise at patch 4 (Figure 4-10). Modest increases for patches 1-3 were caused by decreasing patch density causing the patch to fill less of the smallest circumscribing circle. The large increase at patch 4 was likely due to a similar density effect as well as apparent narrowing and elongation in the north-south direction.

The radius of gyration metric calculates the mean distance between each cell of the patch and the geometric patch centroid, and as such represents a density-weighted measure of patch areal extent and a measure of patch elongation. This metric increased for all four patches, albeit to a lesser degree for patch 4 (Figure 4-11). Increased patch linear extent led to increased radius of gyration, though this was tempered somewhat by decreased patch density, particularly for patch 4.

4.4 Discussion

4.4.1 *Landscape-Scale Investigation*

At landscape scale, the image data collected in this study captured classes of seagrass and bivalves, moving the frame of reference beyond binary classification to a patch-mosaic landscape model representative of increased thematic complexity (Wedding et al. 2011). Although seagrasses have been a primary focus of most marine studies using landscape metrics, bivalve landscape structure has also been explored, particularly with respect to the fractal geometry of blue mussel patch shape (Snover & Commito 1998, Kostylev & Erlandsson 2001, Crawford et al. 2006). Co-occurrence of both bivalves and seagrass on soft sediments have been studied with respect to plant growth, sediment biogeochemistry, and water clarity (Reusch et al. 1994, Wall et al. 2008, Vinther et al. 2012), primarily in European waters. However, studies applying landscape metrics to coexisting seagrass and bivalve habitats are absent from the scientific literature. In Atlantic Canada, no previous studies have described such a mosaic due to the rarity of soft-bottom mussel reef formations in the region.

The distribution of seagrass and mussels throughout the landscape depicts a complex assemblage of patches varying in size and configuration. The total area of each patch type was very similar, though configuration and distribution were markedly variable. Eelgrass formed discrete patches of various sizes in the upper part of the landscape that fused into a larger aggregation in the lower region. By contrast, mussels formed a much larger number of patches packed in a tight matrix without visibly distinctive patch boundaries at landscape scale. These differences were quantified by the metrics representing patch number, mean patch area, and patch density. The clumpiness

index indicated that both patch types were highly clumped, though eelgrass exhibited the highest degree of aggregation. This is reflected in the smaller number of patches and larger mean patch size of eelgrass relative to mussels.

Despite the very high resolution of the imagery collected in this study, fine-scale mussel patterns were difficult to capture due to the relatively small size of most mussel patches. The mean patch size of 0.041 m² was greatly influenced by a single complex aggregation comprising 50.2% of total class area. Omission of this largest patch corresponded to a mean patch size of 0.021 m² for the remaining 29,731 patches, equivalent to only ~10 pixels per patch. The relative paucity of pixels introduces a large amount of error into the calculation of landscape metrics, suggesting that alternative sampling methods or higher-resolution imagery would be preferable for mapping fine-scale mussel bed landscape structure. Previous investigations of mussel patch structure focused on the extent of a sampling quadrat (e.g., ~ 0.25 - 1 m²) allowing the determination of very fine-scale patch metrics at the expense of spatial extent (e.g., Crawford et al. 2006). This shows the importance of spatial scale in mapping patch patterns, as a trade-off exists between resolution and spatial extent, with the low-altitude photography used in this study representing a compromise between the two. Further, the spatial scales appropriate for mapping seagrass patches may not be similar to those in bivalve assemblages. This suggests that some of the structuring processes operate at different spatial scales.

The topography of the mussel bed exhibited high relief in the vertical dimension, creating multiple spectral signals between dry and inundated regions. This was further complicated by difficulty in discriminating between live and dead mussels, as both return

a similar optical signal. The image classification algorithm also had difficulty with the scattering of light caused by glare on water ripples over inundated areas of the landscape. Subtidally, mussels were difficult to differentiate from seagrasses under varying levels of inundation due to the attenuation of light in seawater creating a depth-dependent response. Confusion between mussels and seagrass was also caused by the close coupling of mussel and seagrass patches, with mussels commonly being found within or underneath the seagrass canopy. In particular, it was difficult to differentiate between mussel and seagrass habitats in the lower portion of the image where patch boundaries were not readily apparent. The eelgrass canopy may have obscured smaller interspersed patches of mussels. However, this close association of mussel and eelgrass patches suggests that cohabitation may confer benefits to one or both of these biogenic landscape components.

4.4.2 Patch-Scale Investigation

The overall changes in seagrass metrics observed at the patch-scale are consistent with the expansion of patch borders at the expense of patch density and integrity. Patches 1-3 exhibited similar changes in several of the calculated metrics, with differences only in degree. These changes generally represented increasing patch size and linear as well as areal extent, decreasing density due to the establishment and enlargement of internal gaps, and increasing shape complexity due to growth in patch perimeter length relative to area and internal gap expansion. Patch 4 behaved similarly with the notable exceptions of a slight decline in patch area, a very small increase in patch linear extent, and a comparatively large increase in patch elongation as estimated by the related

circumscribing circle metric. Though it is difficult to separate the effects of these changes on each individual metric, metrics that measure multiple aspects of spatial pattern, such as radius of gyration, can be used to clarify the spatial dynamics of landscape change.

It has been frequently noted that landscape metrics can be redundant or highly correlated, with several metrics available to capture aspects such as the extent, density, and complexity of landscape structure (Wagner & Fortin 2005, Cushman et al. 2008). This was observed to some degree in this study. Many metrics are derived from measures of patch area and perimeter length, causing inherent correlation. Although recent studies have worked to determine which suites of metrics best apply to marine habitats such as seagrasses (e.g. Sleeman et al. 2005), more work is required, and it is likely that a variable suite of metrics will be required to address site-specific differences in landscape structure.

Seagrass patches can be formed either through the fragmentation of an existing meadow or through colonization of previously unoccupied habitat (Duarte et al. 2006). The establishment of new patches can occur through reproductive seed dispersal or the uprooting and export of entire plants during storm events. Once established, patches expand clonally through horizontal rhizome expansion followed by the sprouting of new leaves (Duarte et al. 2006). Studies have shown that the horizontal rhizome elongation rate of *Zostera marina*, the primary mechanism of clonal patch expansion, occurs at a mean rate of 0.26 m y^{-1} (Marbà & Duarte 1998), though other seagrass species experience rates an order of magnitude higher.

Patch expansion as estimated by the radius of gyration metric indicated rates well within values for *Z. marina* found in the literature. However, this metric is weighted by

patch density as well as extent, confounding insight into the magnitude of lateral patch expansion. Radius of gyration could have increased due to lateral expansion, through the “thinning” of patch interior, or through a combination of both processes. The circumscribing circle radius metric was adapted to provide an estimate of the maximum lateral expansion for comparison to literature rates. The mean patch expansion rate of 0.29 m y^{-1} fell very close to values reported in the literature (e.g., Marbà & Duarte 1998), though this metric does not account for corresponding decreases in patch density.

The use of high resolution low-altitude aerial photography added value that could not be easily matched using satellite imagery. In particular, we were able to track the evolution of patch metrics over the course of a 26 month period. The relatively low cost of the method allowed multi-temporal sampling and monitoring of the ongoing growth and fragmentation at the patch-scale, as opposed to most seagrass monitoring that occurs at coarser resolution. The high resolution also allowed the detection of internal patch gaps, adding valuable information to the analysis and greatly impacting the results. If these intra-patch gaps had not been detected, it would not have been possible to detect the decreases in density that occurred alongside overall patch growth and expansion. This would likely lead to a very different interpretation of the trajectory of the landscape, with major ramifications for management of the resource.

Notably, image acquisition dates for the patch-scale investigation occurred 27 months apart, with the first acquisition in July 2008 and the second in October 2010. In Nova Scotia, October is the end of the eelgrass production season, at which point new growth slows and some meadows may begin to decline in extent (Robertson & Mann 1984). Seasonal changes in the eelgrass bed may have influenced the quantification of

the change in patch metrics through time. Eelgrass blades also may have begun to defoliate, accounting for the apparent reduction density despite patch expansion. Assessing the effects of seasonal dynamics would require regular data acquisition and monitoring throughout the growing season.

Short-term temporal dynamics also may have impacted the results of this study. The tidal height at time of acquisition also differed between the two sample dates, from 0.25 m above “lower low water, large tide” (LLWLT) in 2008 and 0.57 m above LLWLT in 2010, though both sampling dates were planned to coincide with the ideal tide and sun angle conditions. The balloon platform can only be flown in dry, low-wind weather conditions, complicating the timing of repeated surveys. However, weather-dependence is common to all aerial photographic methods, and is likely more easily managed given the simplicity of the platform in comparison to powered aircraft or satellites (McKenzie et al. 2001).

4.4.3 Drivers of Landscape Structure

Landscape structure is formed and maintained through the interaction of multiple dynamic physical, chemical, and biological processes. Physical factors related to the hydrodynamic regime strongly influence the landscape structure of seagrass habitats (Fonseca et al. 1983, Fonseca & Bell 1998). Seagrasses in high-energy environments tend to exist as fragmented meadows, while intermediate-energy areas form dense and continuous meadows (Bell et al. 2006). They generally require an intermediate level of hydrodynamic exposure for optimal growth, as low-flow environments can create poor

conditions due to the establishment of epiphytes that inhibit photosynthesis and other effects related to light availability (Fonseca & Kenworthy 1987, Madsen et al. 2001).

Hydrodynamic processes can also affect patch structure directly through physical disturbance or removal from high-energy storm events causing “blowouts” (Patriquin 1975). Erosion caused by current scouring can expose the rhizomes, causing mortality and creating internal patch gaps similar to those seen in patch 3 (Figure 4-3). Reduced current speeds over dense seagrass can also lead to the deposition of suspended sediments, causing burial and mortality inside of larger patches. This effect may be particularly apparent following mass sedimentation following storm events. Interaction between these processes often result in hollowed-out “donut” shapes as blowouts increase in size and frequency (Fonseca & Kenworthy 1987). Under high hydrodynamic stress, patches also may form “C” shapes as sediments migrate through the patch, often resulting in patch mortality. Patch survival from large disturbances such as storms appears to be size- and density-dependent. Larger and denser patches are able to withstand greater hydrodynamic stress due to mutual sheltering and greater anchoring from root and rhizome structures (Bos & van Katwijk 2007).

Hydrodynamic pressures were likely a main driver of pattern at Eastern Passage at both landscape and patch scales. At the patch scale, all four patches persisted over the course of the study, successfully resisting dislodgement from hydrodynamic forces. All four similarly increased in spatial extent, and all but the smallest patch increased in area as well. However, the increased internal gap area observed at each patch was most likely a result of hydrodynamic stress causing blowouts and sedimentation, as has been witnessed in previous studies (Fonseca et al. 1983, Fonseca & Kenworthy 1987). Patch 3

in particular resembled the characteristic “donut” shape, and was likely progressing towards a “C” shape as was visible in other patches throughout the landscape. At the landscape scale, the irregular pattern of the seagrass bed results from frequent blowouts coupled with the growth and establishment of new patches, creating a spatially and temporally dynamic landscape similar to the “leopard skin” pattern seen in previous studies (e.g., Fonseca et al. 1983). Despite the hydrodynamic pressure, the bed shows some signs of stability, persisting in its present location at Eastern Passage for at least 10 years. This suggests that the seagrass bed has reached a dynamic equilibrium, even as patch and landscape structure varied widely over the same time span.

At the scale of individual plants, the physical environment influences morphology as well as reproductive strategy (Moore & Short 2006). Under high hydrodynamic stress, seagrasses tend to devote a greater share of resources to belowground biomass (i.e., roots and rhizomes) to protect against uprooting (Fonseca et al. 1983). In Nova Scotia, the commonly perennial species *Z. marina* has been seen to occur as an annual variety in intertidal areas in response to ice scouring, a particularly important structuring factor in high-latitude areas (Keddy & Patriquin 1978, Robertson & Mann 1984). Physical disturbance also correlates with the relative amount of energy devoted to reproduction vs. clonal growth, with seagrasses growing in highly dynamic areas typically expending relatively more energy on sexual reproduction.



Figure 4-12. Waterfowl (probably American black duck, *Anas rubripes*) grazing within eelgrass patches at the study site during imagery acquisition on 20 September 2010. Internal patch gaps are clearly evident.

Seagrasses can also be subject to bioturbation from grazing species of waterfowl (van der Heide et al. 2012) or invasive species such as the green crab (Garbary et al. 2014). Eelgrass is an important food source and habitat for many migratory seabirds in Atlantic Canada (Seymour et al. 2002, Hanson 2004). The effects of grazing on seagrasses are complex, though consumption by waterfowl has been linked to significant decreases in seagrass biomass in multiple studies (Valentine & Heck 1999). Grazing by waterfowl may also lead to stimulation of growth, as in terrestrial ecosystems, though this has been relatively understudied (Valentine & Duffy 2006). Waterfowl such as the American black duck (*Anas rubripes*) are commonly found grazing within seagrass

meadows at the Eastern Passage study site, as evidenced by photos captured during data collection (Figure 4-12). Eelgrass beds in Nova Scotia also have historical importance for local and migratory populations of species such as the Atlantic Brant (*Branta bernicla hrota*) and Canada goose (*Branta canadensis*) (Hanson 2004). The magnitude and influence of waterfowl grazing on patch growth and survival at this site are unknown, though it is a possible cause of increased internal gaps over the study period.

Other factors known to affect the growth and survival of seagrasses include water temperature, sediment geochemistry, anthropogenic disturbance and eutrophication, and disease (Duarte et al. 2006). Seagrasses can be damaged by low-oxygen sediments stimulating sulfide production (Pedersen et al. 2004), and this has been hypothesized as a driving factor of patch shape in some environments (Borum et al. 2013). Sulfide dynamics are known to play an important role in nutrient cycling at the Eastern Passage tidal flat (Grant 1986) and cannot be ruled out as a potential driver of seagrass landscape structure at the site.

Several studies have described patterns in vegetation as a product of self-organization, where emergent patterns are shaped by interactions between environmental pressure and intraspecific biological interactions (Fonseca et al. 2007, van der Heide et al. 2010, van der Heide et al. 2012). Patch structure is formed and maintained through feedback between physical forcing and seagrass response, for example when seagrasses respond to hydrodynamic pressure by devoting greater resources to below-ground biomass. Patterns may arise from feedbacks driven by reduced stress from water movement and increased light availability (Fonseca et al. 2007). High-density patches are also subject to increased intraspecific competition for light and nutrients. The

benefits of mutual anchoring at the local or patch scale are mediated by competition for light and nutrients at landscape scale. This type of self-organization can manifest as regularly spaced bands of patches oriented perpendicular to the flow, or as irregular patchiness in more complex systems.

While the patch metrics implemented in this study effectively chart the type and magnitude of patch-scale change, determination of causation is a greater challenge. While hydrodynamics are undoubtedly a main driver of patch pattern, feedback from these stresses and other biotic and abiotic factors may also have played important roles. Currently, the ability to predict self-organized patterns in response to environmental drivers is lacking (van der Heide et al. 2010). Predictive models would be greatly beneficial for understanding spatial and temporal dynamics, benefitting the monitoring and management of seagrass habitat (Bell et al. 2006).

Principles of self-organization are also apparent in soft-sediment bivalve reef habitats (van de Koppel et al. 2005). Mussels clump together into aggregations intertwined by byssal threads, providing mutual anchoring support against dislodgement (Reusch & Chapman 1995, van de Koppel et al. 2005). Hydrodynamic forces can strongly influence the distribution of mussels, particularly in soft-sediment areas where they are not directly attached to stable hard substrate. The positive benefits of mutual anchoring are mediated by competition for food suspended in the water column. Mussel beds often form regular elongated patches perpendicular to the direction of flow, though patterning is more fractal and irregular when exposed to storms or variable hydrodynamic conditions (van de Koppel et al. 2005).

At the landscape scale, mosaic structure is shaped by physical and intraspecific processes as well as interspecific relationships between multiple ecosystem components, such as the eelgrass and mussels described in this study. Studies of seagrass–bivalve relationships have been equivocal, with hypothesized positive and negative effects for both species. Positive mechanisms include mutual protection against hydrodynamic stressors, reduced turbidity and increased light through bivalve filter-feeding, reduction in epiphytes, and nutrient fertilization through biodeposition to the sediments (Reusch et al. 1994, Reusch & Chapman 1995, Peterson & Heck 2001). These positive influences are offset by potential negative impacts such as changes in nutrient cycling, anoxia due to organic matter deposition, competition for space, and locally increased current speeds due to geomorphological changes (Vinther et al. 2008).

Eelgrass and soft-sediment mussels respond similarly to hydrodynamic forces, forming patch-scale aggregations to resist dislodgement. The resultant effects on landscape pattern depend on feedback responses to these forces, which would be expected to vary greatly between bivalve and macrophyte groups. Apparent differences in the size structure, configuration, and dispersion of mussel and eelgrass classes likely resulted from differential responses to similar hydrodynamic conditions in the tidal flat. Interactions between the eelgrass and mussels also influenced the persistence of both habitats. Previous studies have shown seagrass to prevent the dislodgement of mussel beds through current attenuation, and to catch dislodged mussel aggregations (Reusch & Chapman 1995). Similarly, the presence of mussels has been shown to provide shelter for eelgrass (van Katwijk et al. 2009).

4.4.4 *Implications for Landscape Analysis*

The use of low-altitude aerial photography allowed for the detection of changes in patch metrics at a spatial scale that is difficult to match using other data sources. Many landscape metrics are known to be highly sensitive to spatial scale, and can misrepresent landscape structure if there is a scale mismatch with the landscape of interest (Wiens 1989, Qi & Wu 1996). The high-resolution imagery collected for this study allows for the detection of patterns that would be obscured at coarser resolution. The patch-scale component of this study focused explicitly on patch metrics at very fine resolution, with pixel edge lengths (< 5 cm) an order of magnitude smaller than most aircraft-based aerial photography, and two or more orders of magnitude finer than common satellite-based remote sensing. By comparison, the highest-resolution multispectral satellite data currently available to non-military users is limited to a 2 m pixel edge length. Given the sensitivity of landscape analysis to spatial scale (Wiens 1989, Wedding et al. 2011), enhanced resolution imagery offers insight to landscape patterns that are difficult to detect and interpret from other aerial datasets.

The aerial photography platform used for this study provided very high-resolution spatial data representing the structure of an intertidal-subtidal landscape. Image acquisition was inexpensive and efficient with respect to time and cost in comparison to aircraft or satellite platforms, allowing for frequent surveys to monitor and detect changes in landscape structure. The balloon platform also allows for multi-scale analysis as demonstrated in this study, increasing the ability to detect and analyze scale-dependent patterns. Few previous studies have used low-altitude photography from balloon or kite

platforms to map marine landscapes (though see Edwards & Brown 1960, Guichard et al. 2000, Bryson et al. 2013) despite clear benefits of the approach. Combined with increased flexibility for dealing with constraints due to weather and environmental conditions, the balloon platform used in this study represents an effective and efficient data source for conducting analyses of intertidal and shallow subtidal landscape structure. Improvements to the quality and resolution of marine landscape data add to the ability of researchers to understand the spatial and temporal dynamics of coastal habitats in the face of increasing stress on coastal health worldwide (Orth et al. 2006).

Most landscape metrics commonly applied to seagrasses were originally devised for terrestrial habitats, and direct assessments of their applicability in the marine context are relatively rare (though see Sleeman et al. 2005, Wedding et al. 2011). Collection of landscape data in the marine environment presents challenges that may limit the effectiveness or complicate interpretation of certain metrics. Determining which suite of metrics best describe important aspects of seagrass landscape structure is recognized as a crucial area for future research (Bell et al. 2006, Wedding et al. 2011). In some cases, the patch-mosaic model of discrete patches that has dominated landscape analysis may not easily describe continuous phenomena, such as near-continuous seagrass beds lacking clear patch borders (Barrell & Grant 2013) or 3D features such as seafloor topography (McGarigal et al. 2009). The continued establishment of landscape metrics for quantifying spatial structure of marine habitat will likely require further studies of metric applicability as well as the development of new methods for analyzing marine landscape structure.

While the discrete patch remains the focal point of most studies of seagrasses applying landscape metrics, the focus is commonly on class- or landscape-level metrics summarizing the spatial attributes of a large number of patches or over a very large extent (~kms) relative to the current study (Wedding et al. 2011). This has in part been driven by difficulties in collecting fine-resolution data over large spatial extents at high temporal frequency. Ongoing improvements in remote sensing technology, image classification, and landscape analysis highlights the need for continued research into the application of landscape ecology techniques in seagrass ecosystems and the marine environment.

4.4.5 Conclusions

The dynamics of coastal landscapes are spatially and temporally complex, involving multiple physical and biological processes with nonlinear interactions. Detection of fine-scale patch pattern is a crucial prerequisite for understanding the spatial dynamics of the relationship between eelgrass and blue mussels at the landscape scale. Quantification of landscape mosaic structure provides critical information for many aspects of conservation, coastal management, and marine spatial planning (Boström et al. 2011). Understanding of the landscape-scale relationship between seagrasses and bivalves has great implications for habitat restoration (Bell et al. 1997). For example, landscape context can strongly influence ecosystem service valuation (Barrell et al. 2014), and has been shown to affect the successful persistence of restored habitats (Bos & van Katwijk 2007). Knowledge of the spatial scale of variation is also a critical component of ecosystem monitoring (Neckles et al. 2012) and predictive modeling.

The use of low-altitude aerial photography in this study demonstrates a low-cost method for collecting high-resolution data representing intertidal-subtidal landscape structure. The application of spatial metrics at landscape- and patch-scale quantified elements of the configuration and composition of an uncommon seagrass-bivalve habitat mosaic. This approach allowed for the tracking of patch metrics through time, depicting landscape change at the patch-scale. Continued development and application of landscape metrics in marine habitats will increase understanding of the ecological function of these areas.

Chapter 5. Conclusions

5.1 Synopsis

This thesis represents advancement in the application of remote sensing to spatial landscape analysis in seagrass habitats through multiple avenues. Acoustic (Chapters 2 & 3) and optical (Chapters 3 & 4) remote sensing were applied for the quantification of seagrass landscape pattern, leading to new insights on the distribution and spatial pattern of coastal habitats. Collectively, the content of this thesis integrates field data collection using state of the art technology with novel spatial analysis techniques to increase understanding of the spatial dynamics of important coastal marine habitats. These advances offer many potential benefits for the management and conservation of coastal resources.

In **Chapter 2**, acoustic single-beam data was used to describe seagrass landscape pattern using the novel application of local spatial statistics. The Getis-Ord G_i^* statistic allowed for the detection of areas of high and low cover within a spatially continuous seagrass bed. This technique was also able to discern boundary zones not easily detectable with optical data, and used the quantitative measure of percent cover provided in the acoustic data more comprehensively than in previous studies. Local spatial statistics also depicted spatial pattern at multiple spatial scales as defined by the neighborhood search radius.

Chapter 3 comprised a detailed comparison of acoustic and optical remote sensing for the collection of seagrass spatial data, and also served to identify multiple ways of conceptualizing seagrass habitat. The implications of uncertainty in seagrass

mapping and monitoring were also explored. The results highlighted the importance of considering spatial scale when mapping submerged aquatic vegetation.

Chapter 4 described a unique landscape of seagrass and bivalves occurring in close proximity to an urban area. The low-altitude aerial photography platform aided in the collection of very high-resolution data representing this mosaic, showcasing a promising source of data representing coastal landscapes. Temporal change in eelgrass patch structure was observed and quantified, highlighting the temporal dynamics of coastal landscapes.

5.2 Future Work

Many suggestions for future work were identified in the composition of this thesis. These suggestions are both theoretical and methodological in scope. Improvement in spatial data collection from acoustic and airborne remote sensing, as detailed in the preceding chapters, has opened many new avenues for research through the increasing availability of high-resolution broad extent spatial datasets representing seagrass habitat. Researchers can now access data at spatial resolution and extent previously inaccessible to remote sensing, and can do so with much greater temporal resolution as costs continue to decline. This wealth of data also raises many new questions and challenges that will need to be addressed for the advancement of spatial ecology in the coastal zone.

5.2.1 Applications to Management

The increase in spatial knowledge and tools developed through this thesis suggest several potential applications for the management of seagrasses and coastal marine habitats in general. The foundation of landscape pattern analysis is also apparent in the spatially-explicit concepts of marine spatial planning, integrated coastal zone management, and ecosystem-based management. These holistic approaches to marine management utilize and require high-quality spatial data for a diverse array of activities including monitoring, predictive modelling, design of marine protected areas, and habitat restoration.

The application of landscape concepts and pattern metrics to compensatory habitat restoration in particular stands out as a worthwhile avenue for future research. In 2013, I worked on a service contract with DFO-Maritimes to write a technical report about the use of quantitative metrics for aiding habitat restoration as part of the SPERA (Strategic Program for Ecosystem-Based Research and Advice) program (Barrell et al. 2014). In Canada, damage to marine habitat supporting commercial or recreational fisheries requires compensation through the restoration, construction, or enhancement of high-value habitat to restore lost ecosystem services. This amount of habitat necessary to restore the lost services is determined through habitat equivalency analysis intended to balance lost habitat with gains through restoration, often of vegetated seagrass habitat.

The current approach does not consider landscape context in determining the value of damaged and restored habitat, instead scaling value to overall area, despite apparent benefits (Bell et al. 1997). In reality, seagrass habitat value varies as a function of its landscape structure and arrangement. The size, shape, and distribution of patches

affects faunal dynamics, nutrient cycling, hydrodynamics, and sedimentary processes, altering the provision of several services (Ackerman & Okubo 1993, Irlandi et al. 1995, Bradley & Stolt 2006, Hirst & Attrill 2008). Further, several services require a minimum threshold quantity of habitat and may not scale linearly with habitat area (Barbier et al. 2008, Koch et al. 2009). For example, the service of wave attenuation varies depending on the density and orientation of seagrass patches relative to the direction of currents (Chen et al. 2007). Landscape context also affects habitat value through relationships with the wider landscape mosaic. Seagrasses support adjacent habitats through the export of nutrient subsidies (Heck et al. 2008), and also can benefit from close proximity to non-vegetated areas.

As illustrated in Chapter 4, seagrasses often occur in conjunction with other ecosystem components such as mussels, potentially benefitting both habitats through mutualistic interactions (Peterson & Heck 2001, Bos & van Katwijk 2007). The consideration of landscape principles could serve to improve the valuation of marine habitats, with consequent benefits to habitat restoration, by better encompassing the range of landscape configurations exhibited by seagrasses themselves and in the larger mosaic of coastal marine and terrestrial habitats. This premise is supported by the recent release in the journal *Landscape Ecology* of a special edition focused on ecosystem services (Iverson et al. 2014 and references therein).

Predictive modelling of seagrass spatial pattern in relation to environmental variables remains a primary, though elusive, goal. Previous efforts at predictive vegetation mapping (PVM; Franklin 1995) have had limited success predicting the presence or absence of seagrasses based primarily on exposure to waves and currents,

though largely limited to coarse resolution over broad spatial extents. The apparent pattern of a seagrass bed effectively integrates the influences of historical (e.g., storms) as well as active processes (e.g., growth, reproduction) and their interactions. The biotic and abiotic factors that shape seagrass landscapes are numerous and vary widely over spatial and temporal scales, and often the ability to detect and quantify these processes at an adequate spatial resolution is limited. Further development of PVM will allow researchers to effectively link spatial patterns to the ecological processes responsible, with implications for numerous aspects of management.

The ability to detect and quantify seagrass spatial patterns at very fine scales, as demonstrated in this thesis, lays the foundation for greatly improved PVM capabilities. Linking fine-scale heterogeneity to environmental variables can improve predictions of response to environmental changes, with applications in assessing the impacts of changes to the ecosystem due to factors such as local development or long-term climate change. Additionally, this can benefit the application of seagrasses as indicators of ecosystem health through monitoring of landscape change. The application of PVM can also assist in the identification of priority areas for conservation as well as candidate areas for habitat restoration and the establishment of marine protected areas (MPAs).

5.2.2 Acoustic Remote Sensing

The use of single-beam acoustic data for mapping seagrasses holds great potential for additional insights due to its flexibility. The spatial scale of data collection can be manipulated in several ways in order to view the consequences on output maps. Most

simply, altering the spacing of transect lines would change the proportion of sampled to unsampled area and produce a different representation of the seagrass bed. Estimates of the spatial heterogeneity of the bed could be compared while varying transect spacing to extend the analysis to multiple spatial scales. This type of experiment could also be conducted with existing datasets through omission of alternating transects, or through analysis of random or stratified subsets of the entire dataset. Similarly, the spatial scale of data collection could be altered through manipulation of vessel speed or ping rate of the echosounder. Examining the impact of transect spacing or data volume on spatial statistics and landscape metrics would allow further insight into the characteristic scales of variation present at the study site.

The orientation of transects may also impact the quantification of pattern in seagrass beds. The ability to detect directional patterns is in part dependent on the sampling design of the survey relative to the patch structure of the habitat. For transect sampling, data density is always highest in the along-transect direction. If transects are biased towards one orientation (e.g., parallel or perpendicular to the shoreline), it is possible to mischaracterize the heterogeneity of the landscape by over- or under-sampling patches formed by anisotropic processes. For example, in Chapter 2 geostatistical analysis detected distinct anisotropy in the dataset, as evidenced by the variogram map (Figure 2-3). Detection of anisotropic pattern aids interpolation and extrapolation of data to unsampled areas, and also may allow insights into the processes responsible for seagrass landscape structure, a crucial aspect for the formulation of predictive models.

Single-beam acoustic data also provides an estimate of the canopy height of vegetation in addition to percent cover. This opens the possibility of extending analysis

of seagrass landscapes into three dimensions, and is mostly unexplored in studies of seagrass landscapes. The inclusion of canopy height data could greatly add to understanding of the spatial dynamics of seagrass beds, but raises many questions in practice. For example, it would be necessary to account for the effect of water movement on measured canopy height; currents cause eelgrass blades to lean down away from the direction of the current, making the acoustically measured canopy height a function of current speed and direction, and confusing the link to shoot length. Further, this effect could be expected to change with the reversing of the tides.

Despite these obstacles, the expansion into three dimensions could help explain patterns that are entirely obscured to aerial optical remote sensing, allowing for new insights into the spatial dynamics of seagrass landscapes. Recent advances looking at continuous landscapes using surface pattern metrics are promising and interesting (Hoechstetter et al. 2008, McGarigal et al. 2009). This also may benefit the analysis of seagrass metrics such as biovolume, an estimate the proportion of the water column filled by aquatic vegetation (Thomas et al. 1990, Valley et al. 2005). In general, the development of additional quantitative metrics derived from acoustic data would be a beneficent avenue for further research.

5.2.3 Aerial Remote Sensing

Object-based image analysis is quickly becoming a new paradigm in the classification of remote sensing data (Blaschke 2010). This method is particularly relevant to landscape analysis due to its implicit focus on multi-scale objects rather than

pixels. OBIA has been used with both acoustic and image data for classifying various marine ecosystems such as seagrasses (e.g., Lathrop et al. 2006, Mahoney et al. 2007, Urbański et al. 2009, Chapter 3 of this thesis), corals, and sediments (e.g., Lucieer 2008). For this thesis, I was unable to secure access to the necessary software due to very high costs, though these are rapidly decreasing as the method increases in popularity. Additional research could improve upon the foundation laid in Chapter 2 by varying the parameters of OBIA to investigate its effects on accuracy in landscape pattern analysis, and to elucidate new insights on scale-dependent patterns in seagrass ecosystems.

One issue frequently noticed in the composition of this thesis was the recurring issue of boundary detection and analysis. This problem merges both methodological and theoretical aspects; detection of transition zones is largely a function of sensor design, while the implications of landscape fragmentation and complexity are potentially very diverse. The detection of boundaries between ground cover categories is very important for the spatial analysis of aerial imagery, in particular when applying landscape metrics of patch shape or complexity. Recent studies have expounded the study of boundaries (e.g., Kent et al. 2006, Hufkens et al. 2009), and further developments specific to the marine environment could greatly improve the mapping of marine landscapes. Notably, this issue also applies to acoustic data, as illustrated in Chapter 2.

Aerial seagrass mapping is now conducted in various ways, largely displacing the standard approach involving manual classification of analog aerial photography. This raises new issues when comparing maps produced with different methodology between sites or regions, or when making comparisons to historical datasets. There are currently no signs of deceleration in the rapid evolution of remote sensing technology, making the

development of static standardized methods unlikely. Anticipation of future developments should continue to motivate researchers to consider the effects of spatial, spectral, and radiometric resolution in order to derive maximum benefits from these technological improvements.

Appendix A. Technical Details

A.1 Acoustic System Specifications

The single-beam acoustic sensor used to collect datasets for Chapters 2 and 3 was a Biosonics DE-X system operating at a frequency of 430 kHz with a 6.2° beam angle.

The acoustic output data were georeferenced by a JRC differential GPS antenna linked to the nearby Port Escuminac, NB reference station for all acoustic surveys performed at the Richibucto site.

For data analysis using the EcoSAV algorithm, individual pings are first analyzed for features suggesting the presence or absence of vegetation. Groups of sequential pings are then summarized to produce an estimate of percent cover, determined as the proportion of pings classified as vegetated for each group. Group size was determined by the number of pings occurring between DGPS readings, and was either 10 or 15 pings for all of the data used in this thesis.

The area ensonified by each ping is a function of many factors including the beam angle, distance from transducer face to seafloor, water temperature and salinity, and vessel speed. Most simply, through trigonometry it can be estimated that a single ping in water depth of 1 meter results in an ensonified circle with a diameter of 11 cm and an area of approximately 0.01 m².

A.2 Acoustic Ground Reference Data

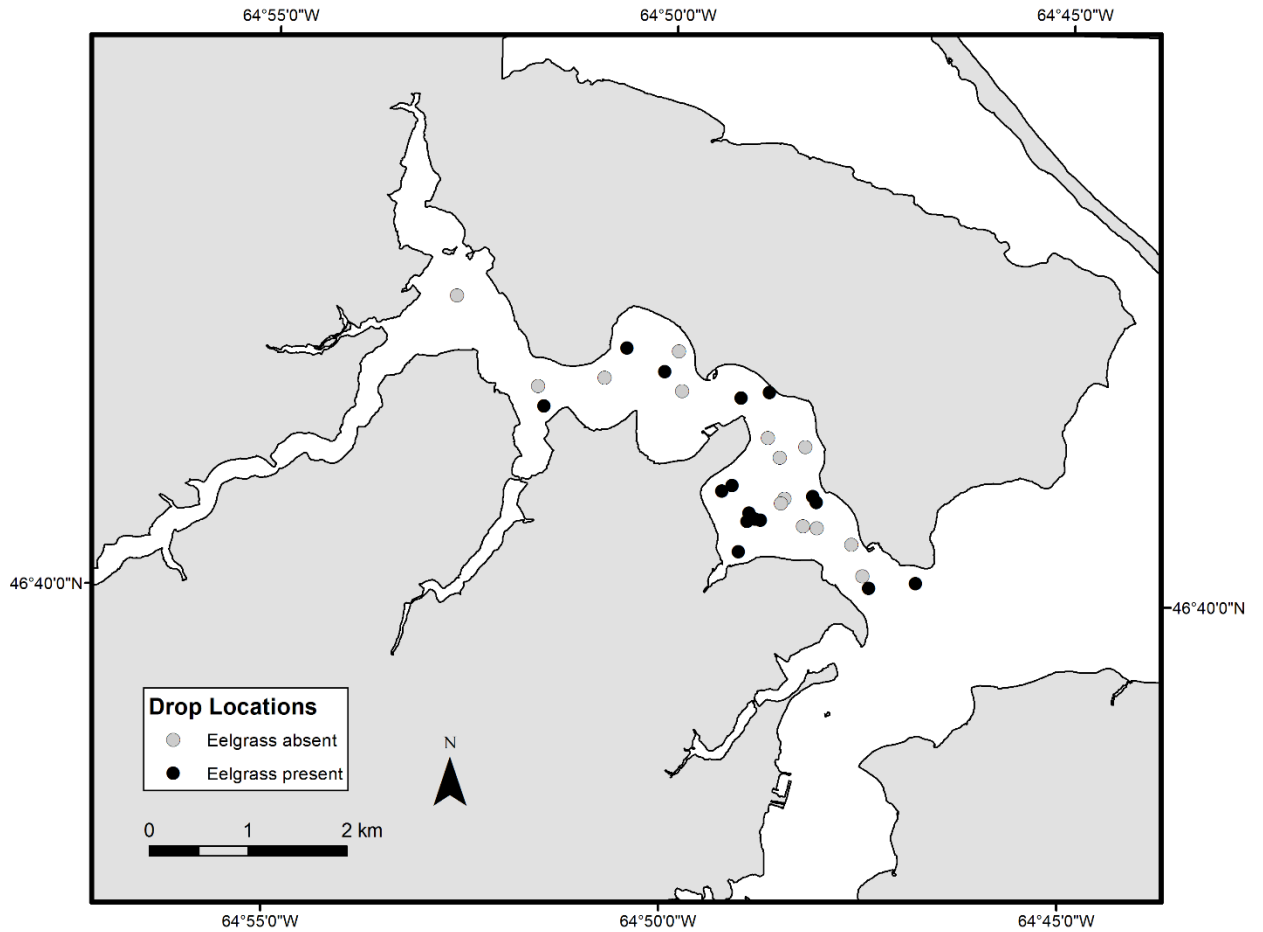


Figure A-1. Map of locations sampled by drop-camera for the purpose of ground-truthing acoustic data gathered in the Richibucto estuary, with the classification of eelgrass presence or absence noted.

The acoustic data used in this thesis were initially compared to independent ground-reference data collected with an underwater video camera to ensure that areas defined as vegetated contained eelgrass and to assist with tuning the vegetation detection algorithm. The camera system used was a Seaviewer drop-camera deployed from the acoustic survey vessel. At each reference site, the video was allowed to run for 30 seconds – 1 minute, collecting video representation at and around the reference waypoint. The live video feed was recorded to a handheld camcorder and overlaid with GPS coordinates. The camera was equipped with LED lights to provide illumination, and was used both with and without a wire frame mount. Parallel lasers attached to the camera housing were used to specify a 10 cm distance in the collected imagery.

Camera drops were performed throughout the Richibucto estuary intermittently through the first two field seasons, 2006 – 2007, in the months from July-October (Figure A-1). Drops occurred at times during acoustic surveys, and at other times in the days immediately before and after so that maximum time in ideal conditions could be allotted to surveying. In both cases, drop locations coincided with acoustic survey areas. The underwater videos were also collected in conjunction with another study into the benthic macrofaunal community at the same site (Lu et al. 2008). The resultant videos were viewed and segmented into still images for classification of eelgrass presence-absence. Drop locations were primarily located in the western part of the estuary where the majority of acoustic work was conducted.

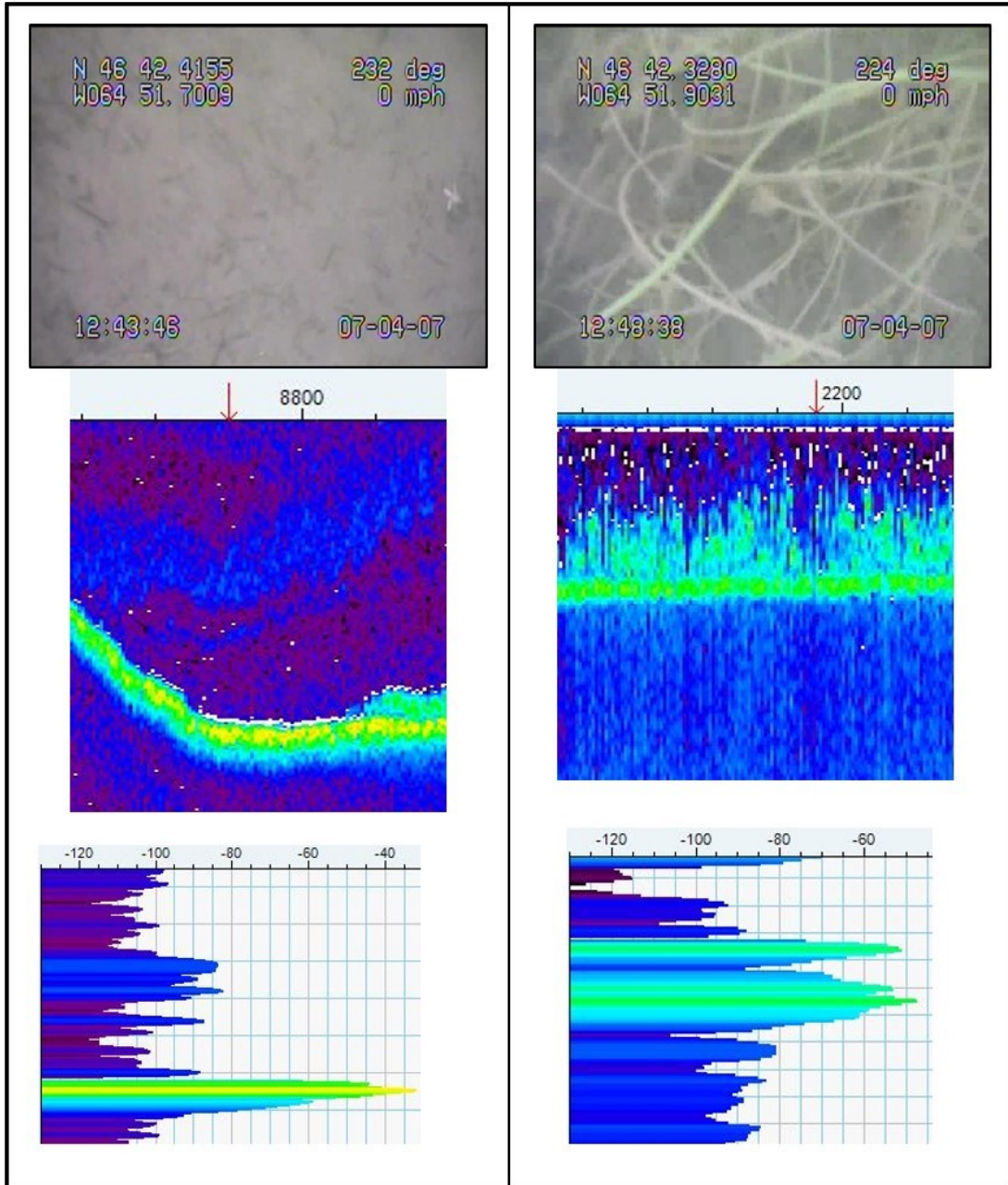


Figure A-2. Characteristic acoustic results for areas with (*left*) absence and (*right*) presence of vegetation. Depicted for each category is (*top*) a screen capture from the underwater video; (*center*) echogram profile showing the structure of the seafloor; and (*bottom*) ping profile used through the classification algorithm.

At the Richibucto site, the composition of the seabed was mostly uniform muddy sand (Lu et al. 2008), aside from deeper areas in tidal channels that were not surveyed for vegetation. Lacking hard substrate, the seabed classification at the site was largely limited to two categories: vegetated, and unvegetated bare sediments. Given the relatively small ensonified area for each individual ping ($\sim 0.01 \text{ m}^2$ in water depth of 1 meter) and the strong acoustic reflectivity of eelgrass, it was expected that even a very small quantity (>1 intact shoot) would result in a positive identification of vegetation through the processing algorithm. This logic was applied to the analysis of ground reference video data for determining eelgrass presence/absence.

Of the 30 locations sampled by the drop-camera, 16 (53.3%) were classified as vegetated and 14 (46.7%) as bare sediments. Of those classified as bare sediment, 7 occurred inside the deep tidal channel where no live eelgrass was observed. These results were compared to raw acoustic echograms as well as to output from the EcoSAV algorithm, and were used in part for tuning of the algorithm. The drop camera also validated expectations that eelgrass would be absent inside the deep tidal channel present at the site.

Comparison of acoustic echograms to screen captures from the underwater camera qualitatively showed 100% agreement in the detection of presence or absence of submerged aquatic vegetation. Macrophytes reflect a large amount of acoustic energy that can be easily recognized in raw echogram imagery, commonly appearing as a characteristic “double-peak” and/or a particularly wide bottom signal (Figure A-2). By contrast, unvegetated seafloor results in a comparatively narrow bottom signal and a single peak associated with the bottom signal.

Notably, the EcoSAV algorithm did not always agree with the author's qualitative interpretation, requiring large amounts of effort in tweaking the algorithm to properly recognize vegetation. The version of EcoSAV used in this thesis did not provide visual output, leading to a laborious tuning process. Since this work was conducted, newer visual approaches have been implemented in software from Biosonics, and have also been demonstrated in the scientific literature. This function allows for faster editing and additional control of the output, greatly streamlining the process.

Appendix B Copyright Information

Chapter 2 of this thesis, “Detecting hot and cold spots in a seagrass landscape using local indicators of spatial association,” is a manuscript version of a paper published in the journal *Landscape Ecology* as:

Barrell J, Grant J (2013) Detecting hot and cold spots in a seagrass landscape using local indicators of spatial association. *Landscape Ecology* 28:2005-2018

Permission was obtained from the publisher for use in this thesis as described in the email messages below. The final publication is available at Springer via

<http://dx.doi.org/10.1007/s10980-013-9937-2>

8/12/2014

Gmail - published article archived with PhD thesis

inip



Jeff Barrell <jeffbarrelldal@gmail.com>

published article archived with PhD thesis

Permissions Europe/NL <Permissions.Dordrecht@springer.com>
To: Jeff Barrell <jeffbarrell@dal.ca>

Tue, Jul 15, 2014 at 10:52 AM

Dear Mr. Barrell,

As long as it's not possible to download the Springer article separately from the thesis, we see no objections.

Please proceed according to the details described in your e-mail below, provided a one year embargo is applied.

With kind regards,

Ingrid Bleeker-de Boer

Springer
Special Licensing / Rights and Permissions

From: Jeff Barrell [mailto:jeffbarrell@dal.ca]
Sent: donderdag 3 juli 2014 15:16
To: Permissions Europe/NL
Subject: published article archived with PhD thesis

Hello,

I am currently preparing my PhD thesis for submission to the Faculty of Graduate Studies at Dalhousie University, Halifax, Nova Scotia, Canada. One of the chapters of my thesis was published in the journal Landscape Ecology as:

Barrell J, Grant J (2013) Detecting hot and cold spots in a seagrass landscape using local indicators of spatial association. Landscape Ecology 28:2005-2018

<https://mail.google.com/mail/u/1/?ui=2&ik=c6723478c5&view=pt&search=inbox&msg=1473a5382cf0ec7f8dsqt=1&siml=1473a5382cf0ec7f>

1/2

I am seeking permission to include a manuscript version of the paper as a chapter in my thesis. I have obtained permission for use of the material at my defense through RightsLink (license # 3421350367355). However, my university also requires me to obtain permission for submission of my thesis to the Library and Archives of Canada, and I would like to request permission to fulfill the following:

Canadian graduate theses are also reproduced by the Library and Archives of Canada (formerly National Library of Canada) through a non-exclusive, world-wide license to reproduce, loan, distribute, or sell theses. I am also seeking your permission for the material described above to be reproduced and distributed by the LAC(NLC). Further details about the LAC(NLC) thesis program are available on the LAC(NLC) website (www.nlc-bnc.ca).

I have included in the thesis full publication details and references to Springer including the DOI as described on your website. I have also applied for a 1-year embargo on any online archiving done by my university or the Library and Archives of Canada.

I am unfortunately in a bit of a rush, as I am set to defend on July 9th, and permission is required prior to that date. If this is possible, I will provide a permission letter that will be included as an appendix to the thesis.

Please let me know if I can provide any more information,

Thanks,

Jeffrey Barrell

PhD Candidate

Dept. of Oceanography

Dalhousie University

Halifax, NS, Canada

B3H 4R2

902-718-6595

jeffbarrell@dal.ca

References

- Ackerman JD, Okubo A (1993) Reduced mixing in a marine macrophyte canopy. *Functional Ecology* 7: 305-309
- Allouche O, Tsoar A, Kadmon R (2006) Assessing the accuracy of species distribution models: prevalence, kappa, and the true skill statistic (TCC). *Journal of Applied Ecology* 43:1223-1232
- Anselin L (1995) Local indicators of spatial association—LISA. *Geographical Analysis* 27:93–115
- Arnot C, Fisher PF, Wadsworth R, Wellens J (2004) Landscape metrics with ecotones: pattern under uncertainty. *Landscape Ecology* 19:181-195
- Barbier EB, Koch EW, Silliman BR, Hacker SD, Wolanski E, Primavera J, Granek EF, Polasky S, Aswani S, Cramer LA, Stoms DM, Kennedy CJ, Bael D, Kappel CV, Perillo GME, Reed DJ (2008) Coastal ecosystem-based management with nonlinear ecological functions and values. *Science* 319: 321-323.
- Barbier EB, Hacker SD, Kennedy C, Koch EW, Stier AC, Silliman BR (2011) The value of estuarine and coastal ecosystem services. *Ecological Monographs* 81:169-193
- Barrell J, Grant J (2013) Detecting hot and cold spots in a seagrass landscape using local indicators of spatial association. *Landscape Ecology* 28:2005-2018
- Barrell JP, Wong MC, Grant J (2014) Evaluating coastal habitat value through metrics of ecosystem function for use in habitat restoration. *Canadian Technical Report of Fisheries and Aquatic Sciences* 3095: v + 21 p.
- Bell S, Fonseca M, Motten L (1997) Linking restoration and landscape ecology. *Restoration Ecology* 5: 318-323
- Bell S, Fonseca M, Stafford N (2006) Seagrass ecology: new contributions from a landscape perspective. In: Larkum AWD, Orth RJ, Duarte C (eds) *Seagrasses: biology, ecology and conservation*. Springer, Dordrecht, p 625–645
- Bell SS, Fonseca MS, Kenworthy WJ (2008) Dynamics of a subtropical seagrass landscape: Links between disturbance and mobile seed banks. *Landscape Ecology* 23:67-74
- Berkenbusch K, Rowden AA (2007) An examination of the spatial and temporal generality of the influence of ecosystem engineers on the composition of associated assemblages. *Aquatic Ecology* 41:129-147

- Blaschke T (2010) Object based image analysis for remote sensing. *ISPRS Journal of Photogrammetry and Remote Sensing* 65:2-16
- Boots B (2002) Local measures of spatial association. *Ecoscience* 9:168-176
- Borowitzka MA, Lavery PS, van Keulen M (2006) Epiphytes of seagrasses. In: Larkum AWD, Orth RJ and Duarte CM (eds) *Seagrasses: Biology, Ecology and Conservation*. Springer, Dordrecht p441–461
- Borum J, Raun AL, Hasler-Sheetal H, Pedersen M, Pedersen O, Holmer M (2014) Eelgrass fairy rings: sulfide as inhibiting agent. *Marine Biology* 161:351-358
- Bos AR, van Katwijk MM (2007) Planting density, hydrodynamic exposure and mussel beds affect survival of transplanted intertidal eelgrass. *Marine Ecology Progress Series* 336:121-129
- Boström C, Jackson E, Simenstad C (2006) Seagrass landscapes and their effects on associated fauna: a review. *Estuarine, Coastal and Shelf Science* 68:383-403
- Boström C, Pittman S, Simenstad C, Kneib R (2011) Seascape ecology of coastal biogenic habitats: advances, gaps, and challenges. *Marine Ecology Progress Series* 427:191–217
- Boyd DS, Foody GM (2011) An overview of recent remote sensing and GIS based research in ecological informatics. *Ecological Informatics* 6:25-36
- Bradley MP, Stolt MH (2006) Landscape-level seagrass-sediment relations in a coastal lagoon. *Aquatic Botany* 84:121-128
- Brown CJ, Smith S, Lawton P, Anderson JT (2011) Benthic habitat mapping: A review of progress towards improved understanding of the spatial ecology of the seafloor using acoustic techniques. *Estuarine, Coastal and Shelf Science* 92:502-520
- Bryson M, Johnson-Roberson M, Murphy RJ, Bongiorno D (2013) Kite aerial photography for low-cost, ultra-high spatial resolution multi-spectral mapping of intertidal landscapes. *PloS One* 8:1-15
- Chen S, Sanford L, Koch E, Shi F, North E (2007) A nearshore model to investigate the effects of seagrass bed geometry on wave attenuation and suspended sediment transport. *Estuaries and Coasts* 30:296-310
- Coen LD, Luckenbach MW (2000) Developing success criteria and goals for evaluating oyster reef restoration: ecological function or resource exploitation? *Ecological Engineering* 15:323–343

- Coen LD, Brumbaugh RD, Bushek D, Grizzle R, Luckenbach MW, Posey MH, Powers SP, Tolley SG (2007) Ecosystem services related to oyster restoration. *Marine Ecology Progress Series* 341:303-307
- Congalton R (1991) A review of assessing the accuracy of classifications of remotely sensed data. *Remote Sensing of Environment* 37:35-46
- Congalton R, Green K (2009) *Assessing the Accuracy of Remotely Sensed Data: Principles and Practices*. 2nd Edition. CRC/Taylor & Francis, Boca Raton, FL 183p.
- Costanza R, d'Arge R, de Groot R, Farber S, Grasso M, Hannon B, Limburg K, Naeem S, O'Neill R, Paruelo J, Raskin R, Sutton P, van den Belt M (1997) The value of the world's ecosystem services and natural capital. *Nature* 387:253–260
- Crawford TW, Commito JA, Borowik AM (2006) Fractal characterization of *Mytilus edulis* L. spatial structure in intertidal landscapes using GIS methods. *Landscape Ecology* 21:1033-1044
- Cushman SA, McGarigal K, Neel MC (2008) Parsimony in landscape metrics: strength, universality, and consistency. *Ecological Indicators* 8:691-703
- Dekker A, Brando V, Anstee J, Fyfe S, Malthus T, Karpouzli E (2006) Remote sensing of seagrass ecosystems: use of spaceborne and airborne sensors. In: Larkum AWD, Orth RJ, Duarte C (eds) *Seagrasses: biology, ecology and conservation*. Springer, Dordrecht, p 347–359
- den Hartog C, Kuo J (2006) Taxonomy and biogeography of seagrasses. In: Larkum AWD, Orth RJ, Duarte C (eds) *Seagrasses: biology, ecology and conservation*. Springer, Dordrecht, p 1-23
- Dennison WC, Orth RJ, Moore KA, Stevenson JC, Carter V, Kollar S, Bergstrom PW, Batiuk RA (1993) Assessing water quality with submersed aquatic vegetation. *Bioscience* 43:86-94
- DFO [Fisheries and Oceans Canada] (2009) Does eelgrass (*Zostera marina*) meet the criteria as an ecologically significant species? DFO Canadian Science Advisory Secretariat Science Advisory Report 2009/018.
- DFO [Fisheries and Oceans Canada] (2011) Definitions of harmful alteration, disruption or destruction (HADD) of habitat provided by eelgrass (*Zostera marina*). DFO Canadian Science Advisory Secretariat Science Advisory Report 2011/058.

- Duarte C (1987) Use of echosounder tracings to estimate the aboveground biomass of submerged plants in lakes. *Canadian Journal of Fisheries and Aquatic Sciences* 44:732-735
- Duarte C (2002) The future of seagrass meadows. *Environmental Conservation* 29:192–206
- Duarte C, Fourqurean J, Krause-Jensen D, Olesen B (2006) Dynamics of seagrass stability and change. In: Larkum AWD, Orth RJ, Duarte C (eds) *Seagrasses: biology, ecology and conservation*. Springer, Dordrecht, p 271–294
- Edwards RW, Brown MW (1960) An aerial photographic method for studying the distribution of aquatic macrophytes in shallow waters. *Journal of Ecology* 48:161-163
- Fielding AH, Bell JF (1997) A review of methods for the assessment of prediction errors in conservation presence/absence models. *Environmental Conservation* 24:38-49
- Fisher P (1997) The pixel: a snare and a delusion. *International Journal of Remote Sensing* 18:679-685
- Foley MM, Halpern BS, Micheli F, Armsby MH, Caldwell MR, Crain CM, Prahler E, Rohr N, Sivas D, Beck MW, Carr MH, Crowder LB, Duffy JE, Hacker SD, McLeod KL, Palumbi SR, Peterson CH, Regan HM, Ruckelshaus MH, Sandifer PA, Steneck RS (2010) Guiding ecological principles for marine spatial planning. *Marine Policy* 34:955-966
- Fonseca MS, Zieman JC, Thayer GW, Fisher JS (1983) The role of current velocity in structuring seagrass meadows. *Estuarine, Coastal and Shelf Science* 17:367-380
- Fonseca MS, Kenworthy WJ (1987) Effects of current on photosynthesis and distribution of seagrasses. *Aquatic Botany* 27:59-78
- Fonseca MS, Bell SS (1998) Influence of physical setting on seagrass landscapes near Beaufort, North Carolina, USA. *Marine Ecology Progress Series* 171:109-121
- Fonseca MS, Julius BE, Kenworthy WJ (2000) Integrating biology and economics in seagrass restoration: how much is enough and why? *Ecological Engineering* 15: 227-237
- Fonseca M, Whitfield P, Kelly N, Bell S (2002) Modeling seagrass landscape pattern and associated ecological attributes. *Ecological Applications* 12:218–237

- Fonseca MS, Koehl MAR, Kopp BS (2007) Biomechanical factors contributing to self-organization in seagrass landscapes. *Journal of Experimental Marine Biology and Ecology* 340:227-246
- Foody GM (2008) Harshness in image classification accuracy assessment. *International Journal of Remote Sensing* 29:3137-3158
- Foody GM (2010) Assessing the accuracy of land cover change with imperfect ground reference data. *Remote Sensing of Environment* 114:2271-2285
- Fornes A, Basterretxea G, Orfila A, Jordi A, Alvarez A, Tintore J (2006) Mapping *Posidonia oceanica* from IKONOS. *ISPRS Journal of Photogrammetry & Remote Sensing* 60:315-322
- Fortin M, Dale M (2005) *Spatial analysis: a guide for ecologists*. Cambridge University Press, Cambridge
- Franklin J (1995) Predictive vegetation mapping: Geographic modelling of biospatial patterns in relation to environmental gradients. *Progress in Physical Geography* 19:474-499
- Freeman E, Moisen G (2008) A comparison of the performance of threshold criteria for binary classification in terms of predicted prevalence and kappa. *Ecological Modelling* 217:48-58
- Garbary DJ, Miller AG, Williams J, Seymour NR (2014) Drastic decline of an extensive eelgrass bed in Nova Scotia due to the activity of the invasive green crab (*Carcinus maenas*). *Marine Biology* 161:3-15
- Getis A, Ord J (1992) The analysis of spatial association by use of distance statistics. *Geographical Analysis* 24:189-206
- Getis A (2008) A history of the concept of spatial autocorrelation: A geographer's perspective. *Geographical Analysis* 40:297-309
- Goovaerts P (1997) *Geostatistics for natural resources evaluation*. Oxford University Press, New York, NY
- Grabowski JH, Hughes AR, Kimbro DL, Dolan MA (2005) How habitat setting influences restored oyster reef communities. *Ecology* 86:1926-1935
- Grant J (1986) Sensitivity of benthic community respiration and primary production to changes in temperature and light. *Marine Biology* 90:299-306
- Green EP, Short FT (2003) *World atlas of seagrasses*. University of California Press

- Guan W, Chamberlain R, Sabol B, Doering P (1999) Mapping submerged aquatic vegetation with GIS in the Caloosahatchee Estuary: evaluation of different interpolation methods. *Marine Geodesy* 22:69–91
- Guichard F, Bourget B, Agnard JP (2000) High-resolution remote sensing of intertidal ecosystems: a low-cost technique to link scale-dependent patterns and processes. *Limnology and Oceanography* 45:328-338
- Guichard F, Halpin PM, Allison GW, Lubchenco J, Menge BA (2003) Mussel disturbance dynamics: signatures of oceanographic forcing from local interactions. *The American Naturalist* 161:889-904
- Gutiérrez JL, Jones CG, Strayer DL, Iribarne OO (2003) Mollusks as ecosystem engineers: the role of shell production in aquatic habitats. *Oikos* 101:79-90
- Guyondet T, Koutitonsky V, Roy S (2005) Effects of water renewal estimates on the oyster aquaculture potential of an inshore area. *Journal of Marine Systems* 58:35-51
- Hanson AR (2004) The importance of eelgrass to waterfowl in Atlantic Canada. In: Hanson AR (ed) Status and conservation of eelgrass (*Zostera marina*) in Eastern Canada. Technical Report Series No. 412. Canadian Wildlife Service, Atlantic Region. viii. + 40 pp.
- Harris B, Stokesbury K (2010) The spatial structure of local surficial sediment characteristics on Georges Bank, USA. *Continental Shelf Research* 30:1840-1853
- Hauxwell J, Cebrian J, Valiela I (2006) Light dependence of *Zostera marina* annual growth dynamics in estuaries subject to different degrees of eutrophication. *Aquatic Botany* 84:17-25
- Heck Jr. KL, Carruthers TJB, Duarte CM, Hughes AR, Kendrick G, Orth RJ, Williams SW (2008) Trophic transfers from seagrass meadows subsidize diverse marine and terrestrial consumers. *Ecosystems* 11:1198-1210
- Hess, G (1994) Pattern and error in landscape ecology: a commentary. *Landscape Ecology* 9:3–5
- Hinchey EK, Nicholson MC, Zajac RN, Irlandi EA (2008) Preface: marine and coastal applications in landscape ecology. *Landscape Ecology* 23:1–5
- Hirst JA, Attrill MJ (2008) Small is beautiful: an inverted view of habitat fragmentation in seagrass beds. *Estuarine, Coastal and Shelf Science* 78: 811-818

- Hoechstetter S, Walz U, Dang L (2008) Effects of topography and surface roughness in analyses of landscape structure—a proposal to modify the existing set of landscape metrics. *Landscape Online* 1:1-14
- Hufkens K, Scheunders P, Ceulemans R (2009) Ecotones in vegetation ecology: methodologies and definitions revisited. *Ecological Research* 24:977–986
- Hughes AR, Bando KJ, Rodriguez LF, Williams SL (2004) Relative effects of grazers and nutrients on seagrasses: a meta-analysis approach. *Marine Ecology Progress Series* 282:87-99
- Hutchinson GE (1953) The concept of pattern in ecology. *Proceedings of the Academy of Natural Sciences of Philadelphia* 105:1-12
- Irlandi EA, Ambrose WG, Orlando BA (1995) Landscape ecology and the marine environment: how spatial configuration of seagrass habitat influences growth and survival of the bay scallop. *Oikos* 72: 307-313
- Iverson L, Echeverria C, Nahuelhual L, Luque S (2014) Ecosystem services in changing landscapes: an introduction. *Landscape Ecology* 29:181-186
- Jiménez-Valverde A, Lobo JM (2007) Threshold criteria for conversion of probability of species presence to either–or presence–absence. *Acta Oecologica*, 31:361–369
- Jones CG, Lawton JH, Shachak M (1994) Organisms as ecosystem engineers. *Oikos* 69:373-386
- Keddy CJ, Patriquin DG (1978) An annual form of eelgrass in Nova Scotia. *Aquatic Botany* 5:163-170
- Kent M, Moyeed RA, Reid CL, Pakeman R, Weaver R (2006) Geostatistics, spatial rate of change analysis and boundary detection in plant ecology and biogeography. *Progress in Physical Geography* 30:201-231
- Knudby A, Nordlund L (2011) Remote sensing of seagrasses in a patchy multi-species environment. *International Journal of Remote Sensing* 32:2227-2244
- Koch EW (2001) Beyond light: Physical, geological, and geochemical parameters as possible submersed aquatic vegetation habitat requirements. *Estuaries and Coasts* 24:1-17
- Koch EW, Barbier EB, Silliman BR, Reed DJ, Perillo GM, Hacker SD, Granek EF, Primavera JH, Muthiga N, Polasky S, Halpern BS, Kennedy CJ, Kappel CV, Wolanski E (2009) Non-linearity in ecosystem services: temporal and spatial variability in coastal protection. *Frontiers in Ecology and Environment* 7: 29–37

- Kostylev V, Erlandsson J (2001) A fractal approach for detecting spatial hierarchy and structure on mussel beds. *Marine Biology* 139:497-506
- Krause-Jensen D, Sagert S, Schubert H, Boström C (2008) Empirical relationships linking distribution and abundance of marine vegetation to eutrophication. *Ecological Indicators* 8:515-529
- Kupfer JA (2012) Landscape ecology and biogeography: rethinking landscape metrics in a post-FRAGSTATS landscape. *Progress in Physical Geography* 36:400-420
- Landis JR, Koch GG (1977) The measurements of observer agreement for categorical data. *Biometrics* 33:159-174
- Lathrop RG, Montesano P, Haag S (2006) A multi-scale segmentation approach to mapping seagrass habitats using airborne digital camera imagery. *Photogrammetric Engineering & Remote Sensing* 72:665-675
- Legendre P, Fortin MJ (1989) Spatial pattern and ecological analysis. *Vegetatio* 80:107-138
- Legendre P (1993) Spatial autocorrelation: trouble or new paradigm? *Ecology* 74:1659-1673
- Legendre P, Legendre L (1998) *Numerical ecology*, 2nd English edition. Elsevier Science BV, Amsterdam
- Levin SA (1992) The problem of pattern and scale in ecology. *Ecology* 73:1943-1967
- Li H, Reynolds JF (1995) On definition and quantification of heterogeneity. *Oikos* 73:280-284
- Li H, Wu J (2004) Use and misuse of landscape indices. *Landscape Ecology* 19:389-399
- Liu C, Berry PM, Dawson TP, Pearson RG (2005) Selecting thresholds of occurrence in the prediction of species distributions. *Ecography* 28:385-393
- Lotze HK, Lenihan HS, Bourque BJ, Bradbury RH, Cooke RG, Kay MC, Kidwell SM, Kirby MX, Peterson CH, Jackson JBC (2006) Depletion, degradation, and recovery potential of estuaries and coastal seas. *Science* 312:1806-1809
- Lu D, Weng Q (2007) A survey of image classification methods and techniques for improving classification performance. *International Journal of Remote Sensing* 28:823-870

- Lu L, Grant J, Barrell J (2008) Macrofaunal spatial patterns in relationship to environmental variables in the Richibucto Estuary, New Brunswick, Canada. *Estuaries and Coasts* 31:994–1005
- Lucieer VL (2008) Object-oriented classification of sidescan sonar data for mapping benthic marine habitats. *International Journal of Remote Sensing* 29:905-921
- Lunetta RS, Congalton RG, Fenstermaker LK, Jensen JR, McGwire KC, Tinney LR (1991) Remote sensing and geographic information systems data integration: error sources and research ideas. *Photogrammetric Engineering and Remote Sensing* 53:1259-1263
- MacArthur RH, Wilson EO (1967) *The theory of island biogeography*. Princeton University Press, Princeton, NJ
- Madsen JD, Chambers PA, James WF, Koch EW, Westlake DF (2001) The interaction between water movement, sediment dynamics and submersed macrophytes. *Hydrobiologia* 444:71-84
- Mahoney ML, Hanson AR (2007) Distribution map of eelgrass (*Zostera marina*) in Richibucto Harbour, New Brunswick, 2007, based on QuickBird Satellite Imagery. Canadian Wildlife Service - Environment Canada, Sackville, New Brunswick
- Mahoney ML, Hanson AR, Gilliland S (2007) An evaluation of a methodology for wetland classification and inventory for Labrador. Technical Report Series No. 480. Canadian Wildlife Service, Atlantic Region. viii. + 40 pp.
- Manel S, Williams HC, Ormerod SJ (2001) Evaluating presence-absence models in ecology: the need to account for prevalence. *Journal of Applied Ecology* 38:921-931
- Marbà N, Duarte CM (1998) Rhizome elongation and seagrass clonal growth. *Marine Ecology Progress Series* 174:269-280
- Martínez-Crego B, Vergés A, Alcoverro A, Romero J (2008) Selection of multiple seagrass indicators for environmental biomonitoring. *Marine Ecology Progress Series* 361:93-109
- McGarigal K, Tagil S, Cushman SA (2009) Surface metrics: an alternative to patch metrics for the quantification of landscape structure. *Landscape Ecology* 24:433–450

- McGarigal K, Cushman SA, Ene E (2012) FRAGSTATS v4: Spatial Pattern Analysis Program for Categorical and Continuous Maps. Computer software program produced by the authors at the University of Massachusetts, Amherst. Available online: <http://www.umass.edu/landeco/research/fragstats/fragstats.html>
- McKenzie L, Finkbeiner M, Kirkman H (2001) Methods for mapping seagrass distribution. In: Short F, Coles R (eds) *Global seagrass research methods*. Elsevier, Amsterdam, p 101–121
- Meager JJ, Schlacher TA, Green M (2011) Topographic complexity and landscape temperature patterns create a dynamic habitat structure on a rocky intertidal shore. *Marine Ecology Progress Series* 428:1-12
- Micheli F, Peterson CH (1999) Estuarine vegetated habitats as corridors for predator movements. *Conservation Biology* 13:869-881
- Moore KA, Short FT (2006) *Zostera: Biology, Ecology, and Management*. In: Larkum AWD, Orth RJ, Duarte C (eds) *Seagrasses: biology, ecology and conservation*. Springer, Dordrecht, p 361-386
- Mumby PJ, Edwards AJ (2002) Mapping marine environments with IKONOS imagery: enhanced spatial resolution can deliver greater thematic accuracy. *Remote Sensing of Environment* 82:248-257
- Mumby PJ, Broad K, Brumbaugh DR, Dahlgren CP, Harborne AR, Hastings A, Holmes KE, Kappel CV, Micheli F, Sanchirico JN (2008) Coral reef habitats as surrogates of species, ecological functions, and ecosystem services. *Conservation Biology* 22:941-951
- Neckles H, Kopp B, Petersen B, Pooler P (2012) Integrating scales of seagrass monitoring to meet conservation needs. *Estuaries and Coasts* 35:23-46
- Nelson T, Boots B (2008) Detecting spatial hot spots in landscape ecology. *Ecography* 31:556–566
- Newton AC, Hill RA, Echeverría C, Golicher D, Benayas JMR, Cayuela L, Hinsley SA (2009) Remote sensing and the future of landscape ecology. *Progress in Physical Geography* 33:528-546
- O'Neill R, Krummel J, Gardner R, Sugihara G, Jackson B, DeAngelis D, Milne B, Turner M, Zygmunt B, Christensen S (1988) Indices of landscape pattern. *Landscape Ecology* 1:153–162
- Ord J, Getis A (1995) Local spatial autocorrelation statistics: distributional issues and an application. *Geographical Analysis* 27:286-306

- Orth R, Carruthers T, Dennison W, Duarte C, Fourqurean J, Heck KL Jr., Hughes A, Kendrick G, Kenworthy W, Olyarnik S, Short F, Waycott M, Williams S (2006) A global crisis for seagrass ecosystems. *BioScience* 56:987–996
- Paine RT, Levin SA (1981) Intertidal landscapes: disturbance and the dynamics of pattern. *Ecological Monographs* 51:145-178
- Pasqualini V, Pergent-Martini C, Clabaut C, Pergent G (1998) Mapping of *Posidonia oceanica* using aerial photographs and side scan sonar: application off the island of Corsica (France). *Estuarine, Coastal and Shelf Science* 47:359-367
- Patriquin DG (1975) ‘Migration’ of blowouts in seagrass beds at Barbados and Carriacou, West Indies and its ecological and geological applications. *Aquatic Botany* 1:163-189
- Paul M, Lefebvre A, Manca E, Amos CL (2011) An acoustic method for the remote measurement of seagrass metrics. *Estuarine, Coastal and Shelf Science* 93:68–79
- Pedersen O, Binzer T, Borum J (2004) Sulphide intrusion in eelgrass (*Zostera marina* L.). *Plant, Cell & Environment* 27:595-602
- Peterson BJ, Heck KL Jr. (2001) Positive interactions between suspension-feeding bivalves and seagrass – a facultative mutualism. *Marine Ecology Progress Series* 213:143-155
- Philibert M, Fortin M, Csillag F (2008) Spatial structure effects on the detection of patches boundaries using local operators. *Environmental and Ecological Statistics* 15:447–467
- Pickett STA, Cadenasso ML (1995) Landscape ecology: spatial heterogeneity in ecological systems. *Science* 269:331-334
- Qi Y, Wu J (1996) Effects of changing spatial resolution on the results of landscape pattern analysis using spatial autocorrelation indices. *Landscape Ecology* 11:39–49
- Reusch TBH, Chapman ARO, Gröger JP (1994) Blue mussels *Mytilus edulis* do not interfere with eelgrass *Zostera marina* but fertilize shoot growth through biodeposition. *Marine Ecology Progress Series* 108:265-282
- Reusch TBH, Chapman ARO (1995) Storm effects on eelgrass (*Zostera marina* L.) and blue mussel (*Mytilus edulis* L.) beds. *Journal of Experimental Marine Biology and Ecology* 192:257-271
- Rivers DO and Short FT (2007) Effect of grazing by Canada geese *Branta canadensis* on an intertidal eelgrass *Zostera marina* meadow. *Marine Ecology Progress Series* 333:271-279

- Robbins BD, Bell SS (1994) Seagrass landscapes: a terrestrial approach to the marine subtidal environment. *Trends in Ecology and Evolution* 9:301–304
- Robertson AI, Mann KH (1984) Disturbance by ice and life-history adaptations of the seagrass *Zostera marina*. *Marine Biology* 80:131-141
- Roelfsema C, Kovacs EM, Saunders MI, Phinn S, Lyons M, Maxwell P (2013) Challenges of remote sensing for quantifying changes in large complex seagrass environments. *Estuarine, Coastal and Shelf Science* 133:161-171
- Sabol B, Melton RE Jr., Chamberlain R, Doering P, Haurert K (2002) Evaluation of a digital echo sounder system for detection of submersed aquatic vegetation. *Estuaries and Coasts* 25:133–141
- Sabol B, Kannenberg J, Skogerboe J (2009) Integrating acoustic mapping into operational aquatic plant management: a case study in Wisconsin. *Journal of Aquatic Plant Management* 47:44–52
- Seymour NR, Miller AG, Garbary DJ (2002) Decline of Canada geese (*Branta canadensis*) and common goldeneye (*Bucephala clangula*) associated with a collapse of eelgrass (*Zostera marina*) in a Nova Scotia estuary. *Helgoland Marine Research* 56:198-202
- Shao G, Wu J (2008) On the accuracy of landscape pattern analysis using remote sensing data. *Landscape Ecology* 23:505–511
- Short FT, Polidoro B, Livingstone SR, Carpenter KE, Bandeira S, Bujang JS, Calumpong HP, Carruthers TJB, Coles RG, Dennison WC, Erftemeijer PLA, Fortes MD, Freeman AS, Jagtap TG, Kamal AHM, Kendrick GA, Kenworthy WJ, La Nafie YA, Nasution IM, Orth RJ, Prathep A, Sanciangco JC, van Tussenbroek B, Vergara SG, Waycott M, Zieman JC (2011) Extinction risk assessment of the world's seagrass species. *Biological Conservation* 144:1961-1971
- Silva TSF, Costa MPF, Melack JM, Novo EMLM (2008) Remote sensing of aquatic vegetation: theory and applications. *Environmental Monitoring and Assessment* 140:131-145
- Simes R (1986) An improved Bonferroni procedure for multiple tests of significance. *Biometrika* 73:751-754
- Sleeman J, Kendrick G, Boggs G, Hegge B (2005) Measuring fragmentation of seagrass landscapes: which indices are most appropriate for detecting change? *Marine and Freshwater Research* 56:851–864

- Snover ML, Commito JA (1998) The fractal geometry of *Mytilus edulis* L. spatial distribution in a soft-bottom system. *Journal of Experimental Marine Biology and Ecology* 223:53-64
- Thomas GL, Thiesfeld SL, Bonar SA, Crittenden RN, Pauley GB (1990) Estimation of submergent plant bed biovolume using acoustic range information. *Canadian Journal of Fisheries and Aquatic Sciences* 47:805-812
- Tobler WR (1970) A computer movie simulating urban growth in the Detroit region. *Economic Geography* 46:234-240
- Townsend EC and Fonseca MS (1998) Bioturbation as a potential mechanism influencing spatial heterogeneity of North Carolina seagrass beds. *Marine Ecology Progress Series* 169:123-132
- Troll C (1939) Luftbildplan und ökologische Bodenforschung (Aerial photography and ecological studies of the earth). *Zeitschrift der Gesellschaft für Erdkunde, Berlin* p 241-298
- Turner MG (1989) Landscape ecology: the effect of pattern on process. *Annual Review of Ecology and Systematics* 20:171-197
- Turner MG, O'Neill RV, Gardner RH, Milne BT (1989) Effects of changing spatial scale on the analysis of landscape pattern. *Landscape Ecology* 3:153-162
- Turner MG, Gardner RH, O'Neill RV (2001) *Landscape ecology in theory and practice: pattern and process*. Springer, New York, NY
- Turner MG (2005) Landscape ecology: what is the state of the science? *Annual Review of Ecology, Evolution, and Systematics* 36:319-344
- UN [United Nations] (2014) UN Atlas of the Oceans. Online: <http://www.oceanatlas.org>, accessed 1 May 2014
- Urbański JA, Mazur A, Janas U (2009) Object-oriented classification of QuickBird data for mapping seagrass spatial structure. *Oceanological and Hydrobiological Studies* 38:27-43
- Valentine JF, Heck Jr. KL (1999) Seagrass herbivory: evidence for the continued grazing of marine grasses. *Marine Ecology Progress Series* 176:291-302
- Valentine JF, Duffy JE (2006) The central role of grazing in seagrass ecology. In: Larkum AWD, Orth RJ, Duarte C (eds) *Seagrasses: biology, ecology and conservation*. Springer, Dordrecht, p 463-501

- Valley R, Drake M, Anderson C (2005) Evaluation of alternative interpolation techniques for the mapping of remotely-sensed submersed vegetation abundance. *Aquatic Botany* 81:13–25
- van de Koppel J, Rietkerk M, Dankers N, Herman PMJ (2005) Scale-dependent feedback and regular spatial patterns in young mussel beds. *The American Naturalist* 165:66-77
- van der Heide T, Bouma TJ, van Nes EH, van de Koppel J, Scheffer M, Roelofs JGM, van Katwijk MM, Smolders AJP (2010) Spatial self-organized patterning in seagrasses along a depth gradient of an intertidal ecosystem. *Ecology* 91:362-369
- van der Heide T, Eklöf JS, van Nes EH, van der Zee EM, Donaldi S, Weerman EJ, Olf H, Eriksson BK (2012) Ecosystem engineering by seagrasses interacts with grazing to shape an intertidal landscape. *PLoS ONE* 7:1-7
- van Katwijk MM, Bos AR, de Jonge VN, Hanssen LSAM, Hermus DCR, de Jong DJ (2009) Guidelines for seagrass restoration: importance of habitat selection and donor population, spreading of risks, and ecosystem engineering effects. *Marine Pollution Bulletin* 58:179-188
- Vandermeulen H (2005) Assessing marine habitat sensitivity: a case study with eelgrass (*Zostera marina* L.) and kelps (*Laminaria*, *Macrocystis*). DFO Canadian Science Advisory Secretariat Research Document 2005/032: ii+53 p
- Vandermeulen H (2009) An introduction to eelgrass (*Zostera marina* L.): the persistent ecosystem engineer. DFO Canadian Science Advisory Secretariat Research Document 2009/085: vi+11 p
- Vandermeulen H (2013) Mapping eelgrass (*Zostera marina*) with a novel towfish: Richibucto and Shippagan, New Brunswick. Canadian Technical Report of Fisheries and Aquatic Sciences 3064: v + 19p.
- Vinther HF, Laursen JS, Holmer M (2008) Negative effects of blue mussel (*Mytilus edulis*) presence in eelgrass (*Zostera marina*) beds in Flensborg fjord, Denmark. *Estuarine, Coastal and Shelf Science* 77:91-103
- Vinther HF, Norling P, Kristensen PS, Dolmer P, Holmer M (2012) Effects of coexistence between the blue mussel and eelgrass on sediment biogeochemistry and plant performance. *Marine Ecology Progress Series* 447:139-149
- Wagner H, Fortin M (2005) Spatial analysis of landscapes: concepts and statistics. *Ecology* 86:1975–1987

- Wall CC, Peterson BJ, Gobler CJ (2008) Facilitation of seagrass *Zostera marina* productivity by suspension-feeding bivalves. *Marine Ecology Progress Series* 357:165-174
- Warren J, Peterson B (2007) Use of a 600-kHz acoustic Doppler current profiler to measure estuarine bottom type, relative abundance of submerged aquatic vegetation, and eelgrass canopy height. *Estuarine, Coastal and Shelf Science* 72:53–62
- Watt AS (1947) Pattern and process in the plant community. *Journal of Ecology* 35:1-22
- Waycott M, Duarte C, Carruthers T, Orth R, Dennison W, Olyarnik S, Calladine A, Fourqurean J, Heck K, Hughes A, Kendrick G, Kenworthy W, Short F, Williams S (2009) Accelerating loss of seagrasses across the globe threatens coastal ecosystems. *Proceedings of the National Academy of Sciences* 106:12377-12381
- Wedding L, Lepczyk C, Pittman S, Friedlander A, Jorgensen S (2011) Quantifying seascape structure: extending terrestrial spatial pattern metrics to the marine realm. *Marine Ecology Progress Series* 427:219–232
- Wiens J (1989) Spatial scaling in ecology. *Functional Ecology* 3:385–397
- Wu J, Hobbs R (2002) Key issues and research priorities in landscape ecology: an idiosyncratic synthesis. *Landscape Ecology* 17:355–365
- Wulder M, Boots B (1998) Local spatial autocorrelation characteristics of remotely sensed imagery assessed with the Getis statistic. *International Journal of Remote Sensing* 19:2223–2231